Identification and characterization of novel keratin associated proteins using a genetic interaction screening system

Dissertation

zur

Erlangung des Doktorgrades (Dr. rer. Nat.)

der

Mathematisch-Naturwissenschaftlichen Fakultät

der

Rheinischen Friedrich-Wilhelms-Universität Bonn

vorgelegt von

Prashanth H.C

aus

Shimoga, Indien

-Bonn, Februar 2009-

Angefertigt mit Genehmigung der Mathematisch-Naturwissenschaftlichen
Fakultät der Rheinischen Friedrich-Wilhelms-Universität Bonn

Erscheinungsjahr: 2009
Tag der Promotion: _._.2009

Gutachter

1. Prof. Dr. Thomas Magin
2. Prof. Dr. Michael Hoch

Die vorliegende Arbeit wurde in der Zeit von April 2005 bis Februar 2009 am Institut für Biochemie und Molekularbiologie der Universität Bonn, Nussallee 11 unter Leitung von Prof. Thomas Magin durchgeführt.

Acknowledgements

I would like to thank **Prof. Thomas Magin** who gave me an opportunity to work in his research group, under whose supervision I chose this topic and began the thesis. His broad knowledge, professional insight was of great importance and his valuable support and guidance helped immensely to accomplish this work.

I would like to extend my sincere gratitude to **Prof. Michael Hoch** for being my second supervisor and for allowing me to use his lab facilities for some of the experiments done in this thesis.

I would like to thank **Prof. Mechthild Hatzfeld** and **Dr. Andreas Schmid** for kindly providing Venus plasmids for this project.

I am very appreciative for the support provided by **Dr. Christof Völker** and **Dr. Mekky Abouzied** to work with recombinant proteins.

I admire and thank sincerely all my former and present colleagues for their help, advice and understanding, whose pleasant company has made my stay in Bonn immensely enjoyable.

I would like to thank all my friends and family members for their untiring support and encouragement.

Index

Figures

List of tables

Abbreviations

µg	Microgram
µl	Microlitre
°C	Grad Celsius
APS	Ammonium persulphate
BiFC	Bimolecular fluorescence complementation
bp	Base pair
BSA	Bovine serum albumin
CO_2	Carbon dioxide
DAPI	4,6-Diamidino-2-phenylindole
DMSO	Dimethyl sulphoxide
DNA	Deoxy ribonucleic acid
dNTP	Deoxynucleoside-triphosphate
E. coli	Escherichia coli
EDTA	Ethylene diamine tetra acetic acid
hr(s)	Hour(s)
IF	Intermediate filament
IL-1	Interleukin 1
K	Keratin protein
kDa	Kilodalton
KO	Knockout
Krt	Keratin gene
L	Litre
LB	Luria-Bertani
ME	Mercaptoethanol
mg	Milligram
min	Minutes
mRNA	Messenger RNA
PAGE	Polyacrylamide gel electrophoresis
PBS	Phosphate buffered saline
PCR	Polymerase chain reaction
PEG	Polyethylene glycol
pmol	Picomole
RT	Room temperature
RT-PCR	Reverse transcription – polymerase chain reaction
SDS	Sodium dodecyl sulfate
PAGE	Polyacrylamide gel electrophoresis
Sec	Seconds
TBS	Tris buffered saline
TNF	Tumor necrosis factor
Ven	Venus

1. Introduction

Intermediate filaments (IFs) are important structural components found in most vertebrate cells. They are expressed in nucleus as well as in cytoplasm providing physical resilience for cells to withstand the mechanical stresses of the tissue in which they are expressed. Intermediate filaments are essential for normal tissue structure and function and are encoded in the human genome by 70 different genes in six subfamilies.

1.1 Keratins

Keratins are the structural intermediate filament proteins and account for most of the majority intermediate filament proteins. They form a dynamic network of 10-12 nm filaments (40–70 kDa) which are prominent structural constituents of the cytoplasm in epithelial cells. Keratins are encoded by a large multigene family of more than 50 individual members and on the basis of gene structure and homology (Hesse et al., 2001; Moll et al., 1982; Schweizer et al., 2006), are classified into two major sequence types, type I (acidic) and type II (basic to neutral). The genes encoding type I and type II keratins are clustered on chromosomal regions 17q12–q21 and 12q11–q13, respectively. Keratin filaments represent obligatory heterodimers of basic and acidic partners. The 28 type I include K9–K23 (epithelial), and the hair keratins K31–K40 and 26 type II include K1–K8, and the hair keratins, K81–K86 which are specifically expressed in and closely restricted to the various compartments of the hair follicle inner root sheath.

Pairs of type I and type II keratins are expressed in highly specific patterns related to the epithelial type and stage of cellular differentiation (Kirfel et al., 2003) (figure1.1). Each keratin pair is characteristic of a particular epithelial differentiation programme, some epithelial cells express more than one pair. The coexpressed pairs of type I / type II keratins can be divided into three expression groups: simple keratins of one-layered epithelia (K8/K18, K20), barrier (keratinocytes) keratins of stratified epithelia (K5/K14, K1/K10, K3/K12, K4/K13, K6a/K16, K6b/K17, K19) and structural keratins which make up hard appendages like hair, nails, horns and reptilian scales.

The present study is focused on keratin pair K5, K14 and their expression profile is introduced briefly in the following section.

1.1.1 Keratin 5 and Keratin 14

K5 (62 kDa) and K14 (51 kDa) occur as heterodimers with varying levels of expression in basal keratinocytes of stratified epithelia. They are strongly expressed in the basal cell layer containing stem cells (Fuchs and Green, 1980), uniformly expressed in stratified follicular outer root sheath, basal and myoepithelial cells of complex glandular epithelial tissue (Purkis et al., 1990). The distinctive expression of specific keratin pairs depends largely on the tissue-type, differentiation status, and the physiological state. For example, as the dividing basal keratinocytes of the skin epidermis exit the cell cycle and embark on a program of differentiation, expression of K5 and K14 is downregulated and a new set of keratins, K1 and K10 are expressed in the suprabasal spinous layer (Byrne et al., 1994) or become activated producing K6 and K16. IL-1 is the primary signal initiating keratinocyte activation and expression of K6 and K16 (Freedberg et al., 2001). The restricted expression of K14 in the basal layer of the skin epidermis is primarily controlled at the level of transcription and regulation of this process has been extensively studied using various complementary approaches. DNAse I hypersensitive site (Hs) mapping of the human K14 gene has identified several Hs in the 5' region that are present selectively in keratinocytes (Sinha et al., 2000; Sinha and Fuchs, 2001).

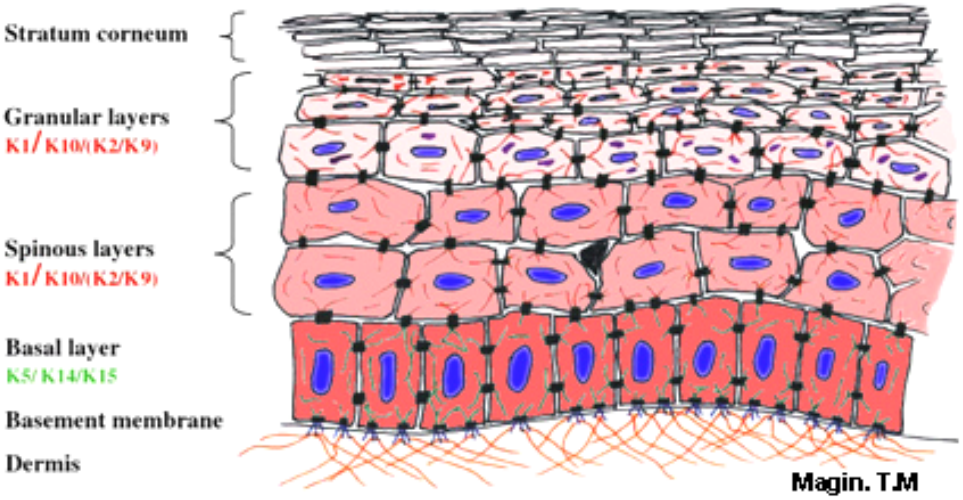

Figure 1.1: Keratin expression in the epidermis. Basal epidermal cells express K5, K14 and K15. As basal cells commit to terminal differentiation, they switch off the expression of K5, K14 and K15 and induce the expression of K1 and K10. As epidermal cells move up through the spinous layers, they express K2e, which can pair with K10. Some keratins are expressed in the epidermis under special circumstances, during wound healing, keratinocytes express K6, K16 and K17. K9 is unique to the suprabasal layers of the palms and soles.

1.1.2 Keratin organization and expression in the cells

Filaments of keratins are organized into a complex supra-molecular network which is extended over the cytoplasm and are attached to the cytoplasmic plaques of the typical epithelial cell–cell junctions, the desmosomes - the peripheral most portion of the cell (figure1.2). The desmosome–intermediate filament complex (DIFC) network or scaffolding maintains the integrity of cells (Garrod and Chidgey, 2008).

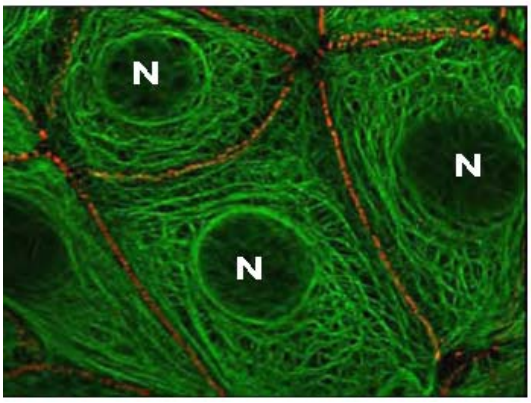

Figure 1.2: Keratin IFs (green) are organized in a network that spans the whole cytoplasm, and are attached to desmosomes (red) at points of cell–cell contacts. N: nucleus. Scale bar, 10 µm (Image: Dr. S. Loeffek. IBMB, Bonn)

In epithelial cells, keratin filaments are attached by adapter proteins to desmosomes (cell-cell adhesion) and hemidesmosomes (cell-matrix adhesion) by a filigree of proteins that make up the desmosomal plaques, like desmoplakin, desmogleins, desmocollins and the armadillo proteins plakoglobin and plakophilin (figure1.3).

Keratins interact with desmoplakins, which are prototypes of the plakin family of cytoskeletal adaptor proteins and are essential for normal desmosomal adhesion. The globular head or plakin domain of desmoplakin is an important region for protein–protein interactions. The C-terminal tail domain consists of three plakin repeat domains (PRDs) and two of them represent an intermediate filament binding site (Choi et al., 2002). The interaction between desmoplakin with keratin filaments is regulated by glycine–serine–arginine rich domain located at the extreme C-terminus (Stappenbeck et al., 1994). Mutations in the K5 tail domain cause migratory circinate erythema, possibly by affecting the interaction between desmosomes and keratins (Betz et al., 2006; Gu et al., 2003; Magin et al., 2004).

Plakoglobin is found in all cell–cell adhesive junctions and forms a bridge between adhesion proteins and cytoskeletal linkers (Kowalczyk et al., 1997; Mathur et al., 1994). The C-terminal end of plakoglobin contains a three-Tyr cluster in its C-terminal domain (Tyr693, Tyr724, and

Tyr729) which is binds to the N-terminal domain of desmoplakin. Loss of plakoglobin leads to decreased number and altered structure of desmosomes in the epidermis of mouse skin

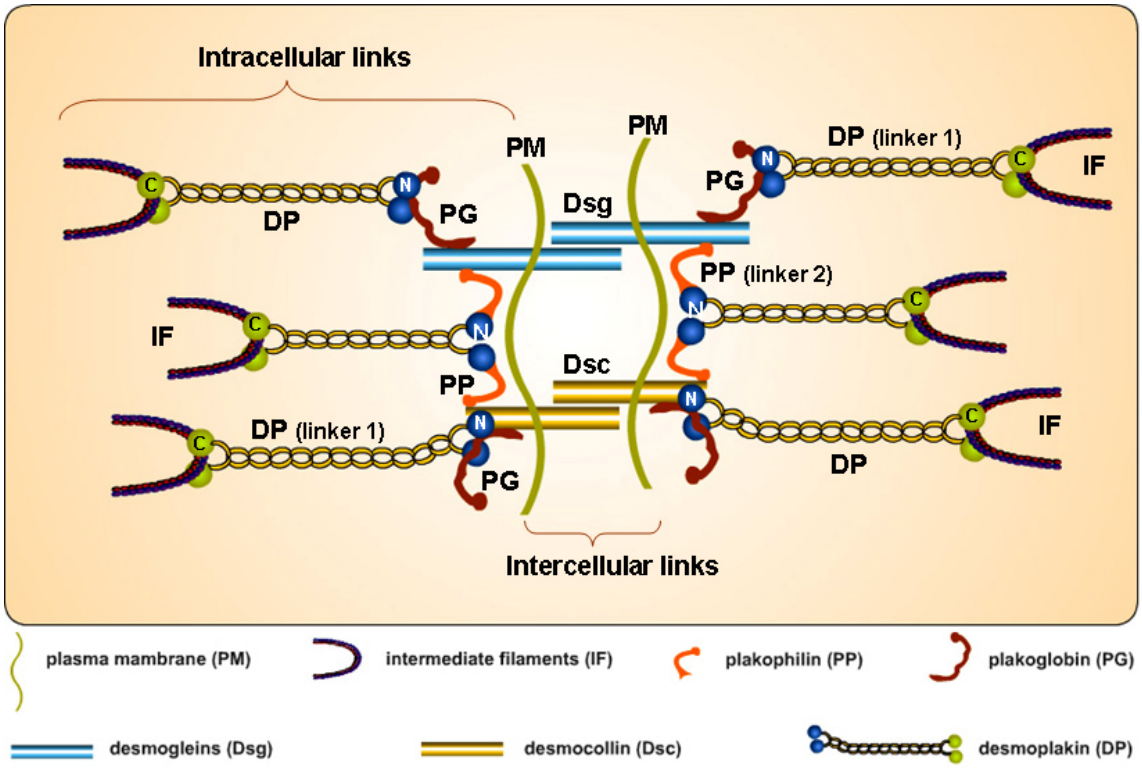

Figure 1.3: **Organization of keratin filaments in cell**

In the cytoplasm, keratin filaments are linked to plasma membrane via two linker proteins desmoplakin (DP) and periplakin (PP). In desmosome, desmogleins (Dsg) bind directly to plakoglobin (PG) and plakophilin (PP), which provide links to the N terminus (N) of desmoplakin (DP)13. DP also binds directly to the juxtamembrane domain of desmocollin-1a (Dsc) and DP C- terminal domain (C) interacts with intermediate filaments (IF).

(Bierkamp et al., 1996), and plakoglobin null keratinocytes exhibit weakened intercellular adhesion (Caldelari et al., 2001; Yin et al., 2005). Likewise, the proper recruitment and distribution of the PG-associated protein DP to desmosomal plaques is required for IF attachment as well as strong intercellular adhesion and epithelial integrity in vitro and in vivo (Huen et al., 2002; Vasioukhin et al., 2001).

Epidermal keratinization is a tightly regulated process that enables epidermal cells to withstand mechanical stress and leads to the formation of cornified cell envelope. Epidermis is the protective layer that acts as a barrier against the environment and water loss. During this process, the keratins expressed are highly specific for the state of differentiation. For example, in the basal layer, as the cells move out of the proliferative compartment, K5 and K14 pair is down-regulated, while the differentiation-specific keratins, K1 and K10 are expressed (Ishida-Yamamoto et al., 1998). These suprabasal keratins account for nearly 85% of the total protein (Fuchs, 1996) of fully differentiated squamous that are sloughed off from the skin surface.

Interestingly, there are also a number of keratins with a restricted tissue distribution. For example, K9 is expressed in the suprabasal cells of palmoplantar skin and K2e is found in keratinocytes of the upper spinous and granular layers of the epidermis (Corden and McLean, 1996). Non-cornifying cells of the stratified mucosa express K4 and K13 and suprabasal cells of the corneal epithelia express K3 and K12. In the normal epidermis, the expression of K6 and K16 is restricted to the outer root sheath of the hair follicle, nail bed, palmoplantar skin and the suprabasal layer of the orogenital mucosa. On the other hand, K17 is expressed in the nail bed, hair follicle, sebaceous glands, and other epidermal appendages (Langbein and Schweizer, 2005).

1.1.3 Structure and organization of keratins

Keratins share common protein structural characteristics (fig. 1.2), comprising an α-helical 'rod' domain of ~ 310 amino acids (with a 50-90% sequence identity among cytokeratins of the same family and around 30% between cytokeratins of different families) constituted with four consecutive domains of highly conserved length (segment 1A accounting for 35, segment 1B for 101, segment 2A for 19 and segment 2B for 121 amino acids). The non-α-helical parts between these segments, also called 'linkers' (L1, L12, L2), are variable in length (8–22 amino acids). The α-helical segments exhibit a heptad substructure in which the first and fourth positions are commonly occupied by apolar amino acids such as Leu, Ile, Met or Val. These hydrophobic amino acids generate a surface that is wound around the axis of a single right-handed α-helix in a left-handed manner, ultimately leading to superhelix, i.e. coiled-coil formation of two such molecules.

The phasing of the heptads is interrupted by deletion or insertion of amino acids in the middle of segment 2B giving rise to a 'stutter' (Steinert et al., 1994) and is conserved in IF proteins.

The stutter represents a helical segment which is not engaged in coiled-coil formation. Moreover, atomic structure analysis showed that the end of segment 2B, representing the evolutionarily conserved IF consensus motif (TYRKLLEGEE), is not entirely part of the coiled-coil structure, but bends away from the coiled-coil axis (Herrmann et al., 2000; Strelkov et al., 2002). The end-domain sequences of type I and II cytokeratin chains contain in both sides of the rod domain the subdomains V1 and V2, which have variable size and sequence. The subdomains V1 and V2 contain residues enriched by glycine/serine, the former providing the cytokeratin chain a strong insoluble character and facilitating the interaction with other molecules. These terminal domains are also important in defining the function of cytokeratin chain characteristic of a particular epithelial cell type.

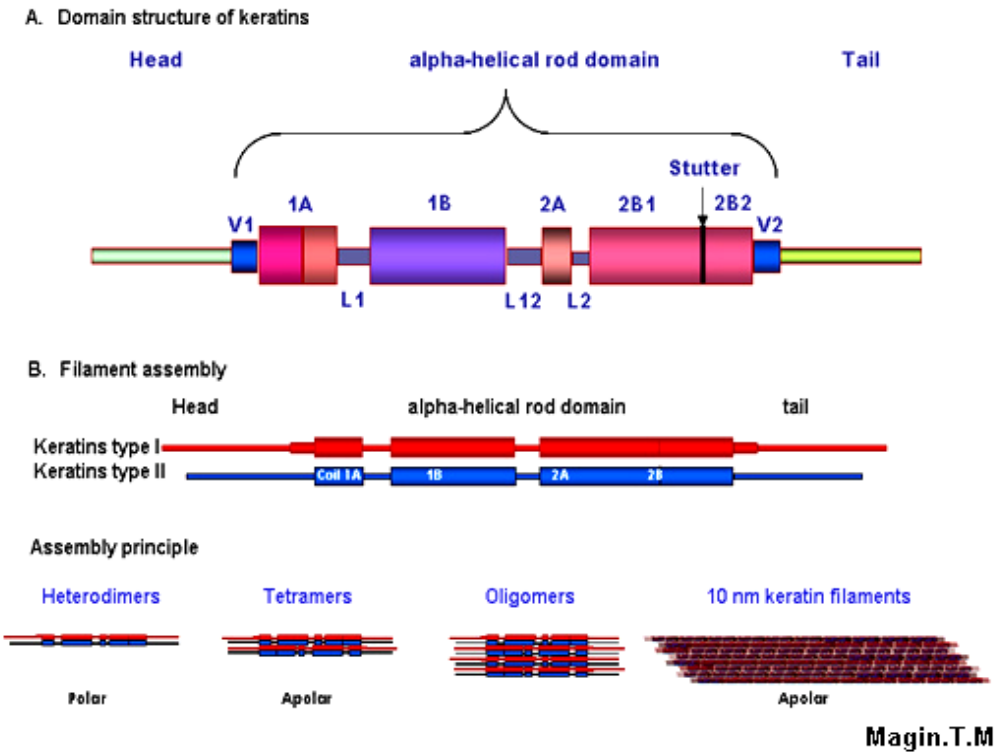

Figure 1.4 (A) The tripartite domain structure of all keratin proteins, with an *a*-helical central rod domain dominated by subsegments (1A, 1B, 2A and 2B) and separated by short linker regions (L1, L12 and L2). The stutter represents a helical segment not engaged in coiledcoil formation. Non-helical head and tail domains at the N and C termini flank the rod domain, respectively. At the beginning and end of the rod domain are the highly conserved helix boundary sequence motives, also known as the helix initiation peptide (HIP) in the 1A domain and the helix termination peptide (HTP) at the end of helix 2B

(B) Type I and type II keratin proteins readily form highly stable coiled-coil dimers (10 nm in length), in which the two participating monomers exhibit a parallel, in-register alignment. Dimers then associate along their lateral surfaces, with an antiparallel orientation, to form apolar oligomers.

Like all intermediate filaments, keratin proteins form filamentous polymers in a series of assembly steps beginning with dimerization; dimers assemble into tetramers and octamers and eventually, the current hypothesis holds, into unit-length-filaments (ULF) capable of annealing end-to-end into long filaments. The process of formation of keratin filament assembly initiates by formation of heterodimers in which compatible type I and type II polypeptide chains align in parallel and in exact axial register (Parry et al., 1985). Two heterodimers associate, forming tetramer units aligned in an antiparallel manner (Geisler et al., 1985) or which may be identical, as in the case of desmin IFs (Sergei et al,). Dimers and/or tetramers polymerize laterally and longitudinally to give rise to higher order structures comprising of equimolar amounts of a type I protein and a type II protein (Steinert, 1990), but no dominant intermediate has been identified or isolated after the tetramer stage.

1.1.4 Known keratin interactions and functions

The variation in expression levels of keratin proteins in different cells (in surface epithelial cells accounting to 30% and about 1% in hepatocytes of their total proteins), and their highly specific patterned expression profile related to the epithelial type and stage of cellular differentiation, might hint towards the diverse role of keratins in cellular machinery.

The characteristic spanning of keratin cytoskeletal network (not so in all cell types, eg. hepatocytes) across cytoplasm weaving the nucleus, and their attachment to cell-cell junctions – desmosomes, itself suggests a major functional role for keratins in regulation and maintenance of integrity and mechanical stability of cells and tissues. Pathogenic mutations have been discovered in different keratin genes (figure 1.5) causing wide range of epithelial fragility disorders affecting skin, mucous membranes, hair, nails, and sebaceous glands (Corden and McLean, 1996; Lane and McLean, 2004; Smith, 2003). The general pathology in these disease conditions corresponds to the expression pattern of the defective keratin protein resulting in structural (eg. EBS - Dowling-Meara) or pigmentation (eg. Dowling–Degos disease) disorders. A brief insight to this is mentioned in the next chapter.

In multilayered epithelia, keratin filaments act as a mechanical scaffold enabling their constituent cells to withstand deformation without breaking (Takahashi et al., 1999; Wilson et al., 1992) This function is crucial in surface epithelia, such as epidermis, oral mucosa, and hair (Wong et al., 2000), and has been demonstrated as well for internal simple epithelia, including liver, trophectoderm and placenta (Hesse et al., 2000; Ku et al., 2001; Magin et al., 1998; Tamai et al., 2000). The reported binding studies between type II keratins and the desmosomal protein desmoplakin (Smith and Fuchs, 1998), perinuclear collapse of keratin IFs around the nucleus in live cells as frequently seen in skin blistering diseases, significantly softens the cytoplasm (Beil et al., 2003), confirms that keratins are organized into a network architecture, which in turn is important for cellular micromechanics (Beil et al., 2003)

Keratins and vesicle transport

The keratinocyte pigmentation disorder Dowling–Degos disease (DDD) (Dowling and Freudenthal, 1938) due to K5 haploinsufficiency, rare skin disorders like EBS with mottled pigmentation (Uttam et al., 1996), and Naegeli–Franceschetti–Jadassohn syndrome are caused by mutations residing in the head domains of K5 and K14 (Betz et al., 2006; Harel et al., 2006; Liao et al., 2007; Lugassy et al., 2006; Uttam et al., 1996). In contrast to most other keratinopathies,

the described haploinsufficiency in K5 (DDD) which results from premature stop codons in the K5 gene, affects melanosome distribution in keratinocytes but not the integrity of the keratin cytoskeleton (Betz et al., 2006; Liao et al., 2007) and is the same in latter mentioned conditions which show an intact keratin organization with disorganized distribution of melanosomes in keratinocytes.

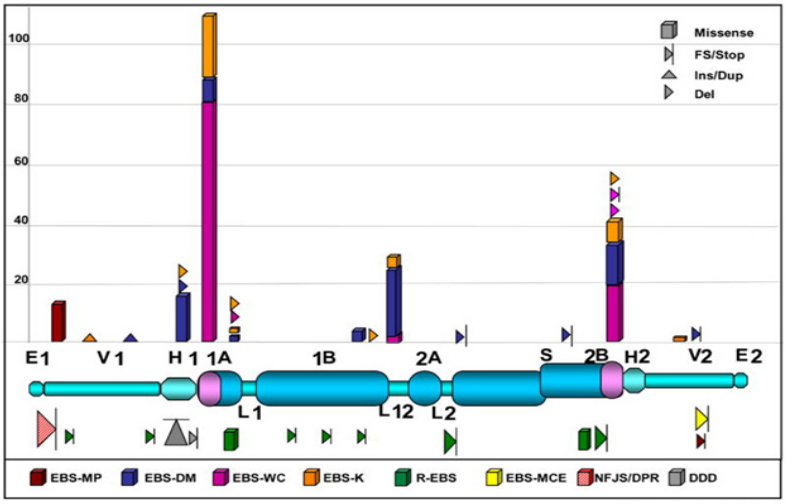

Uitto et al, 2007

Figure 1.5 : Schematic representation of keratin protein depicting the structural domains and common mutation sites in epidermolysis bullosa simplex.

Common sites of dominant mutations and their corresponding EBS phenotypes are depicted above the diagram; the locations of recessive mutations are shown below. The relative height of the bars reflects the relative frequency of the mutations.

Pigmentation of skin depends on melanin synthesis and transport of melanosomes- a lysosome related organelles which form supranuclear caps in keratinocytes. Biogenesis and transport of melanosomes in melanocytes depend on the regulation of actin and myosin motors by the GTPase Rab27a and Rab effectors (Marks and Seabra, 2001). The mechanism of uptake of melanosomes into basal keratinocytes and its distribution, how do the mutations in keratins responsible for pigmentation disorders disturb the physiological cellular process still remains an open question, the reason being, lack of information about the keratin associated proteins which might get affected due to mutations in keratin genes inturn influencing the cellular machinery. Further support for a role of keratins in melanosome transport comes from the analysis of mice with chemically induced mutations in K1, K2e and K4 (Fitch et al., 2003; McGowan et al., 2006; McGowan et al., 2007). The interaction results of the K5 head domain with dynein light and intermediate chains (Betz et al., 2006), report of dynein involvement in the centripetal transport of melanosomes in keratinocytes where they form supranuclear caps (Byers et al., 2003) hints at

the role of keratins in their transport and distribution which holds great promise for the understanding of a general role of IF proteins in vesicle trasnsport.

Role of keratins in wound healing

Re-epithelialization is a pivotal event in wound healing process. It involves the migration and cornification of perilesional basal keratinocytes across wound bed for restoration of an intact epidermal barrier through wound. In the initial process of wound healing the basal keratinocytes express K6 and K16 (Wong and Coulombe, 2003), unlike the normal skin which expresses K5 and K14 pair. More experimental studies have shown that after skin wounding, K6 and K16 are rapidly induced within 6h in human keratinocytes at the wound edge, before migration and regeneration begins (Paladini et al., 1996). In epidermal wounding situation, transcription of the Krt6/16/17 genes is induced and Krt1/10 gene expression is reduced (Zhong et al., 2004), presumably providing the cell with a more pliable cytoskeleton that favours keratinocyte migration for wound closure. K6a knockout mice showed delayed re-epithelialization upon partial thickness skin wounding (Wojcik et al., 2000) and loss of K17 compromised wound healing in mouse embryos (Mazzalupo et al., 2003).

Role of keratins in microtubule localization

It has been shown that intermediate filaments mediate cross-talk among other components of the cytoskeleton (Chang and Goldman, 2004). Centrosomes are known to be located under the apical domain in simple epithelial cells, instead of a perinuclear localization as in other cell types (Apodaca et al., 1994; Meads and Schroer, 1995; Salas, 1999). Several research groups have shown that γ-tubulin–containing structures are attached to intermediate filaments (IFs) (Figueroa et al., 2002) and that this attachment is responsible for the apical distribution of centrosomes in simple epithelial cells (Mulari et al., 2003; Salas, 1999). Similarly, overexpressed keratin accumulates around the centrosome (Blouin et al., 1990), this colocalization can be disrupted by Cdk1/cyclinB mediated phosphorylation in interphasic cells, and is naturally lost in mitotic cells. Keratin knock-downs in tissue culture cells where the apical localization of centrosomes and non-centrosomal γ–TurCs is abrogated (Salas, 1999) and the phenotype of the K8-null mice villus enterocytes (Ameen et al., 2001) coincided to show loss of the apical γ–tubulin layer and disorganization (not depolymerization) of MTs with loss of the apico-basal arrangement. Yet, a full mechanistic explanation for these phenotypes has to be established. An interesting possibility

of interactions between keratin filaments and molecular motors (Betz et al., 2006) (kinesins and cytoplasmic dyneins) which may participate in the organization of the microtubular architecture similar to that of vimentin (Helfand et al., 2004) still remains and has not been demonstrated so far.

Role of keratins in epithelial polarization

K8-null mice show decreased expression of apical proteins in the apical membrane. In some cases, mispolarization or intracellular localization was observed, suggesting that membrane traffic was the cause, rather than transcriptional/translational defects. In general, the effects were observed in epithelia where K7, a type II keratin redundant to K8, was not expressed.
It might also be due to the changes in MT architecture and even, that IFs may serve as scaffolds for extrinsic membrane proteins that, in turn interact with membrane proteins.
An example of this possibility is the phenotype of transgenic mice overexpressing K8 which showed an extensive atrophy of the intestinal brush border. An analysis of the subcellular localization of ezrin showed it bound to the abnormal cytoplasmic IFs while lacking under the apical membrane (Wald et al., 2005). Ezrin is known to connect actin to the PDZ protein EBP50, and to membrane proteins (Bretscher et al., 2002), interactions that aid in the retention of apical membrane proteins such as CFTR (Guggino and Stanton, 2006). More data will be necessary to determine the relevance of these and other possible mechanisms in the function of IFs.

Keratin response in stress conditions

The studies in mice that overexpress Arg89→Cys K18 as well as in K8-null mice demonstrated the importance of an intact IF network in imparting protection to hepatocytes from several stresses (Ku et al., 1999; Zatloukal et al., 2000). Pancreatic acinar cells were far more resilient than their hepatocyte counterparts upon exposure to two established pancreatic injury models (Toivola et al., 2000) suggesting that the same keratins may function differently in the pancreas and liver, or that other stress-related compensatory mechanisms are found in the pancreas. Along with the strong association of simple epithelial keratins with cytoprotection upon exposure to nonmechanical stresses (Ku et al., 1999), the induced expression of keratins upon injury to the liver (Cadrin et al., 2000; Denk et al., 2000) and pancreas suggests that keratins may function as stress proteins similar like heat shock protein (Hsp) family. Recent studies using transgenic mice over expressing K8 G61C mutant (inhibits phosphorylation of K8 at S73 by stress-activated

protein kinases such as p38, JNK and p42) has shown an increased susceptibility to stress-induced liver injury and apoptosis (Ku and Omary, 2006). Consequently, a similar susceptibility to stress was also observed in the S73A mutant wherein the site for phosphorylation is destroyed. Such a role can be envisaged to occur either directly and be affected by scaffolding, chaperone or 'sponge'-type activities absorbing the stress-activated phosphate kinases, thereby reducing their untoward effects and hence protect the cells from injury, or indirectly via the known association of keratins with Hsp family members. During oxidative stress or exposure to other toxins disrupts the keratin-Raf-1 association (Ku et al., 2004) in a phosphorylation-dependent manner, suggesting keratins regulate Raf-1 kinase signaling potential by kinase sequestration, activation, inactivation or compartmentalization.

The results of the spatiotemporal and differential regulation of keratin phosphorylation like Phosphorylation of K20 S13 in mucus-secreting goblet cells, but not in the other K20-expressing enterocytes (Tao et al., 2006), and hyperphosphorylation of K20 during starvation-induced mucin secretion indicates the complex functional properties of specific epithelial cell types.

Loss of maternal TNFα increased the survival of keratin deficient embryos (Caulin et al., 2000; Jaquemar et al., 2003) and keratins have been shown to moderate apoptosis in Fas mediated apoptosis (Ku et al., 2003) pathway either induced by death receptor or cell-intrinsic pathways.

1.1.5 Keratin disorders in humans

Mutations in 19 different keratin genes have so far been identified as the cause of at least 15 different genetic diseases (table 1.1). Most disorders are transmitted in an autosomal dominant mode, although there are some reports of recessive transmission (Corden and McLean, 1996; Irvine and McLean, 1999; Lane and McLean, 2004; Porter and Lane, 2003; Smith, 2003). The phenotypes of keratin disorders usually reflect the expression pattern of the mutated keratins ranging from very severe to relatively mild blistering because of fragile basal layer of epidermal keratinocytes to pigmentation disorders. In general, a mutation in either one of a particular keratin pair leads to the same disorder. However, there are instances in which distinctly different phenotypes result from mutations in the same keratin (table 1.1).

Most pathogenic keratin mutations are dominant mutations caused by missense mutations that alter amino acids at the start of '1A' rod domain and the end of the '2B' rod domain (fig1.2 A) which are called as helix initiation and termination motifs respectively. These helix boundary peptides represent genetic "hot spots" for mutations in almost all hereditary keratin disorders. The most commonly affected amino acid is an arginine residue near the start of helix 1A that is

conserved in all type I keratins (Rugg and Leigh, 2004). Mutations occurring outside the helix boundary regions are frequently associated with milder or unusual phenotypes. Mutations that affect residues in the head and tail domains often result in conditions that are distinct from those caused by mutations in the central region of the keratin molecule suggesting that these regions of the keratin molecules may have different functions to the rod domain.

The precise phenotype of each disease apparently reflects the spatial level of expression of the mutated genes, as well as the types and positions of the mutations and their consequences at mRNA and protein levels.

Disorders of K5 and K14

The first keratin disorder to be identified was epidermolysis bullosa simplex (EBS). EBS is caused by mutations in the genes for keratins 5 (KRT5)/14 (KRT14), describes a heterogeneous group of heritable skin-blistering disorders in which is characterized by rupture of the basal keratinocytes of the epidermis in response to mild physical trauma. Based on severity, distribution, and seasonal variations in blistering, EBS is categorized in three groups.

I. EBS Dowling-Meara (EBS-DM): is the most severe subtype characterized by widespread, herpetiform blistering and intracellular keratin aggregates. Pathogenic defects are due to missense mutations clustering at the highly conserved boundaries of the alpha-helical rod of K5 or K14. In most of the identified mutations, a particular arginine codon within the helix initiation peptide in K14 (R125) is found to be replaced either by cysteine/histidine and in K5 substitution of a highly conserved amino acid isoleucine to threonine (I466T) within this critical region.

II. EBS Kobner (EBS-K): is characterized by milder, generalized blistering of the skin without apparent clustering, often in response to minor trauma and induced by increased ambient temperature. Hands, feet and extremities are most consistently affected. Pathogenic condition arises due to T-to-C transition within exon 7 of the KRT5 gene at the nucleotide level which results in substitution of a leucine by a proline at the amino acid level. In KRT14 a heterozygous mutations at 2B helix domain G1231T creates a premature stop codon and G1237A mutation that produces a conservative amino acid change (alanine to threonine) at position 413 (A413T) have been identified as the cause of EBS-K.

III. EBS Weber-Cockayne (EBS-WC): is the most common, relatively mild, localized subtype of EBS, characterized by blisters or pigmentation disorders that are confined to the hands, feet and areas of friction or trauma. In this relatively form of EBS, pathogenic mutations lie in most cases outside of the helix boundaries, elsewhere in the rod domain of K5 (T-->G point mutation in the

second base position of codon 161) or K14 (in-frame deletion), including the non-helical L12 linker motif or in the amino terminal homologous domain of K5 resulting in amino acid substitutions.

Table 1.1 gives an overview of other types of disorders caused due to the discrepancies in kerartins. The detrimental effects caused by mutations in keratins have various underlying molecular mechanism which still remain elusive. Identification of keratin associated proteins involved in various cellular processes will be a major advantage to this end.

Different available techniques which can be used to identify keratin associated proteins are briefly introduced in the next chapter.

Type II	Type I	Expression pattern	Human disease
K1*	K10*	suprabasal cells of cornified squamous epithelia	Bullous congenital ichthyosiform erythroderma or epidermolytic hyperkeratosis
			Autosomal recessive epidermolytic hyperkeratosis
			Diffuse non-epidermolytic palmoplantar keratoderma*
			Ichthyosis hystrix Curth-Macklin*
			Palmoplantar keratoderma with tonotubules*
K3	K12	Corneal epithelium	Meesmann corneal epithelial dystrophy
K4	K13	suprabasal cells of non-cornified squamous epithelia	White sponge nevus
K5*	K14*	basal cells of stratified epithelia	Epidermolysis bullosa simplex types Weber-Cockayne, Koebner, Dowling-Meara
			Autosomal-recessive Epidermolysis bullosa simplex
			EBS with mottled pigmentation*
			Dowling-Degos disease*
K6a	K16*	suprabasal orogenital mucosa; palmoplantar epidermis; epidermal appendages, epidermal expression induced by trauma/wound healing	Pachyonychia congenita type I
			Focal non-epidermolytic PPK*
K6b	K17*	like K6a/K16	Pachyonychia congenita type II
			Steatocystoma multiplex*
K2 (K2e)		Upper spinous and granular layer of cornified squamous epithelia	Ichthyosis bullosa of Siemens
K9		Suprabasal layers of palmoplantar epidermis	Epidermolytic palmoplantar keratoderma
K8	K18	Simple epithelia	Various liver diseases, inflammatory bowel disease
K31 (Ha1)	K81 (Hb1)*	Hair shaft	Monilethrix*
K33 (Ha3)	K83 (Hb3)*		
K36 (Ha6)	K86 (Hb6)*		

Table 1.1: Expression patterns of keratins and the associated human disorders. The former designation is given in brackets. * indicates diseases for which mutations have been found in only one of a keratin pair

1.2 Protein-protein interactions

Proteins control and mediate many of the biological activities of cells. Although some proteins act as single monomeric units (enzymes that catalyze changes in small-molecule substrates), a significant percentage, if not, the majority of all proteins function in association with partner molecules or as components of large molecular assemblies. Their intrinsic biochemical and/or catalytic activities are, to large extent, regulated/modulated by dynamic, spatially and temporally confined physical (direct) and functional (indirect) protein–protein interactions. Protein–protein interactions (PPIs) are an essential aspect in virtually all biological processes, including the formation of macromolecular structures, cell signaling (Choi et al., 1994), regulation (Kischkel et al., 1995), and metabolic pathways. In addition, PPIs have emerged as important drug targets with small molecules binding to 'hotspots' on the protein contact surfaces (Ryan and Matthews, 2005; Wells and McClendon, 2007). Aberrant protein-protein interactions have the potential to cause or contribute to human disease. The modulation of these interactions by drug-like molecules would offer previously unavailable opportunities to explore the relevance and therapeutic significance of pre-selected protein-protein interactions.

The availability of completed genome sequences of several eukaryotic and prokaryotic species has shifted the focus towards the identification and characterization of all gene products that are expressed in a given organism. In order to cope with the huge amounts of data that have been generated by large-scale sequencing projects, high-throughout methodologies (Auerbach et al., 2002) has to be applied in the process of identifying the interacting partners and their functional significance.

1.2.1 General classification of detection methods

The study of protein-protein interactions can be conceptually divided into three major domains: identification, characterization and manipulation. At present different methods have been developed to study and analyse protein-protein interactions, they can be broadly categorized as :

I. Genetic approaches

1. Two Hybrid Systems
    a) Yeast two hybrid system (Y2H)
    b) Bacterial two-hybrid system (B2H)
    c) Mammalian two-hybrid system (M2H)
    d) Phage display system
    e) Protein fragment complementation assays (PCA)

2. Three-hybrid systems
    a) Kinase three-hybrid system (tri-brid)
    b) Protein three-hybrid system
    c) Peptide ligand and small ligand three-hybrid system
    d) RNA three-hybrid system

II. Biochemical methods

a) Pull down studies using tagged fusion proteins
b) Coimmunoprecipitation
c) Far western blot technique
d) Protein microarrays
e) Matrix assisted laser desorption/ionization-time of flight(MALDI-TOF)

III. Physical methods

a) Protein Affinity Chromatography
b) Affinity Blotting
c) Tandem Affinity Purification (TAP)

IV. Biophysical methods

a) Fluorescence resonance energy transfer (FRET)
b) Bioluminescence resonance energy transfer (BRET)
c) Bimolecular fluorescence complementation (BiFC)
d) Atomic force microscopy (AFM)

Living cells monitor parameters of interest in their environment for any given interaction between the proteins. Each of the above mentioned techniques have been widely used to identify & characterize the interaction partners. As each technique has unique advantages & limitations, appropriate method has to be selected to create nearest internal representations of physiological conditions to implement appropriate adaptive responses to changing conditions depending on the scope and goal of the study to be conducted.

In this present study two of the systems has been successfully used and are briefly introduced in the next section.

1.2.2 Yeast two-hybrid

The yeast two-hybrid system is an in vivo assay that detects binary physical interactions. The interaction between a 'bait' fusion and a 'prey' fusion re-constitutes a functional secondary signal which is used as read-out of the assay (growth at restrictive temperature, formation of

functional transcription factor). Many improvised methods have been established since its first application in 1989 (Fields and Song, 1989). The system is economical, scalable and hence perfectly suited for automated high-throughput approaches (Drewes and Bouwmeester, 2003).

Sos recruitment system (SRS)

This system is based upon generating fusion proteins whose interaction in the yeast cytoplasm activates the Ras-signaling pathway, inducing cell growth. This system enables the study of protein interactions that cannot be assayed by conventional two-hybrid or interaction trap systems. These include proteins that are transcriptional activators or repressors, proteins that require post-translational modification in the cytoplasm, and proteins that are toxic to yeast in conventional two-hybrid systems.

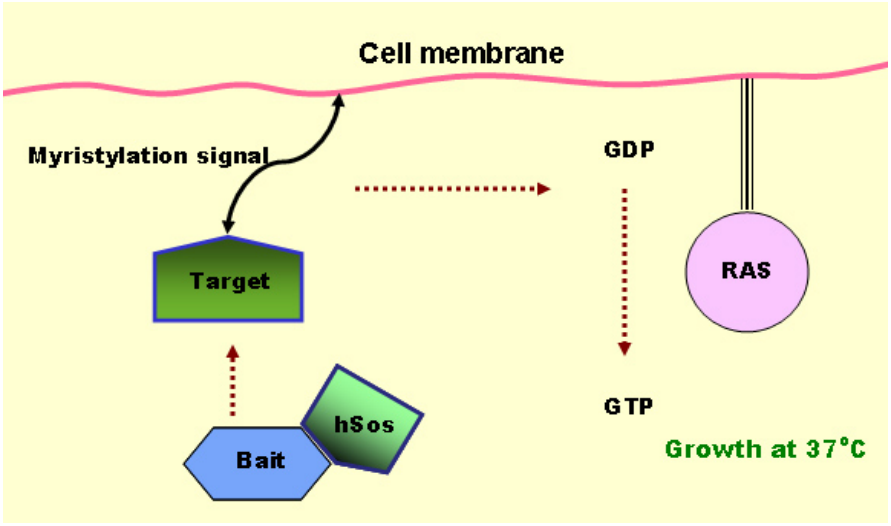

Figure 1.6: Schematic representation of SRS

In this system yeast *S. cerevisiae* temperature-sensitive mutant strain cdc25H, containing a point mutation in CDC25 gene which is the yeast homolog of human Sos(hSos) gene, coding for guanyl nucleotide exchange factor that binds and activates Ras (Aronheim et al., 1994), beginning the Ras signal transduction pathway. The CDC25 mutated gene is complemented with hSos fused with the bait protein and the target protein/expression library is expressed as a fusion protein with a myristylation sequence that anchors the hSos to the plasma membrane. These fusion proteins are coexpressed in the cdc25H yeast strain, and the yeast cells are incubated at the restrictive temperature of 37°C. Physical interaction between bait and target proteins recruit hSos protein to membrane, thereby activating the Ras-signaling pathway and allowing the cdc25H yeast strain to grow at restrictive temperature 37°C.

1.2.3 The Bimolecular Fluorescence Complementation assay

Direct visualization of protein complexes in living cells enables investigation of interactions in their normal environment. Many proteins can be divided into fragments that can associate to produce a functional complex. Direct visualization of protein complexes in living cells enables investigation of interactions in their normal environment. Bimolecular fluorescence complementation (BiFC) analysis is based on the formation of a fluorescent complex by fragments of fluorescent proteins, whose association is facilitated by an interaction between proteins that are fused to the non- fluorescent fragments. BiFC analysis enables visualization of protein interactions in living cells and organisms with minimal perturbation of the normal cellular environment.

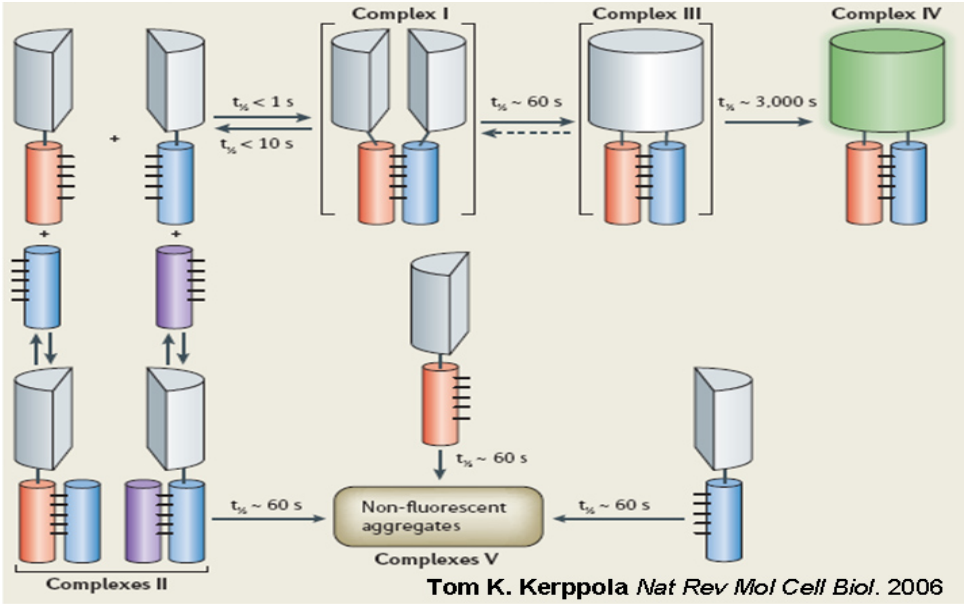

Figure 1.7: Principle and dynamics of bimolecular fluorescence complementation

The most exciting feature of this method is that the complex can be directly visualized in living cells without the need for staining with exogenous molecules that could affect detection of the interaction. This system does not require structural information about the interaction partners, nevertheless, steric constraints can prevent association of the fragments within a complex which can be overcome by using peptide linkers between the fragments and the interaction partners.

In this system interaction occurs in competition with mutually exclusive interactions with alternative interaction partners. A stable intermediate complex is formed on association of two non-fluorescent protein fragments that undergoes slow maturation to produce irreversible mature fluorophore complex, but sometimes in the presence of cellular chaperones might get dissociated. The spectral characteristics of the bimolecular fluorescent complex are comparable

to that of the intact fluorescent protein. The fluorescence intensity produced by BiFC complexes in living cells is generally less than 10% of that produced by expression of an intact fluorescent protein, nevertheless, because autofluorescence is detected in the visible range similar to that of emitted by intact fluorescent proteins with the same excitation (514 nm) and emission maximum of 527nm. Fluorescent-protein fragments that have not associated with complementary fragments undergo irreversible misfolding in vitro thereby reducing any non-specific signals.

2. Aim

'Keratins' – the largest subgroup of intermediate filament proteins, form a complex network of keratin filaments in the cytoplasm of epithelial cells provides stability and integrity thereby protecting the cells from mechanical and non-mechanical stress. The keratin family comprises more than 50 individual members (Hesse et al., 2001; Moll et al., 1982; Schweizer et al., 2006) which are expressed in a tissue type-restricted pattern and differentiation stage. This raises the question on functional importance of the multiplicity of keratin sequences according to their expression profile, and is supported by the recent findings revealing the key role of keratins in regulatory functions of the cellular machinery like organelle transport apart from its well established structural functions. Understanding the molecular mechanism by which keratins exert regulatory functions will help to know about the unidentified contributions of keratins and their extended role beyond scaffolding cytoarchitecture.

To understand the novel functions of keratins, knowledge of keratin-associated proteins is a major pre-requisite. As a first step, this study was designed with the aim of identifying associated proteins of "K5 and K14", followed by the characterization of identified keratin associated proteins.

3. Materials and Methods

3.1 Materials

3.1.1 Chemicals used

Unless otherwise stated, chemicals were purchased from Serva (Heidelberg, Germany), Sigma (Deisenhofen, Germany), Roche (Basel, Switzerland), Fermentas (St.Leon-Rot, Germany), Merck (Darmstadt, Germany), Fluka (Deisenhofen, Germany), Invitrogen Life Technologies (Karlsruhe, Germany), or Applichem (Darmstadt, Germany).
All media base and salts for yeast culture were purchased from Becton, Dickinson and company, Sparks. MD21152
All cell culture solutions, buffers, DNase I, antibiotics & normal goat serum were from Sigma (Deisenhofen, Germany), Invitrogen/Life technologies (Karlsruhe, Germany) & GibcoBRL (Karlsruhe).
In vitro High Prime DNA labeling kit was from purchased from Roche (Basel, Switzerland).
[α-32P]-dCTP was obtained from Amersham Biosciences (Buckinghamshire, UK).
Restriction enzymes, protein and DNA markers dNTPs and NTP's were from Fermentas (St.Leon-Rot,Germany).
PCR reaction mix (Buffers, Taq polymerase enzyme, MgCl2), RT-PCR kit were purchased from Invitrogen/Life technologies (Karlsruhe, Germany).

3.1.2 Ready-to-use solutions / reagents

Acetic Acid
Acrylamide solution (37.5:1) Acrylamide/Bisacrylamide for protein-SDS-gel
Chloroform
DAB substrate (Biogenex, DC138R006)
Dimethylsulfoxide (DMSO)
PBS- (Dulbecco's Phosphate buffered saline) for cell culture
Ethanol
Ethidiumbromide, 10mg/ml
Formaldehyde, 37 %
Isopropanol
Methanol
ProLong® Gold antifade reagent (Molecular Probes, P36930)
Roti-Phenol TE equilibrated for purification of nucleic acids

TEMED for protein-SDS gel

TRIzol for isolation of RNA

Taq-Polymerase (Invitrogen, 10342-020)

Tween-20

Triton-X100

3.1.3 Kits

High Prime DNA labeling system (Roche, 11585584001)

QIAEX II Gel Extraction Kit (Qiagen, 20021)

Nucleospin Plasmid for plasmid DNA miniprep (Macherey-Nagel, 740 588.250)

Nucleobond AX for plasmid DNA midiprep (Macherey-Nagel, 740 410.100)

Superscript II Reverse Transcriptase (Invitrogen, 18064-014)

Protino Ni-IDA for recombinant protein purification (Macherey-Nagel, 745 210.5)

3.1.4 Solutions for DNA analysis

Name	Final Concentration	Constituents and their amounts
Sodium acetate	3 M	40.82 g Sodium acetate in 100ml water. pH was adjusted 5.2 with acetic acid and stored at room temperature.
DNA loading Buffer	30%	Ficoll Type 400
	100 mM	3.72 g EDTA
	0.25%	125 mg Bromphenolblue
	0.25%	125 mg Xylenecyanol
	0.25%	Orange G
	2%	20% SDS
Lysis buffer	100 mM	1 ml of 0.5 M EDTA
	5 mM	1 ml SDS-solution, 20 %
	0.2%	4 ml 5 M NaCl
	200 mM	The above ingredients were added to 84ml of DNase/RNase free water and stored as 10ml aliquots at -20°C
	10 ml of 1 M Tris-HCl	
10 x TBE	0.89 M	54 g Tris-base
	0.89 M	27.5 g Boric acid
	8 mM	20 ml from 0.5 M pH 8 EDTA
		The solution was autoclaved and stored at room temperature.

20x SSC transfer buffer	1.5 M	175.3 g NaCl
	0.5 M	88.2 g Sodium citrate
		pH was adjusted to 7.0 with a few drops of 10N NaOH solution. The volume was adjusted to 1L and sterilized by autoclaving.
DNA denaturation solution	0.4 M	16 g NaOH in 1 L of water. Stored at room temperature.
Hybridization buffer	50%	250 ml Formamid ultrapure.
	5x	125 ml 20x SSC
	5x	5ml 100x Denhardt's solution
	1%	25 ml 20% SDS
	0.1 mg/ml	5ml DNA, MB-grade; from fish sperm 10 mg/ml
	10%	50 g Dextransulfate
		The contents were mixed and the volume was adjusted to 500 ml with sterile water, aliquoted and stored at -20°C
Proteinase K solution	20 mg/ml	1 g Proteinase K (Applichem, A38300025) was added to 50 ml DNAase/RNAse free water, aliquoted and stored at -80°C.
RNase Solution	20 mg/ml	500 mg RNase was dissolved in 25 ml DD water and heated for 15 min at 95°C. Aliquoted and stored at -80°C.
TBE (10 x)	900 mM	109 g Tris-base
	900 mM	55.6 g Boric acid
	25 mM	0.93 g EDTA
		Dissolved in 1L water and pH adjusted to 8.3
TE buffer	10 mM	121 mg Tris
	1 mM	37.2 mg EDTA
		Dissolved in 100 ml DD water, pH adjusted to 8.0 and sterilized by autoclaving. Stored at RT
DNAse solution	1 mg/ml	3 mg DNAse I
	50%	0.5 ml 0.3 M NaCl
	50%	0.5 ml glycerol
		Stored at -20°C.
β-Mercaptoethanol	0.1 M	69 µl of 14.4 M β-mercaptoethanol in 10 ml of DD water. Stored at 4°C.

Pepsin stock solution	10%	1 g of pepsin dissolved in 10 ml of DD water. Stored at –20°C. Pepsin working dilution: 50 µl pepsin stock solution was added to 70ml of DD water containing 700 µl of 1 M HCl.
10x PBS	137 mM 2.7 mM 10 mM 2 mM	40 g NaCl 1 g KCl 89 g Na2HPO4.2H2O 12 g KH2PO4 Salts were dissolved in 4.5 L water, pH was adjusted to 7.4 with HCl,and volume was adjusted to 5 L with water and autoclaved. Stored at RT.
Magnesium chloride	1 M	101.65 g MgCl2 in 500 ml water.
PBS Magnesium Chloride	0.25 M	5 ml 1 M Magnesium chloride 95 ml 1x PBS Prepared fresh

Table No 3.1.1: Solutions for DNA analysis

3.1.5 Solutions for bacterial cultures

Name	Final Concentration	Constituents and their amounts
Ampicillin solution	5%	50 g ampicillin in 50 ml of water. Sterile filtered. End concentration used was 100 mg/ml.
LB Agar	2%	1 L LB Medium 32 g LB Agar in 1 L water Sterilized by autoclaving. Antibiotics were added at 55°C and plates were poured.
LB Medium		25 g LB medium was dissolved in 1 L water and sterilized by autoclaving.

Table No 3.1.2: Solutions for bacterial cultures

3.1.6 Media and reagents for yeast two hybrid screening

Name	Final Concentration	Constituents and their amounts
Synthetic Glucose Minimal Medium [SD/Glucose (–UL)	1.7grams 5 grams 20 grams 17grams	Yeast nitrogen base without aminoacids Ammonium sulfate Dextrose Bacto agar for SD dropout agar plates Adjust the total volume to 900 ml with dH2O Autoclave for 15 minutes at 121°C, cool to 55°C. Add 100 ml of the appropriate filter-sterilized 10× dropout solution
Synthetic Galactose Minimal Medium [SD/Galactose (–UL)] (per Liter)	1.7grams 5 grams 20grams 10grams 17 grams	Yeast nitrogen base without aminoacid Ammonium sulphate Galactose Raffinose Bacto agar for SD dropout agar plates Adjust the total volume to 900 ml with dH_2O. Autoclave for 15 minutes at 121°C, cool to 55°C. Add 100 ml of the appropriate filter-sterilized 10× dropout solution
Cell Lysis Buffer for Protein Isolation	140 mM 2.7 mM 10 mM 1.8 mM 1 % 1 mM 10 µg/ml 1 µM 100 µM 1 µg/ml	NaCl KCl Na2HPO4 KH2PO4 Triton® X-100 containing freshly added **Protease inhibitors:** PMSF aprotinin pepstatin A leupeptin chymostatin
LB– Chloramphenicol Agar (per Liter)	3 ml of 10-mg/ml	Prepare 1 liter of LB agar Autoclave. Cool to 55°C Add -filter-sterilized chloramphenicol Pour into petri dishes (~25 ml/100-mm plate)
1.4 M β-ME (yeast competent cells)		Dilute stock -mercaptoethanol 1:10 with sterile dH_2O just prior to use
NaOH/β-ME Buffer	1.85 M	NaOH

	7.5%	β-Mercaptoethanol
Salmon Sperm DNA	20 mg/ml	Boil 400 µl of sheared salmon sperm DNA for 10 minutes
LiSORB (per Liter)	100 mM	LiOAc
	10 mM	Tris-HCl (pH 8.0)
	1 mM	EDTA
	1 M	sorbitol
		Add dH2O to a volume of 1 liter Verify that the pH is 8.0 Autoclave. Store at room temperature
PEG/LiOAc Solution	10 mM	Tris-HCl (pH 8.0)
	1 mM	EDTA (pH 8.0)
	100 mM	LiOAc (pH 7.5)
	40% (w/v)	PEG 3350. Autoclave
YPAD Agar (30–40 Plates/Liter)	1%	yeast extract
	2%	Bacto peptone
	2%	dextrose
	2%	Bacto agar
	40 mg	adenine sulfate
		Autoclave at 121°C for 20 minutes Pour into petri dishes (~25 ml/100-mm plate) Dry plates at room temperature for 2–3 days Store plates in a sealed bag
SU Buffer	5%	(w/v) SDS
	8 M	Urea
	125 mM	Tris-HCl (pH 6.8)
	0.1 mM	EDTA
	0.005% (w/v)	bromophenol blue
		Store at –20°C Add 15 mg of DTT/ml of SU buffer prior to use.
YPAD Broth	1%	yeast extract
	2%	Bacto peptone
	2%	dextrose
	40 mg	adenine sulfate
		Add deionized H2O to a final volume of 1 liter Autoclave at 121°C for 20 minutes
Yeast Lysis Solution for DNA Isolation	2.5 M	LiCl
	50 mM	Tris-HCl (pH 8.0)

	4%	Triton X-100
	62.5 mM	EDTA

Table No 3.1.3: Solutions for yeast cultures

3.1.7 Solutions for protein biochemistry

Name	Final Concentration	Constituents and their amounts
5x Laemmli sample buffer	50 mM	Sodium phosphate pH 6.8
	5%	SDS
	40 mM	DTT
	5 mM	EDTA
	5 mM	EGTA
	20%	Glycerol
	0.01%	Bromophenol blue
		Solution was stored at -20^{o}C and freeze/thawed not more than 5 times.
APS	10%	1g Ammonium persulphate in 10ml water. Stored at 4^{o}C for not longer than 1 month.
Stacking gel buffer (Upper Tris)	0.5 M	15.1 g Tris-base
	0.4%	1 g SDS
		Volume made up to 250 ml after adjusting pH to 6.8, sterile filtered and stored at 4^{o}C.
Separating gel buffer (Lower Tris)	1.5 M	181.7 g Tris
	0.4%	4 g SDS
		Volume made up to 1 L after adjusting to pH 8.8, sterile filtered and stored at 4^{o}C.
SDS-running buffer (1x Laemmli buffer)	23 mM	2.78 g Tris Base
	190 mM	14.26 g Glycine.
	0.1%	5 ml 20% SDS stock
		The contents were mixed in 1 L water and pH was adjusted to 8.8. Stored at room temperature
Coomassie Staining solutio	0.4%	1.0 g Coomassie Brilliant Blue G-250.
	5 %	25 ml Acetic Acid
	40%	200 ml Methanol
		Volume was adjusted to 500 ml with distilled water, filtered through a Whatmann filter paper and stored at room temperature. Solution was used more than once.

Coomassie destaining solution	10% 30% 50 ml Acetic Acid	150 ml Methanol Solution made up to 500 ml with water.
Ponceau staining solution	0.5% 1%	0.5 g Ponceau S 1 ml Acetic acid Contents were dissolved in 100 ml distilled water and filtered; Solution was stored in dark at room temperature.
Transfer buffer (1x Towbin buffer)	25 mM 192 mM 0.1% 10%	3.028 g Tris. 14.41 g Glycine 1 g SDS 100 ml Methanol The contents were dissolved in 1 L water, and pH was adjusted to 8.3. Solution was stored at room temperature
10x Tris buffered saline (TBS)	0.1 M 1.5 M	12.1 g Tris 87.6 g NaCl Contents were dissolved in 750 ml water, pH was adjusted to 7.5 and the volume was made up to 1 L. Solution was sterilized by autoclaving and stored at room temperature.
Western washing buffer	1x 0.1%	100 ml 10x TBS. 1 ml Tween 20 Volume was made up to 1 L with water
Blocking solution	5% 1x 0.5%	5 g Skimmed milk (Sucofin). 100 ml 10x TBS 1 ml Tween 20 Always prepared fresh
Alternative blocking solution	5% 1x 0.5%	5 g BSA fraction V. 100 ml 10x TBS 1 ml Tween 20 Always prepared fresh
Protease inhibitor	1x	Complete Protease Inhibitor Cocktail Tablets. 7 x stock solution was prepared by dissolving one tablet in 1.5 ml water, aliquoted and stored up to 6 months at -20°C.
Phosphatase inhibitor	1x	Phosphatase Inhibitor Cocktail Tablets. 10 x stock solution was prepared by dissolving one tablet in 1 ml water, aliquoted and stored up to 6 months at -20°C.

Table No 3.1.4: Solutions for protein biochemistry

3.1.8 Bacterial strain

Description	Characteristics and Application
E. coli XL1-blue MRF	Genotype: recA1 endA1 gyrA96 thi-1 hsdR17 supE44 relA1 lac [F´ proAB lacIqZΔM15 Tn10 (Tetr)] ; Amplification of plasmid endA1 hsdR17 (rK12- mK12+) supE44 thi-1 recA1 gyrA96 relA1 lacF' [proA+B+ lacIqZΔM15::Tn10(tetR)]
RosettaBlue(DE3)pLysS	(DE3)pLysSRARE (CmR)

Table No 3.1.5: Bacterial strain genotype

3.1.9 Yeast strain

Host strain	Genotype
cdc25H Yeast Strain (α)	*MATα ura3-52 his3-200 ade2-101 lys2-801 trp1-901leu2-3 112 cdc25-2 Gal+*

Table No 3.1.6: Yeast strain genotype

3.1.10 Primers

Name	Sequence	Product
BN1019 pSos-K5HD –-Fwd	5` ATATGGATCCATGGAGCGCGAGCAGATCAAGACC 3`	Keratin5 head domain
BN1020 pSos -K5HD –Rev	5` ATATGTCGACCTACTCGCCCTCCAGCAGCTTGCG 3`	
BN1021 pSos-K14HD –Fwd	5` ATATGGATCCATGGAATGCAGACTCAGTGGAGAA 3`	Keratin14 head domain
BN1022 pSos-K14HD –Rev	5` ATATGTCGACCTAGAACACATTCTGGAGGTAGTT 3`	
BN1186 pSos-K5RD-Fwd	5’ ATATGGATCCATGGAGCGCGAGCAGATCAAGACC 3’	Keratin5 rod domain
BN1187 pSos-K5RD-Rev	5’ TATGCGGCCGCTCACTCGCCCTCCAGCAGCTT 3’	
BN1188 pSos-K5TD-Fwd	5’ TATGGATCCAGATGGAATGCAGACTCAGTGGA 3’	Keratin5 tail domain
BN1189 pSos-K5TD-Rev	5’ ATATATGCGGCCGCTTAGCTCTTGAAGCTCTT 3’	
BN1190 pSos-	5’ ATATGGATCCAAGGTGACCATGCAGAACCT 3’	Keratin14 rod domain

K14RD-fwd		
BN1191 pSos-K14RD- Rev	5’ ATATATGCGGCCGCTCAGAGGTGGGCGTCCTCGCC 3’	
BN1192 pSos-K14TD- Fwd	5’ ATAAGGATCCCACCTCATGTCCTCCTCCCAGTCC 3’	Keratin14 tail domain
BN1193 pSos-K14TD- Rev	5’ ATATATGCGGCCGCGCCTCAGTTCTTGGTGCGAAG 3’	
BN1090 Rab34HA-tag-C e/s Fwd	5’GCGGCGAGTCGACCCGCAGGCAGGATGAACATTCTG 3’	Rab34
BN1091 Rab 34 HA-tag-C e/s FP WIK Kpn I	5’ ATAATCCGGTACCCAGGCAGGATGAACATTCTG 3’	
BN1115 AP2ß HA-tag-C e/s RP	5’ ATTATATGGTACCGTCATTTCCTGTGTTTCTCCTC 3’	AP2β
hZwi-V1/2-FL/HA	5' ATATGTCGACAGCTTTGTGGTGGTGCCATG 3'	p86DM
hZwi-V1/2-FL/HA rev	5' ATA TCG GTA CCC TCA AAC TGT AGA CTG GTC 3'	
pV1-N Zwi fwd	5' ATATAAAGCTTTGTGGTGGTGCCATGCAGCAAGAA 3'	p86DM
pV1-N Zwi rev	5' ATATCGGTACCACTGTAGACTGGTCTCT 3'	

Table No 3.1.7: List of primers used to prepare constructs

3.1.11 Plasmids

	Expression vector	Description
1	pSos	contains DNA encoding amino acids (aa) 1 to 1067 of the hSos gene and unique 3′ cloning sites. It is used for constructing a bait plasmid containing a DNA insert encoding a bait protein
2	pMyr	contains DNA encoding the myristylation membrane localization signal (Myr) and unique 3′ cloning sites and is used for constructing plasmids or cDNA libraries that contain DNA inserts encoding target proteins
3	pSos MAFB	expresses the Sos protein and full-length MAFB as a hybrid protein
4	pSos Cadherin	expresses fused Sos protein and full-length cadherin
5	pSos Col I	expresses fused Sos protein and amino acids 148–357 of murine 72-kDa type IV collagenase
6	pMyr armadillo	expresses the myristylation signal fused to full length armadillo protein
7	pMyr MAFB	expresses a hybrid protein that contains the myristylation signal fused to full-length MAFB
8	pMyr SB	expresses the myristylation signal fused to a Sos-binding protein
9	pMyr lamin C	expresses the myristylation signal fused to amino acids 67–230 of human lamin C
10	pVen1-Flag-C $_{E/S}$	contains amino terminal half of Venus YFP tagged with FLAG tag
11	pVen2-HA- C $_{E/S}$	contains carboxy terminal half of Venus YFP tagged with HA tag
12	pVen1-N $_{E/S}$	contains amino terminal half of Venus YFP
13	pVen2-N $_{E/S}$	contains carboxy terminal half of Venus YFP
14	pET-SUMO	used for expression of recombinant p86DM

Table No 3.1.8: List of plasmids

3.1.12 Antibodies

Name	Antigen/ Anti-species	Source	Subclass	Dilution/ Application	Source
Anti-GFP	GFP	Mouse	Monoclonal IgG2a	1/500, Immunofluoresence	Abcam
Zwi-3	p86DM	Guinea pig		1/2000, Immuno blotting	In-house
Alexa 594	Mouse	Goat	IgG H+L	1/400, Immunofluoresence	Molecular probes
Alexa 488	Mouse	Goat	IgG H+L	1/400, Immunofluoresence	Molecular probes
HRP	Mouse	Goat		1/30,000, Immuno blotting	Molecular probes
HRP	Guinea pig	Goat		1/30,000, Immuno blotting	Molecular probes

Table No 3.1.9: List of antibodies

3.1.13 General Lab Materials

All sterile cell culture plastic-ware were purchased from Falcon, Sarstedt, Nunc and Becton Dickinson

Pipette Tips and tubes were purchased from Sarstedt

Fuji Medical X-Ray film (Fuji)

High density photopaper (Mitsubishi)

Hybond-N- blotting membrane 30cm x 3m (Amersham, RPN303B)

Microscope slides 76 x 26 mm (Engelbrecht)

Protran Nitrocellulose Hybridization Transfer Membrane, 0.2 µm, 30 cm x 3 m Roll (Schleicher &Schuell)

Sterile filters 0.45 µm, 0.2 µm, 0.1 µm (Schleicher & Schuell)

SuperFrost® Plus microscope slides (Menzel #041300)

Universal agarose

Whatman 3mm-Paper GB 002 (Schleicher & Schuell #426693)

Whatmann filter paper (Schleicher & Schuell)

3.1.14 Equipment and materials used

Instrument / Software	Model / Version	Company
Agarose gel electrophoresis system	B2; B1A	Angewandte Genetechnologie
Blotting Chamber	Fast blot B49	Biometra
Centrifuges	5417R, 5810R, 5417C	Eppendorf
CO2 incubator	CB150; CB210	Binder
Film Developer	Curix 60	Agfa
Fluoresence Microscope	AxioPhot II	Zeiss
Incubators for bacterial / yeast cultures	Function line	Heraeus Instruments
Inverted tissue culture microscope	Telaval 31	Zeiss
Laminar flow system-type	Herasafe	Heraeus Instruments
PCR-Thermocycler	TGradient	Biometra
pH-Meter	761 Calimatic	Knick
Scintillation counter	Beckmann LS-6500	Beckmann
UV-spectrophotometer	Genesys 10UV	Thermoelectron corporation
Water purifier	Milli-Q Plus Nanopure	Barnstead
Electroporator	Gene Pulser II	Biorad

Table No 3.1.10: List of equipments

3.2 Methods

3.2.1 Molecular biological methods

3.2.1.1 Polymerase Chain Reaction

Unless specified differently, PCR reactions were performed in a total volume of 25µl. To avoid nonspecific annealing of the primers and undesired PCR amplification, all the constituents (Table No. 3.2.1) were pipetted on ice and transferred to a cycler *(iCycler, BioRad)* immediately. The PCR was performed along with corresponding positive and negative controls. For multiple PCR reactions, a master mix was made and respective templates were added in appropriate aliquots of master mix.

PCR condition optimization Taq polymerase enzyme

PCR conditions (20 µl PCR master mix)

1.0 ng Template DNA (linearised plasmid)
2.5 µl 10x PCR buffer
0.75 µl $MgCl_2$ (50mM)
1.0 µl dNTP's (5mM)
1.0 µl fwd sense primer
1.0 µl rev anti-sense primer
0.2 µl (IU) Taq polymerase
13.55 µl water

PCR programme :

Step	Temperature	Time	Cycles
Denaturation	95.0°C	5 min	1
		30sec	
Annealing	59.2°C, 60.4°C 61.6°C 62.8°C 64.0°C 65.1°C	30 sec	35
Extension	72.0°C	60 sec per kb	
Final extensior	72.0°C	10 min	1
Storage	4.0°C	∞	1

Table 3.2.1: PCR program for optimization of conditions using Taq polymerase enzyme

PCR amplification using proof reading Taq polymerase enzyme

PCR conditions (20 µl PCR master mix)

10.0 ng (1.0 µl) Template DNA (linearised plasmid)

5.0 µl 5x high fidelity PCR buffer with $MgCl_2$ (50mM)

1.0 µl dNTP's (5mM)

1.0 µl fwd sense primer

1.0 µl rev anti-sense primer

0.25 µl (IU) Taq polymerase

10.75 µl water

PCR programme :

Step	Temperature	Time	Cycles
Denaturation	95.0°C	5 min	1
		30sec	20
Annealing	X°C from optimization reaction	30 sec	
Extension	72.0°C	60 sec per kb	
Final extensior	72.0°C	10 min	1
Storage	4.0°C	∞	1

Table 3.2.2: PCR program for optimization of conditions using proof reading Taq polymerase enzyme

3.2.1.2 Ligation of PCR products

PCR products were ligated with the TOPO® cloning kit (Invitrogen). To avoid auto degradation of adenosine overhangs upon longer storage intervals, freshly prepared PCR products were used. If blunt end producing (3´-5´ exonuclease activity, proof reading activity) polymerase was used, the ligation was carried out using the Zero Blunt® TOPO® PCR cloning kit (Invitrogen). The ligation was done according to the manufacturer's directions.

3.2.1.3 Transformation and culture of E. coli

The ligation product (2 µl) was mixed with 20 µl of competent E. coli (XL1 blue) and incubated on ice for 30 min. The cells were heat shocked at 42°C for 90s and were quickly placed on ice for 2 min. 500 µl LB medium was added and cells were incubated in a bacterial shaker at 37°C for 1 h. The cells were spread on LB-plates with respective antibiotic.

After 14-20 h of incubation at 37°C, colonies were chosen and kept for overnight cultures in 5 ml LB-growth medium with the respective antibiotic.

3.2.1.4 Preparation of plasmid DNA

3.2.1.4.1 Plasmid DNA isolation (mini preparation)

For analytical purposes, 5 ml of overnight bacterial culture was used. The plasmids were isolated using silica columns according to manufacturer's instructions (NucleoBond PC20, Machery-

Nagel).

3.2.1.4.2 Preparative Plasmid DNA isolation (midi/maxi preparations)

For preparative purposes, 50 ml - 100 ml of overnight bacterial culture was used. The plasmids were isolated with silica columns according to manufacturer's instructions (NucleoBond PC100, Machery-Nagel).

3.2.1.5 DNA restriction digestion

Digestions of DNA with restriction endonucleases were performed according to the instructions given by the manufacturer (Fermentas Life sciences).

3.2.1.6 Agarose gel electrophoresis

Agarose gel electrophoresis was used to resolve DNA constructs. Agarose gels were casted in TAE Buffer. 0.5 µg/ml ethidium bromide was added while casting gel. DNA samples were diluted in 10x loading dye before loading on agarose gels. One kb and 100 bp molecular weight ladders (Invitrogen) were used to analyze the molecular size of the DNA. Gels were run at 80-120 V in TAE buffer.

3.2.1.7 Isolation of DNA fragments from agarose gel

Under UV-light desired bands were cut out from the gel using a sterile scalpel. DNA was extracted from the agarose using the Qiagen gel extraction kit.

3.2.1.8 DNA precipitation in ethanol / isopropanol

Ethanol and isopropanol precipitation was used for the purification of DNA and RNA. Ionic concentration of the aqueous DNA and/or RNA solution was increased by addition of 1/10 volume 3 M sodium acetate solution (pH 5.2). About 2.5 times volumes of ethanol/isopropanol were added. The DNA and/or RNA was incubated at -20°C for 30-60 min. Afterwards the sample was centrifuged at 14,000 rpm, the pellet was washed with 70% ethanol and dried for 10 min at 60°C. Then the DNA and/or RNA pellet was dissolved in the desired quantity of Sigma water or TE buffer pH 8.0

3.2.1.9 Concentration determination of nucleic acids

To determine the concentration of DNA or RNA in a solution the optical density (OD) was measured. Nucleic acids have an absorption maximum at 260 nm and proteins absorb UV light maximally at a wavelength of 280 nm. An OD unit corresponds to the amount of nucleic acid in µg in a 1 ml volume using a 1 cm path length quartz cuvette that results in an OD260 reading of 1.

For DNA OD260 1 = 50 mg / ml,

For RNA OD260 1 = 40 mg / ml,

For single stranded oligonucleotides OD260 1 ~ 33 mg / ml

The ratio of readings taken at 260 nm and 280 nm wavelengths indicates of the purity of the nucleic acid.

For pure DNA OD260/OD280 = 1.8

For pure RNA OD260/OD280 = 2.0

3.2.1.10 Sequencing of DNA

The sequencing of plasmids was performed by the Macrogen Incorporations in Seoul (South Korea).

3.2.1.11 Southern blotting

Rod domains of Keratin 5 and 14 were amplified by PCR and obtained 929bps and 932bps amplified product respectively. The PCR products were loaded on a 0.7% agarose gel in 1x TBE- buffer with 0.5 µg/ml ethidiumbromide. The samples were run for about 400- 700 Vh with a maximum of 80 V. Photograph of the gel was taken by exposing to limited UV. Gel was incubated 30- 40 min in 0.4 M NaOH and Hybond N+ and 3 sheets of filter paper were kept. Buffer reservoir with 300- 400 ml 20x SSC - 2x filter papers - Gel – membrane - 2x filter paper - pile of paper cloths - glass plate- about 200 g- weights were used. Transfer was carried out and then the membrane was removed carefully and the gel run was marked with a pencil. Membrane was washed for 15 seconds in 2 x SSC and dried totally on filter paper. DNA present on the membrane was baked at 80°C for 2 h or can be UV cross linked for ~30 sec (0.16kJ/m^2). The membrane was washed with 5X SSPE and then incubated in 25 ml hybridization buffer for 30 min (or longer – maximum overnight) at 42°C. In the meantime probe was prepared. Labeling of the probe was done using dCTP. 25ng of DNA is mixed with 10 µl of buffer and made up to 40µl with water. The sample is kept in boiling water bath for 10 mins and snap cooled in ice. To the snapped chilled sample 3 µl MixC (dNTP without

dCTP), 5µl radioactive labelled dCTP, 1µl Klenow enzyme was added and incubated at 37°C for 5mins.To the above sample 4µl of dNTP was added and incubated at 37°C for 10 mins and the reaction was stopped by the addition of 1µl EDTA (0.5M). The sample is made to 200µl with TE and then to that 400µl of 70% Ethanol, 40 µl NaAcetate, 1µl glycogen. Spun for 15 min 14.000 rpm in room temperature and the supernatant was collected for scintillation counter. The pellet was washed twice with 70% ethanol and dissolved in 50µl Sigma water. 1µl was taken into counter.

Calculation:

counts supernatant + counts probe = counts total (~ 50-60 Mio in 5µl fresh dCTP). Incorporation rate = counts probe / counts total.

Salmon sperm DNA (100 µg/ml hybridization solution) was added to the hybridization tubes containing the labeled probe and incubate 5 min at 95°C before adding probes. Spun briefly for a few seconds and the probe were added to the hybridization tubes (do not add directly on membrane) followed by incubation at 42°C for at least 16 h. After the hybridization, membrane was washed for Wash 20- 30 min at 68°C in the shaking water bath with 300 ml of pre-warmed washing solution. Exposed along with StrataLogos.

3.2.1.12 Isolation of RNA

For the isolation and the analysis of RNA some precautionary measures were followed. For all buffers and solutions sterile milli Q water was used. All used glassware was baked for at least 4 h at 180°C before use. Metallic parts such as spatulas, pincets or the homogenizer were washed thoroughly with RNase off and followed by sterile milli Q water. The RNA was isolated with TRIzol reagent (Invitrogen). 1 mL TRIzol reagent was used per 10 cm^2 cultured dish. The suspension was homogenized in TRIzol reagent with a homogenizator (T8 ultra turrax, IKA) and passed through a 21 G needle at least 10 times. Homogenized samples were left at room temperature for 5 min in 2 ml eppendorf tubes to allow complete dissociation of nucleoprotein complexes. The homogenate was centrifuged at 5,000 rpm at 4°C for 5 min. The supernatant was then mixed with 1/10 volume 1-Bromo-3-chloro-propane by vortexing. The mixture was incubated for 3 min and centrifuged at 4°C at 14,000 rpm. The aqueous phase was carefully transferred into a fresh tube and mixed with an equal volume isopropanol and incubated for 10 min. Afterwards the sample was centrifuged at 4°C at 14,000 rpm. The resulting RNA pellet was washed with 75% ethanol. The pellet was dried in air for 10-15 min and dissolved in milli Q water by incubating 15 min at 55°C. The RNA concentration was estimated by reading O.D. using the Genesys 10uv.

3.2.1.13 Amplification of p86DM by RT-PCR from isolated RNA

For the reverse transcription reaction, 1 µg total RNA isolated from Caco-2 cells was incubated with 20 pmol of oligonucleotide primers at 70°C for 10 min. After a short cooling on ice, 1x first strand buffer, 10mM dithiothreitol, 1 mM dNTP's, 20 U of RNAsin (1U) were added to a total volume of 19 µl with RNase free water, mixed and incubated at 42oC for 2 min. 200 U of Superscript II reverse transcriptase was added to the reaction mix, mixed by pipetting up and down and incubated at 42°C for 50 min. The reaction was stopped by incubating the reaction at 72°C for 15 min. The reaction mix was taken directly for the PCR reaction. PCR was performed in a 25 µl reaction mixture containing 1 µl of template cDNA, as detailed in section 3.2.1.1.

3.2.2 Cell culture methods

Common cell culture methods

All cell lines were cultivated at 37°C in an incubator with 5% CO2 and humid atmosphere. Adherent growing cells were grown in tissue culture dishes on 6 or 10 cm diameter dishes.

3.2.2.1 Passage of mammalian cells

Almost confluent (80-90%) grown cells were passaged into a new culture dish. First the medium was removed and cells were washed with 10 ml PBS. Approximately 2 ml of a trypsin/EDTA solution (Invitrogen) were added and the plate was incubated at 37°C for 3-5 min to dislodge the cells. Trypsinization was inhibited by addition of 5 ml growth medium. Cells were mixed well by pipetting up and down with a 10 ml glass pipette and transferred into a Falcon tube. The cells were pelleted by centrifugation (1,200 rpm, 2 min), resuspended in growth medium and seeded at suitable density.

3.2.2.2 Freezing and storage of cells

A 15 cm confluent culture dish was passaged as above. Cells were resuspended in 5 ml freezing medium with 10% DMSO and transferred with a sterile 1 ml pipette in cryotubes. The cells were stored overnight at –20°C prior to -80°C long term storage.

3.2.2.3 Thawing of cells

Cells were thawed in a 37°C water bath as quickly as possible. In order to minimize the toxic effect of the DMSO, 5 ml fresh growth medium were added and cells were pelleted by centrifugation at 1,200 rpm for 2 min. The cell pellet was resuspended in the appropriate cell

culture medium and seeded depending upon desired cell density in tissue culture dishes and cultivated under standard conditions.

3.2.2.4 Cell counting

The cell number was determined using a Neubauer modified cell chamber. The cell number per ml was calculated by determining the average number of cells in the 4 large squares and multiplying by 10^4.

3.2.2.5 Transient transfection of eukaryotic cells

Cells were grown to 60-80% confluence before transient transfection. Transfection was performed using Lipofectamine reagent (Invitogen) according to the manufacturer's instructions.

3.2.2.6 Immunocytochemistry

Transiently transfected cells were cultured on glass cover slips to 50-80% confluence. Cells were fixed in 4% paraformaldehyde for 10 min followed by permeabilization with 0.1% Triton X-100 for 10 min and blocking with 5% BSA for 1 h. Cells were incubated with desired primary antibody/antibodies, for 2 h in 1% BSA. Primary antibodies were detected by using conjugated secondary antibodies diluted as per the manufacturer's instructions. Coverslips were mounted on glass slides using 15% Mowiol mounting medium. Images were acquired on a fluorescence inverted microscope (Zeiss).

3.2.3 Screening of keratin associated proteins using Sos recruitment system

3.2.3.1 Establishing streaked yeast agar plate

Cells were obtained from the glycerol stock by scraping off splinters of solid ice with a sterile wire loop or sterile inoculating stick. Splinters were streaked on an YPAD agar plate.
The plate was incubated at room temperature (22–25°C) until colonies appeared (~4 days).

3.2.3.2 Preparation of - 80°C yeast glycerol stock

Single colony grown on YPAD agar plate was inoculated in 10ml of YPAD broth and were grown to late log phase ($OD_{600} = 0.8–1.0$) at room temperature (22–25°C). 4.5 ml of a sterile solution of 50% glycerol in liquid YPAD (prepared as 5 ml of glycerol + 5 ml of YPAD broth) was added to the yeast culture from step with continuous mixing. Glycerol-containing cell suspension was aliquoted into sterile centrifuge tubes (1 ml/ tube) and stored at –80°C.

3.2.3.3 Verification of yeast host strain marker phenotype

Yeast from the –80°C glycerol stock was streaked onto each of the four agar "dropout" (tryptophan (Trp), leucine (Leu), histidine (His), and uracil (Ura)) plates and the plates were incubated at room temperature (22–25°C) for 4–6 days. Simultaneously sample of the same glycerol stock was streaked onto a YPAD agar plate and incubated at room temperature (22–25°C) for 4–6 days. After the phenotype has been verified (growth on the YPAD plate and no growth on any of the four SD agar dropout plates), colonies from the YPAD plate were used for the preparation of competent yeast cells.

3.2.3.3 Preparation of cdc25H yeast competent cells

In the preparation of the competent cell, if revertants have arisen, then it is not suitable for two-hybrid screening experiments. Fresh plate of cdc25H (*a*or α,) was prepared from the glycerol stock by scraping off splinters of solid ice with a sterile wire loop and streaked the splinters onto a YPAD agar plate. Plate was incubated at room temperature (22–25°C) until colonies appeared (~4 days). 4–5 cdc25H yeast colonies were picked (from a plate that is less than one week old) into separate 1.5-ml microcentrifuge tubes containing 1 ml YPAD. Cell clumps were completely dispersed by vortexing and yeast cell suspensions were diluted to 50 ml with YPAD followed with incubation for 14–16 hours at room temperature (22–25°C) with shaking at 220–250 rpm till the OD_{600} of the cultures was >1.

Cultures were diluted for a total diluted culture volume of 300 ml (OD_{600}=0.2) and incubated at room temperature (22–25°C) with shaking at 220–250 rpm for 3 hours (OD_{600}>0.7). 75 µl (approximately 1×10^6 cells) of each culture was plated on YPAD agar plate, sealed and incubated at 37°C. The plates were observed daily for 4–6 days, checking for temperature-sensitive revertants. Plates with more than 30 colonies after 6 days of incubation were discarded.

Remaining volume of the yeast cultures was pelleted by centrifugation at 1000×g for 5 minutes at room temperature, yeast cell pellets were resuspended in 50 ml of dH_2O and spun at 1000×*g* for 10 minutes at room temperature. Supernatant was discarded and the pellet was resuspended in 50 ml of LiSORB followed by incubation at room temperature for 30 minutes. At the end of the 30-minutes incubation, yeast cells were pelleted by spinning at 1000 × *g* for 5 minutes at room temperature and resuspend in 300µl of LiSORB. 600 µl of sheared salmon sperm DNA mixture was added to the 300 µl of yeast cells from the previous step. Mixed thoroughly, to each cell preparation 5.4ml of PEG/LiOAc solution and 530 µl of DMSO was added and mixed. Cells were aliquoted in volumes of 500µl and 100µl in separate micro

centrifuge tubes.

3.2.3.4 Transforming yeast and detecting protein-protein interactions

Yeast transformation mixtures were prepared as outlined in Table No: 3.2.3. Plasmid DNA was added in the combinations listed to separate aliquots of freshly prepared cdc25H yeast competent cells. 2 µl of 1.4 M β-mercaptoethanol was added to each tube and mixed the contents thoroughly but gently by inversion or tapping.

Transformation suspensions were incubated at room temperature for 30 minutes with occasional tapping. Cell suspensions were subjected to heat-shock treatment by incubating the transformation suspensions at 42°C for 15 minutes. Placed immediately on ice and left for 3 min. Cells were collected by centrifugation for 30 seconds at 14,000 rpm at room temperature and the supernatant was discarded. Cells were resuspended in 0.5 ml of 1 M sorbitol. Each of the transformation mixture was spread on agar plates using sterile glass beads as indicated in Table No: 3.2.3. For transformation group1, 10 µl and 100 µl of the cells were plated on separate 150 mm SD/glucose (–UL) agar plates and incubated these plates at room temperature (22–25°C). These platings were used to determine cotransformation efficiency. Remainder of transformation reaction 1 was plated on a150-mm SD/glucose (–UL) agar plate and Incubated at 37°C, this plate was observed daily for 4–6 days to check for temperature-sensitive revertants.

After incubation of this plate 37°C for 4–6 days, observed for any growth of colonies (no colonies should appear. Colonies present on this plate indicate that the cells used for the transformation contained temperature-sensitive revertants or were not cdc25H).

Transformation efficiency for the competent cell preparation was evaluated if the reversion control plates met the above criteria. Number of colonies on plates from transformation group1 (Table No: 3.2.3) incubated at room temperature (22–25°C) were counted. Cotransformation efficiency was calculated using the following equation (The transformation efficiency should be at least 0.5×10^3–1×10^4 cfu/µg).

$$\frac{\text{Number of cfu} \times \text{Total suspension volume (500 µl)}}{\text{Volume of transformation plated (µl)} \times \text{Amount of DNA used (2µg)}} = \text{cfu/µg DNA (Transformation efficiency)}$$

For transformations 2–12, the entire transformation reaction mixture was plated on a 100-mm SD/glucose plate (either SD/glucose (–U), SD/glucose (–L) or SD/glucose (–UL) according to Table No: 3.2.3). Incubated at room temperature (22–25°C) until colonies were seen (4–6 days). Three colonies from each of these transformations (5–8, and 10-12) were selected for transfer to SD/glucose (–UL) and SD/galactose (–UL) to test for protein-protein interactions that allow

Number	Plasmid(s)	Amount of Plasmid	Volume of Yeast Competent Cells	Medium for Plating
1	pSos + pMyr	2 µg each	500 µl	SD/glucose (–UL)
2	pSos MAFB	100 ng	100 µl	SD/glucose (–L)
3	pMyr SB	100 ng	100 µl	SD/glucose (–U)
4	pMyr Lamin C	100 ng	100 µl	SD/glucose (–U)
5	pSos MAFB + pMyr MAFB	300 ng each	100 µl	SD/glucose (–UL)
6	pSos MAFB + pMyr Lamin C	300 ng each	100 µl	SD/glucose (–UL)
7	pSos Col I + pMyr MAFB	300 ng each	100 µl	SD/glucose (–UL)
8	pSos MAFB + pMyr SB	300 ng each	100 µl	SD/glucose (–UL)
9	pSos Bait	100 ng	100 µl	SD/glucose (–L)
10	pSos Bait + pMyr Lamin C	300 ng each	100 µl	SD/glucose (–UL)
11	pSos Bait + pMyr SB	300 ng each	100 µl	SD/glucose (–UL)
12		300 ng each	100 µl	SD/glucose (–L)

Table 3.2.3: Transforming yeast and detecting protein-protein interactions

growth at 37°C. Each picked colony was resuspended in 25 µl of sterile H_2O and transferred to separate wells of sterile 96-well plate. 2.5µl of the yeast/ H_2O suspensions was spotted onto each of two SD/galactose (–UL) agar plates and two SD/glucose (–UL) agar plates. One plate of each type was incubated at 37°C. The second plate of each type was kept at room temperature (22–25°C) for 5 days. Growth in SD/galactose (–UL) agar plates that are incubated at 37°C was scored after 7–10 days incubation.

3.2.3.5 Library screening

40µg of pSos bait construct, 40µg of pMyr cDNA plasmid library and 200 µl of 1.4M β-

mercaptoethanol was added to 10ml of freshly prepared cdc25H (α) yeast competent cells. The contents were mixed thoroughly and the contents were transferred into 20 separate microcentrifuge tubes. Cotransformation was done as mentioned in the previous section. Cells were resuspended in 0.5 ml of 1 M sorbitol. The entire transformation reaction in each tube was plated on a 150-mm SD/glucose (–UL) agar plate. Plates were incubated at room temperature (22–25°C) for 2-4 days. The transformants were replica plated onto SD/galactose (–UL) agar plates and the plates were incubated at 37°C.

After 6 days, colonies (interactor candidates) from the experimental library screen transformation replicates were picked on galactose incubated at 37°C. In order to repress *GAL1* promoter-driven expression from the pMyr library prior to interaction tests, cells from the interactor candidate colonies were patched onto an SD/glucose (–UL) agar plate (candidate patch plate), and the plate incubated at 22–25°C for 48 hours. The original galactose transformation replica plates were returned to 37°C after picking colonies, since some additional colonies appeared much later (10 days).

After 48 hrs incubation, cells from the SD/glucose (–UL) candidate patch plates were patched onto two fresh SD/glucose (–UL) plates and one SD/galactose (–UL) plate. As a primary test to identify interactors among the candidates, one SD/glucose (–UL) and the SD/galactose (–UL) plate was incubated at 37°C for approximately 48 hours. The other SD/glucose (–UL) agar plate was kept at room temperature (22–25°C) as a re-patching source plate.

After the 48 hour incubation, the primary interaction test plates (see step 16) were evaluated, identifying the patches growing at 37°C on SD/galactose (–UL) plates, but not on SD/glucose (–UL) plates. A secondary interaction test was performed by re-patching the interactor candidates from the re-patching source plate kept at 22–25°C onto another set of one SD/glucose (–UL) and one SD/galactose (–UL) agar plate, and both plates were incubated at 37°C for 48 hours. The candidates producing patches that grow on SD/galactose (–UL) plates but not on SD/glucose (–UL) plates at 37°C in both the primary and secondary interaction tests should be considered "putative positive" clones and analysed further.

3.2.3.6 Verification of interaction by yeast co transformation

Putative positive colonies were grown in SD/glucose (–UL) media, cDNA library inserted plasmid 'pMyr' was isolated from this yeast culture by lysing yeast cells followed by phenol/chloroform extraction. Top aqueous phase containing the DNA was transferred to a new microcentrifuge tube and DNA was precipitated with 100% (v/v) ice-cold ethanol at –20°C overnight or at –80°C for 15 minutes. Suspension was spun at 14,000 × *g* for 10 minutes at 4°C.

DNA pellet was washed with 70% (v/v) ethanol and centrifuged at 14,000 × *g* for 5 minutes at room temperature and the pellet was air dried, resuspended in 40 µl of dH_2O.

DNA was precipitated with 3M NaOAc (pH 5.2) and ethanol. The above mentioned washing steps were repeated twice. DNA pellet was resuspended in 20 µl of dH_2O followed by retransformation in high-efficiency electroporation-competent *E. coli* cells. Transformed colonies were selected for pMyr cDNA plasmid by plating on LB-chloramphenicol agar plates. Colonies that contain the pMyr cDNA plasmid were identified by preparing miniprep. Isolated plasmid DNA was subjected to restriction digest analysis and the cDNA insert was identified by sequencing.

3.2.4 Expression, purification and analysis of recombinant p86DM

3.2.4.1 Expression His SUMO fused-p86DM protein

p86DM was cloned into pET-SUMO expression vector and retransformed (as mentioned in previous section) in Rosetta competent cells. Transformed cell suspension was spread on LB agar plate and incubated at 37°C for 12-16h. Positive clone was picked and inoculated in LB broth followed with incubation at 37°C until the absorbance showed 0.5 at OD600. Grown culture was shifted to 27°C, expression of fusion protein was induced by adding 1mM IPTG at 27°C for 210 min. The cells were pelleted by centrifugation at 3,000 g at 4°C for 10 min, supernatant was discarded. Cell pellet were resuspended in 3 ml ice-cold PBS buffer per 50 ml culture and centrifuged at 3,000 g at 4°C for 10 min and the pellets were frozen at -80°C for 1 hr. The cells were thawed on ice and re-suspend cells in 3 ml of ice-cold PBS buffer per 50 ml culture. Cells were broken by brief pulses of sonication on ice until the sample was no longer viscous. 10 µl aliquots sample from both soluble and insoluble fractions for SDS-PAGE analysis were taken (by adding equal volume of 5X SDS sample loading buffer, boil for 5 min and run SDS-PAGE to determine the amount and solubility of the fusion protein).

3.2.4.2 Purification of recombinant His SUMO fused-p86DM protein

An appropriate amount of High-Affinity His resin (50% slurry) was transferred to a disposable column using a pipette. (Usually 1 ml of resin can bind more than 6 mg of His protein). The resin was equilibrated with 10 bed volumes of cold lysis buffer. Clear solution (supernatant of the cells lysed by sonication) containing fusion protein was applied to the pre equilibrated column and with the flow rate at 5 ml/min. Column was washed with 20 bed volumes of washing buffer containing protease inhibitors. The fusion protein was eluted with 10-15 bed volumes of freshly

made elution buffer containing 250mM imidazole. 10-20 µl aliquots of flow through, wash and the eluted protein were analyzed by running SDS-PAGE to confirm the presence of the target protein. The eluted fractions were pooled and dialysed against TBS at 4°C to remove imidazole.

3.2.4.3 SDS –Polyacrylamide gel electrophoresis (SDS-PAGE)

Protein lysates were separated on a SDS-polyacrylamide gel prepared according to the compositions mentioned in table 3.1.

Preparation of stacking gel (for 2 /10 gels 10/50 ml)

Ingredients	Maxi gels		Mini gels	
	Stacking	Separating	Stacking	Separating
30% Acrylamide	1.6 ml (4%)	22.2 ml	440 µl	3.3 ml
Lower Tris	---	16.7 ml	---	2.5 ml
Upper Tris	3 ml	---	1.0 µl	---
Water	7.4 ml	27.8 ml	2.6 ml	4.2 ml
Temed	20 µl	67 µl	6 µl	10 µl
10 % APS	100 µl	70 µl	40 µl	100 µl

Table 3.2.4: Composition of SDS polyacrylamide gels

The protein samples were denatured at 98°C for 5 min, centrifuged briefly and allowed to cool to room temperature. Depending on the molecular weight of the protein analysed, the samples were loaded onto SDS-PAGE of 8% or 10% gels, in an apparatus containing running buffer in both chambers. A constant voltage of 40 V was applied per gel until the loading dye (bromophenol blue) entered the separating gel. Then the voltage was increased to 80 V until the dye reached the bottom of the gel. The proteins were then blotted onto PVDF membranes.

3.2.4.4 Western Blotting

PVDF membrane was activated in methanol for 1 min and then equilibrated for 10 min in 1x Towbin buffer. The SDS-polyacrylamide gel was dismantled from the electrophoresis equipment and the stacking gel was excised. The separating gel was equilibrated in 1x Towbin buffer for 10 min and set up for semi-dry blotting as per manufacturers' directions. Protein transfer was achieved at a constant current of 1.0 mA/cm^2 of membrane. After blotting, the membrane was stained with Coomaasie G250 stain and destained with destaining solution. The marker was re-marked using a pencil and the membrane was scanned for future reference.

For Western blotting, the membrane was washed with TBST buffer. Non specific binding sites were blocked by incubating the membrane with either 5% skimmed milk powder or 5% BSA in

TBS containing 0.1% tween-20 (TBS-T) for 1h. After blocking, the membrane was incubated with primary antibody diluted in blocking solution for 1 hour at RT or o/n at 4°C and washed thrice with TBS-T for 5 min each at RT, to remove any unbound antibodies. The membrane was then incubated with corresponding secondary antibody, diluted in blocking solution for 1 hour at RT and washed thrice with TBS-T for 5 min each at RT. A final wash was carried out with 1x TBS, pH 7.5. Bound antibodies were visualised with ECL system (Amersham Pharmacia) according to the manufacturer's protocol or with indigenous ECL system.

4. Results

4.1 Screening of keratin associated proteins by yeast two hybrid system

4.1.1 Target cDNA library construction

In order to construct a cDNA library to identify the K5 and K14 associated proteins, total RNA was isolated from human skin sample (kindly provided by Prof. Bruckner-Tuderman, Freiburg) and 500,000 cDNA fragments were prepared using random primers. The average size of the fragments measured 1.2 kb ranging from the smallest fragment 500 bp to 4 kb, which were subsequently inserted into pMyr expression vector as Myr-target fusions.
Multiple cloning site of the pMyr expression vector was modified by inserting SalI and NotI restriction sites at 5` and 3´ ends respectively, to facilitate the insertion of the cDNA fragments.

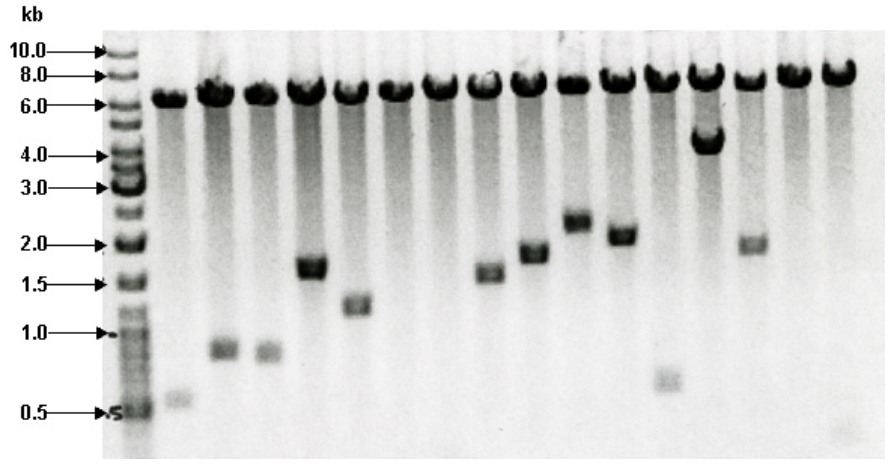

Figure 4.1: Size range from 500bp – 4kb of inserted cDNA fragments in the target cDNA library

cDNA fragments from purified total RNA were inserted into the modified pMyr by RZPD GmbH. Berlin. This cDNA library was used in the screening experiments for identifying K5 and K14 associated proteins.

4.1.2 Bait plasmid construction

Head, rod and tail domains of K5 and K14 were used as baits to identify their interacting partners using Sos recruitment method.
DNA encoding the head, rod and tail domains of K5 and K14 protein were prepared from the full length cDNA by PCR amplification using specific primers. PCR amplified product was cloned into the cloning vector, plasmid DNA was isolated by miniprep, specificity of the PCR amplified product was confirmed by sequencing. DNA coding for the respective domain was obtained by

digesting the cloning vector containing desired insert with the restriction enzymes, purified by gel extraction and ligated into the pSos expression plasmid as gene fusion with hSos protein.

	Bait domain	Insert length	Insertion sites		Position in pSos expression vector
			5′	3′	
1	Keratin5 head (K5Hd)	510 bp	BamHI	SalI	3223 - 3733
2	Keratin5 rod (K5Rd)	929 bp	BamHI	NotI	3223 - 4512
3	Keratin5 tail (K5Td)	343 bp	BamHI	NotI	3223 - 3566
4	Keratin14 head (K14Hd)	363 bp	BamHI	SalI	3223 - 3586
5	Keratin14 rod (K14Rd)	932 bp	BamHI	NotI	3223 - 4155
6	Keratin14 tail (K14Td)	149 bp	BamHI	NotI	3223 - 3372

Table 4.1: Cloning details of the bait inserts as fusion with hSos gene in pSos expression vector.

The pSos vector contains DNA encoding amino acids (aa) 1 to 1067 of the hSos gene and unique 3′ cloning sites with ADH1 promoter for the expression of the hSos-bait insert fusion.
It contains the pUC and 2μ origins for replication in E. coli and yeast, respectively. The pSos also carry yeast biosynthetic genes LEU2 for selection of yeast transformants based on nutritional requirements. The pSos vector contains the ampicillin-resistance gene which enables for the selection while recovering plasmids from E. coli. Details of the cloned bait plasmids is listed in the above table No.4.1

4.1.3 Verification of yeast host strain marker phenotype

In the present study yeast strain cdc25H (α), genotype: 'MATα ura3-52 his3-200 ade2-101 lys2-801 trp1-901 leu2-3 112 cdc25-2 Gal+' was used. The phenotype of the yeast host strain was verified prior to competent cell preparation for the subsequent experiments. Cells were obtained from the glycerol stock and were grown at 24°C on SD agar plates lacking the nutrients tryptophan (Trp), leucine (Leu), histidine (His), and uracil (Ura). The plates were incubated for 6

days at 24°C. Simultaneously another culture from the same stock was inoculated on YPAD agar plate and incubated at 24°C or 6 days.

Growth media	Growth
SD agar(-Trp)	–
SD agar(-Leu)	–
SD agar(-His)	–
SD agar(-Ura)	–
YPAD agar	+

Table 4.2: Verification of yeast host strain marker phenotype by testing for growth using dropout media.

Growth on YPAD agar plate and absence of growth on any of the four SD agar dropout plates as indicated in the table confirmed the phenotype of the yeast strain.
The yeast colonies from the YPAD agar plates were used for preparing the competent cells.

4.1.4 Confirmation for absence of temperature revertants

The screening procedure is based on the selection of temperature sensitive growth of the yeast colonies for the detection of positive keratin interacting partners. So it is of utmost importance to check for the absence of temperature revertants in the prepared competent cells to avoid false positives in the process of screening for keratin associated proteins.
Competent cells of cdc25H(α) were prepared from the phenotype verified yeast colonies, and cotransformed with the set of negative control plasmids pSos MAFB and pMyr Lamin C as described in methods. The cotransformed cells were plated on SD/glucose (–UL) dropout agar plate and incubated at 37°C for 6 days.
The incubated plate was observed daily for 6 days. No colonies were observed till 6^{th} day of incubation at 37°C. This confirms that there were no temperature revertant CFUs present in the stock of yeast competent cells used for detection of keratin interacting partners.

4.1.5 Control plasmids

For validation of screening process, different sets of control plasmids have been used. These were cotransformed as control groups along with test groups which were used for the identification of positively interacting candidates.

The different combinations of control plasmids mentioned in section 3 were cotransformed in competent cells of cdc25H(α). Cotransformation was done in duplicate sets, first set of transformed mixture was spread on SD-glucose(-U,L) agar plates and incubated at 24°C for 4-6 days till the colonies were visible. The other set of transformed mixture was spread on agar plates containing SD-galactose(-U,L) and the plates were incubated at restrictive temperature 37°C for 6 days and observed daily for growth. The growth profile of the transformed colonies is tabulated below in table No: 4.3

Combination of control plasmids cotransformed		SD (–UL)/24°C		SD (–UL)/37°C	
Sos fusion	**Myr fusion**	**Glucose**	**Galactose**	**Glucose**	**Galactose**
MAFB	MAFB	+	+	–	+
Cadherin	Armadillo	+	+	–	+
MAFB	SB	+	+	–	+
MAFB	Lamin C	+	+	–	–
Col I	MAFB	+	+	–	–

Table 4.3: Growth profile of the cdc25H(α) yeast cells cotransformed with control plasmids.

Growth was observed in both sets of transformation which were spread on the agar plates containing SD-glucose(-U,L)/SD-galactose(-U,L), incubated at 24°C. Agar plates with SD-galactose(-U,L) containing yeast cells cotransformed with positive control plasmids were able to grow when incubated at restrictive temperature 37°C, where as the plates containing yeast cotransformed with negative control plasmids failed to grow at restrictive temperature.

These results validate the system to be used for the screening studies of keratin associated proteins.

4.1.6 Verification of bait plasmid suitability for screening assays

The constructed bait plasmids (pSos-bait) were verified for their compatibility with the system in order to avoid false positives arising from them.

4.1.6.1 Verification for auto-activation

The fusion of bait sometimes results in self-activation of the signal recruitment system. Therefore, it is essential to test each bait for its inability to confer growth of cdc25H at the restrictive temperature. Prior to initiating the yeast two-hybrid screen using the constructed pSos bait plasmids, it was verified that the pSos-bait fusion does not interact with the myristylation signal in the absence of an interaction partner. The individual pSos bait plasmids (containing the genes of head, rod and tail domains of K5 and K14) were cotransformed into the yeast host with either pMyr empty vector or pMyr Lamin C to establish that the bait protein does not interact with the myristylation signal provided by the negative control plasmids. Co-transformation was performed according to the protocols outlined in Methods. After cotransformation, the plates containing glucose were initially incubated at room temperature (24°C) to allow colony formation. Colonies which were grown on these plates were patched onto fresh plates containing galactose, and assayed for growth at 37°C.

If the bait plasmid cotransformed with the pMyr empty vector or pMyr Lamin C can induce cdc25H yeast growth at 37°C, then the bait plasmid is unsuitable for detecting protein-protein interactions in the CytoTrap system. Induction of growth of the yeast host at 37°C by the bait plasmid may also occur if the bait protein contains sequences that target them to the membrane.

In the figure: 4.2/4.3 a, b and c, absence of growth of yeast colonies at 37°C cotransformed with the above mentioned pSos bait constructs and pMyr Lamin C indicates that there is no auto activation as bait proteins do not interact with the myristylation signal from the negative control plasmid and hence are suitable for the screening experiments.

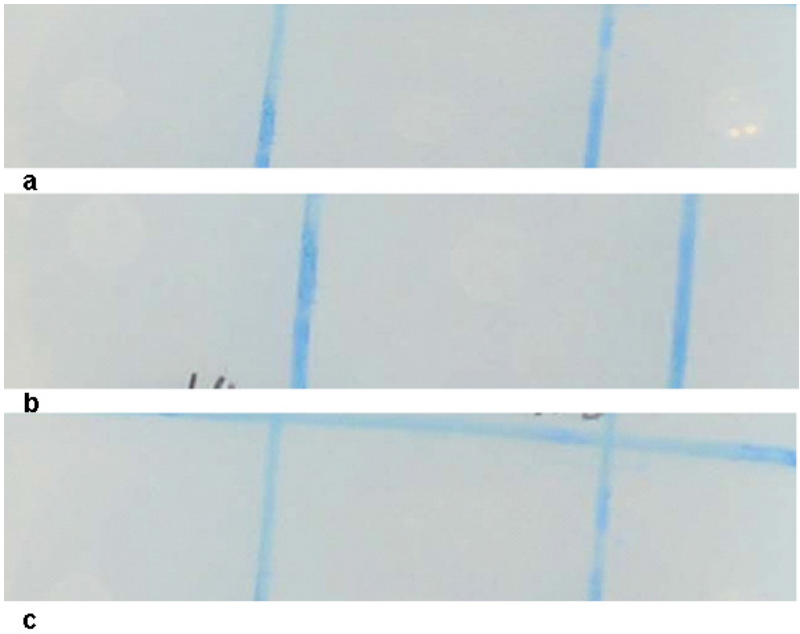

Figure 4.2: No growth confirms suitability of the K5 bait constructs for two hybrid screening

a) pSos-K5Hd, b) pSos-K5Rd, c) pSos-K5Td, and pMyr Lamin C were cotransformed in cdc25 H yeast strain, plates containing glucose (-Leu/-Ura) were initially incubated at room temperature (24°C) for 4 days to allow colony formation. Three individual colonies grown at permissive temperature were selected and spotted onto fresh plates containing galactose(-Leu/-Ura), and assayed for growth at restrictive temperature (37°C) for 6 days to check if the bait plasmid cotransformed with the pMyr Lamin C can induce cdc25H yeast growth at 37°C.

Bait plasmids constructed using PCR amplified product of head, rod and tail domain encoding DNA of K5 was inserted in pSos vector, expressing as fusion protein with Sos protein. 300ng of each of the bait plasmid along with 300ng of pMyr Lamin C were cotransformed in 100µl of competent cdc25H(α) cells previously tested for absence of temperature revertion. Growth was observed after 4 days of incubation at permissive temperature on agar plates containing SD-glucose(-U,L). Three of the grown colonies were picked randomly, resuspended in 20µl of sigma water and spotted on agar plates containing SD-galactose(-U,L). Plates were inverted and incubated at restrictive temperature and were observed daily for 6 days.

No growth was observed till 6 days of incubation at 37°C indicating that, the bait plasmids constructed with different domains of K5 do not possess self-activation property and are suitable for the screening assay.

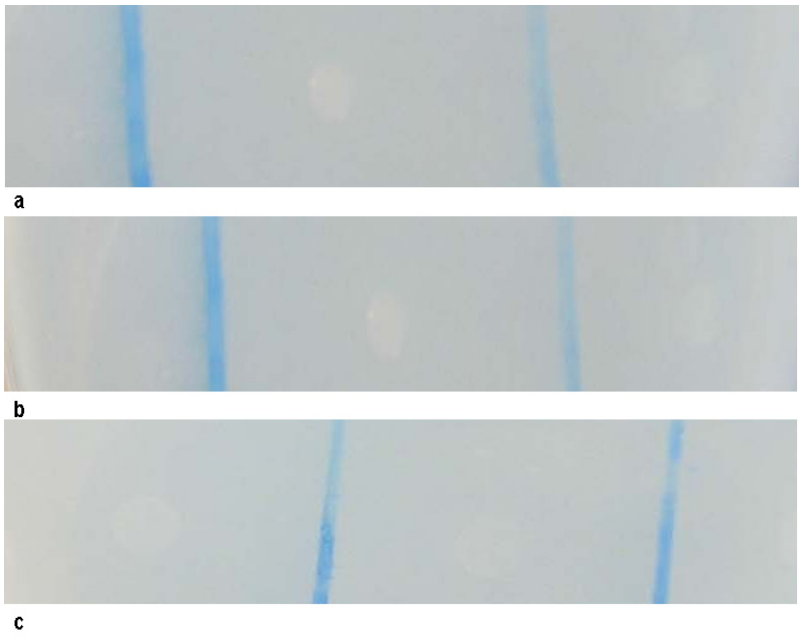

Figure 4.3: No growth confirms the suitability of K14 bait constructs for two hybrid screening

a) pSos-K14Hd, b) pSos-K14Rd, c) pSos-K14Td, and pMyr Lamin C were cotransformed in cdc25 H yeast strain, plates containing glucose (-Leu/-Ura) were initially incubated at room temperature (24°C) for 4 days to allow colony formation. Three individual colonies grown at permissive temperature were selected and spotted onto fresh plates containing galactose(-Leu/-Ura), and assayed for growth at restrictive temperature (37°C) for 6

days to check if the bait plasmid cotransformed with the pMyr Lamin C can induce cdc25H yeast growth at 37°C.

Bait plasmids constructed comprising head, rod and tail domains of K14 were cotransformed along with pMyr Lamin C (300ng each) in 100µl of competent cdc25H(α) cells previously tested for absence of temperature revertion. Absence of growth on SD- galactose(-U,L) plates incubated at 37°C was evaluated similar to that of previous results of K5 domain expressing bait constructs. Absence of growth indicated that, the bait plasmids constructed with different domains of K14 do not possess self-activation property and are suitable for the screening assay.

4.1.6.2 Verifying bait insert cloning and expression

The nucleotide sequence of the cloning junctions between pSos and DNA insert encoding for bait protein was determined by sequencing the column purified plasmid DNA. Which in turn also confirmed that the bait protein will be expressed in frame with the Sos domain and the DNA insert does not contain mutations.

Expression of the bait protein can be verified by either

a) Western blot analysis using an antibody that immunoreacts either with the protein expressed from the DNA insert or with the hSos protein
b) The cytoplasmic localization of the bait protein can be verified by cotransformation of pMyr SB and the pSos bait plasmid followed by patching on galactose containing medium and assaying for growth at 37°C.

In the present set of studies verification of expression of the DNA encoding bait proteins as fusion protein along with Sos protein was confirmed by the genetic interaction of the expressed Sos protein with the SB protein, which is expressed from pMyr SB to rescue the growth at restrictive temperature 37°C that confirms the integrity and cytoplasmic localization of the pSos vector.

Expression and cytoplasmic localization of K5 and K14 domains in frame with Sos protein

The cytoplasmic localization of the head, rod and tail domains of K5 bait protein was verified by cotransforming the pSos-K5 bait constructs with pMyr SB followed by patching on galactose containing dropout medium and assayed for growth at 37°C.

Ability of the cotransformed colonies (figure 4.4) confirms that bait proteins pSos-K5Hd, pSos-K5Rd and pSos-K5Td are intact and their cytoplasmic localization.

Expression and cytoplasmic localization of K14 bait constructs pSos-K14Hd, pSos-K14Rd and pSos-K14Td was also confirmed in the similar set of experiments.

Ability for the growth of cotransformed yeast cells with pSos-K14bait and pMyr SB at restrictive temperature 37°C on galactose containing dropout media (figure 4.5) confirms the integrity and cytoplasmic localization of K14 bait fusion proteins.

Expression and cytoplasmic localization of K5 head, rod and tail domains

Figure 4.4: Growth of cotransformed yeast colonies confirms the integrity & expression of Sos-K5 head, rod and tail domains in cdc-25H

a) pSos-K5Hd, b) pSos-K5Rd, c) pSos-K5Td, and pMyr SB were cotransformed in cdc25 H yeast strain, plates containing glucose (-Leu/-Ura) were initially incubated at room temperature (24°C) for 4 days to allow colony formation. Selected individual colonies grown at permissive temperature were selected and spotted onto fresh plates containing galactose(-Leu/-Ura), and assayed for growth at restrictive temperature (37°C) for 6 days to check if the bait plasmid cotransformed with the pMyr SB can induce cdc25H yeast growth at 37°C.

Expression and cytoplasmic localization of K14 head, rod and tail domains

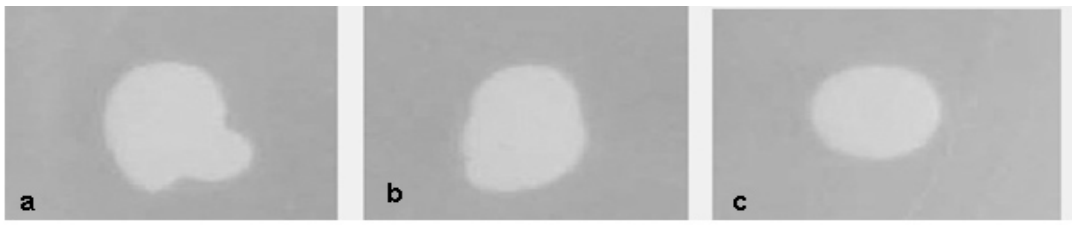

Figure 4.5: Growth of cotransformed yeast colonies confirms the integrity & expression of Sos-K14 head, rod and tail domains in cdc-25H

a) pSos-K14Hd, b) pSos-K14Rd, c) pSos-K14Td, and pMyr SB were cotransformed in cdc25 H yeast strain, plates containing glucose (-Leu/-Ura) were initially incubated at room temperature (24°C) for 4 days to allow colony formation. Selected individual colonies grown at permissive temperature were selected and spotted onto fresh plates containing galactose(-Leu/-Ura), and assayed for growth at restrictive temperature (37°C) for 6 days to check if the bait plasmid cotransformed with the pMyr SB can induce cdc25H yeast growth at 37°C.

4.1.7 Detection of keratin associated proteins by cotransformation of K5/ K14 bait plasmids and target cDNA library

Screening for the identification of novel keratin associated proteins was performed by introducing the keratin bait and target cDNA containing plasmids into the cdc25H(α) yeast strain by cotransformation. This strategy of cotransformation allows results to be generated faster than mating technique as the latter method limits the number of generations of growth prior to the

interaction assay, and thus reduces the incidence of cdc25H reversion leading to false positives. Cotransformation is especially useful if the bait plasmid is toxic to the yeast cells.

Number	Plasmids Transformed	SD Glucose (–UL) /24°C	SD (–UL)/37°C	
			Glucose	Galactose
1	pSos + pMyr	+	NA	–
2	pSos MAFB + pMyr MAFB	+	–	+*
3	pSos MAFB + pMyr SB	+	–	+*
4	pSos Col I + pMyr MAFB	+	–	–*
5	pSos MAFB + pMyr Lamin C	+	–	–
6	pSos K5Hd + pMyr cDNA lib	+	–	+
7	pSos K5Rd + pMyr cDNA lib	+	–	+
8	pSos K5Td + Myr cDNA lib	+	–	+
9	pSos K14Hd + pMyr cDNA lib	+	–	+
10	pSos K14Rd + pMyr cDNA lib	+	–	+
11	pSos K14Td + pMyr cDNA lib	+	–	+

Table 4.4: Combination of the plasmids cotransformed and the growth profile of the transformed cdc25H(α) yeast cells.

Group 1 is used for verification of temperature revertants and to calculate cotransformation efficiency. Groups 2-5 served as positive and negative contols. Groups 6-11 represent the test groups for identification of positively interacting protein partners from cDNA library. * Colonies grown at 24°C on SD glucose containing plates were picked randomly and spotted on galactose containing plates followed with incubation at growth restrictive temperature 37°C.

Cotrasformation of competent cdc25H(α) yeast cells was performed as detailed in the methods section. Growth profile of the transformed yeast colonies is outlined in table No. 4.4. The first group with empty pSos and pMyr plasmids was used to test for the temperature revertants and to

calculate the cotransformation efficiency. Second and third group served as positive controls (figure 4.5), fourth and fifth group of cotransformation were used as negative control (figure 4.6) for the experiment.

Initially, the pMyr cDNA library and pSos bait cotransformant colonies are selected at permissive temperature 24°C on glucose containing SD droupout media. Candidate interactors are identified by replica plating the cotransformants to 37°C. "Putative positives" are identified among the candidates by two rounds of testing for galactose dependent growth at 37°C.

The putative positives colonies obtained after the initial screening were picked individually and inoculated in glucose containing SD broth, incubated for four days at 24°C with shaking.

Yeast DNA was isolated from the grown cultures and was retransformed into XL1 blue *E.coli* by electrotransformation. Transformed bacterial cells were spread on LB agar plates containing chloramphenicol for the selection of the bacterial cells containing cDNA fragments inserted pMyr plasmid. Column purified plasmid DNA containing putative interacting fragments from the cDNA library was isolated by miniprep. Each of the isolated samples were subjected to restriction with Sal I and Not I restriction enzymes to check for the size of inserted fragment. As mentioned in the previous section the minimum size of the inserted DNA fragment in the pMyr cDNA library was about 500bp, so only the fragments which were more than 500bp were selected for the further analysis. The number of putative positive candidates obtained by screening of individual bait is tabulated in table No. 4.5.

4.1.7.1 Cotransformation of pSos MAFB – pMyr MAFB (positive control) and pSos Col I – pMyr MAFB (negative control)

Figure 4.6: Positive and negative controls for yeast two hybrid screening

a) pSos and pMyr plasmids encoding for MAFB protein were cotrasformed in cdc25H yeast strain and plated on tbe agar plates containing glucose(-Leu/-Ura), incubated at growth permissive temperature (24°C) for 3-4 days. Individual colonies were selected and spotted onto agar plates containing galactose(-Leu/-Ura). The plates were incubated at restrictive temperature (37°C) for 4-6 days.

b) pSos and pMyr plasmids encoding for Col I, MAFB proteins respectively were cotrasformed in cdc25H yeast strain and plated on tbe agar plates containing glucose(-Leu/-Ura), incubated at growth permissive temperature

(24°C) for 3-4 days. Individual colonies were selected and spotted onto agar plates containing galactose(-Leu/-Ura). The plates were incubated at restrictive temperature (37°C) for 4-6 days.

Cotransformation of pSos MAFB – pMyr Lamin C (negative control)

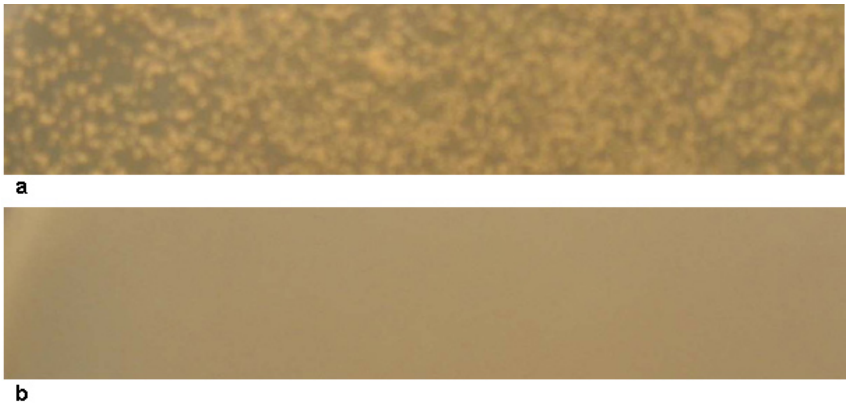

Figure 4.7: Negative control for yeast two hybrid screening

a) pSos and pMyr plasmids encoding for MAFB, laminC proteins respectively were cotrasformed in cdc25H yeast strain and plated on the agar plates containing glucose(-Leu/-Ura), incubated at growth permissive temperature (24°C) for 3-4 days.

b) The colonies which appeared at permissive temperature were replica plated onto agar plates containing galactose(-Leu/-Ura), incubated at growth restrictive temperature (37°C) for 6 days.

The transformation mixture from group 1 (table No. 4.4) was used to check for the temperature revertants and to calculate cotranformation efficiency. 390µl of the transformed mixture was spread on SD glactose (-U, L) agar plates and incubated at 37°C. The plates were observed daily for 6 days to check for growth. No growth was observed indicating the competent cells used for screening experiments were void of temperature revertants. 110µl from the same transformation mixture was spread on SD glucose (-U, L) agar plate and incubated at 24°C for four days to evaluate the transformation efficiency of the competent cells used for screening experiment.

Cotransformation efficiency was found to be **4.3 x 10^3 cfu/µg** of plasmid DNA used which was in the standard range of 0.5 x 10^3 to 1 x 10^4 cfu/ µg DNA.

The transformation mixture of test groups cotransformed with keratin bait plasmids and target cDNA library containing plasmids were spread on SDglucose (-U, L) agar plates (20 numbers) and incubated at room temperature for four days. The colonies grown were transferred on to galactose containing media followed with the incubation at 37°C for 6 days.

The image below (figure 4.8) demonstrates the robustness of the selection system based on the growth of yeast colonies harboring putative positive interaction at restrictive temperature.

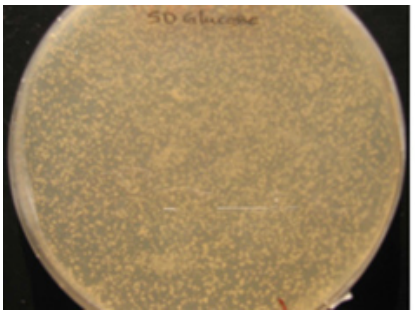

Figure 4.8: Selection of temperature sensitive cotransformed yeast colonies

pSos-K5Hd and pMyr-cDNA library containing plasmids were cotransformed in to cdc25H(α), spread on SDglucose(-U, L) agar plate and incubated for 4 days at 24°C. Approximately 3500 colonies appeared, which were subsequently replica plated on to galactose containing media followed with incubation at restrictive temperature 37°C. Only 8 colonies appeared at restrictive temperature which represents putative positive interacting candidates for keratin 5 head domain.

All the colonies which appeared on galactose containing plates incubated at 37°C, were picked individually and grown in liquid broth for four days. Yeast DNA was isolated from the grown cultures and retransformed into E.coli followed by chloramphenicol selection to isolate pMyr plasmid containing cDNA insert. Column purified plasmid DNA from E.coli was analyzed for the insert size by double digesting with Sal I and Not I restriction enzymes. In total 2475 putative positive candidates were identified as K5 and K14 associated proteins. The below table outlines the number of putative positive candidates obtained for each of the K5 and K14 domain used as bait to identify their interaction partners.

4.1.8 Identification of positive candidates from screening

DNA fragment contained in pMyr plasmid was identified by sequencing the insert using specific primers for the pMyr plasmid. 100 random samples for K5 and K14 associated candidates whose insert size was more than 500 bp were sequenced. Obtained sequence data was analyzed using BLAST bioinformatics tool to identify the interacting protein.

Only the results which covered more than 75% of query length and above 90% sequence identity were considered (Figure: 4.9). The interesting candidates were confirmed for its interaction with their respective keratin domains by cotransforming the specific bait and isolated pMyr plasmids in cdc25H(α) assaying for the growth at restrictive temperature 37°C.

Sl.No	Keratin bait domain	Number of positively interacting candidates isolated
1	Keratin 5 head	434
2	Keratin 5 rod	535
3	Keratin 5 tail	240
4	Keratin 14 head	460
5	Keratin 14 rod	486
6	Keratin 14 tail	320

Table 4.5 : Number of positive interacting candidates isolated using head, rod and tail domains of K5 / K14 as bait against skin cDNA library by 'Sos recruitment' yeast two hybrid genetic screening technique.

Rod domains of keratins are responsible for formation of the keratin heterodimers with the other type of keratins. To evaluate if the candidates obtained by using rod domains as bait contained any keratins, Southern blotting was done using contemporary keratin rod domains as probes. For the candidates isolated with K5 rod as bait, K14 rod was used as probe and for the one identified as K14 rod interacting partners were tested against probe prepared from K5 rod domain.

Among 535 candidates identified with K5 rod domain as bait, seven of them were found to type I keratins. 5 out of 460 candidates obtained as K14 rod interacting partners turned out to be type II keratins.

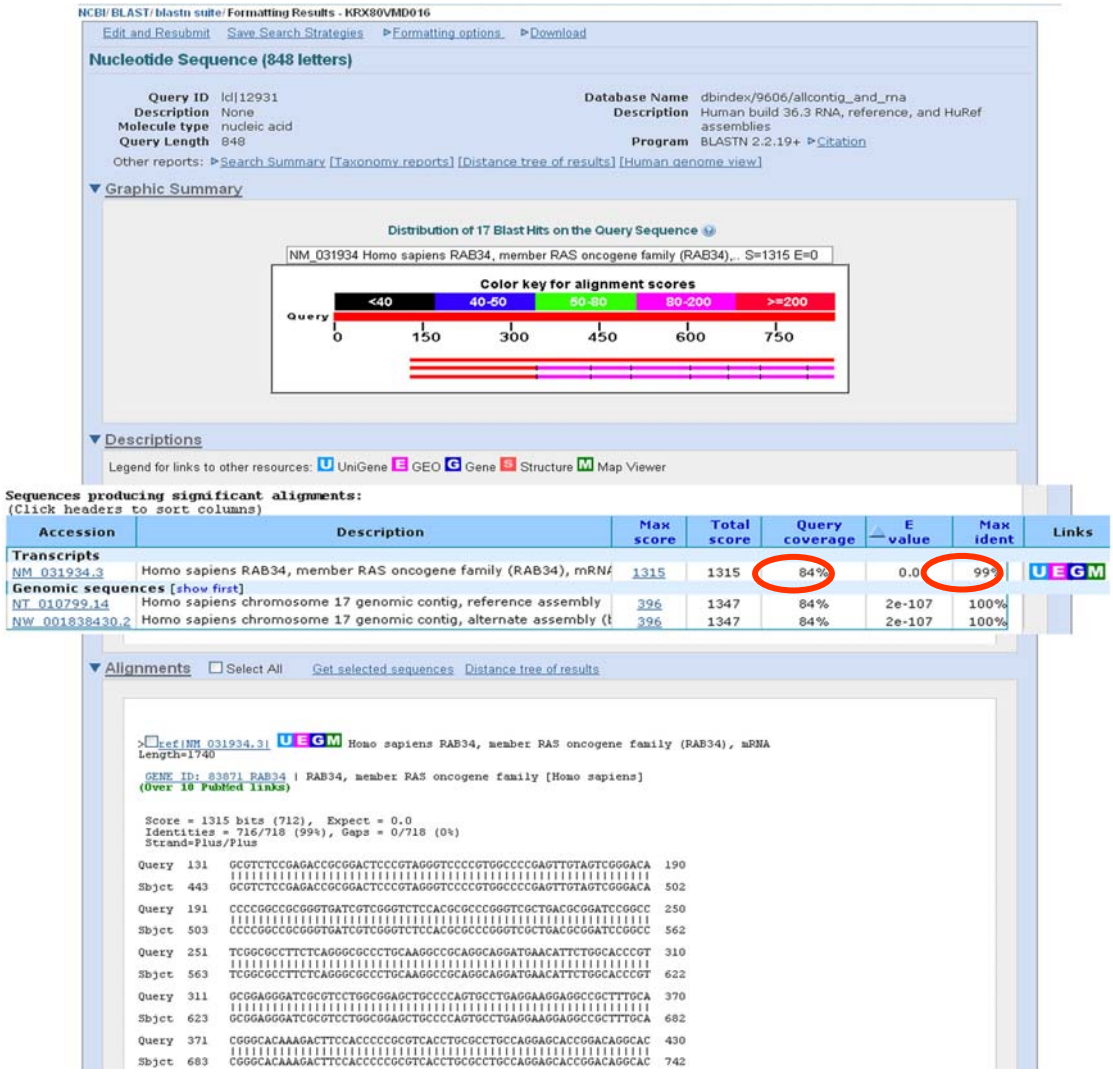

Figure 4.9: An example of BLAST report
Query submitted from results obtained from sequencing the putative positive candidates identified as keratin associated proteins using Sos recruitment system.

The keratin associated proteins identified from BLAST analysis contained well characterized, known proteins to unannotated and hypothetical ones which are yet be investigated for their functions and properties. Few of the candidates from the 200 sequenced results are mentioned in table No. 4.6 and 4.7

Positive interacting protein partners of K5

Number	Name identified by BLAST analysis
1	Homo sapiens Annexin 2
2	Bromodomain and PHD finger containing 3, (BRPF3)
3	Calmodulin-like skin protein (CLSP), the CALML3 gene for calmodulin-like 3 (CLP) and four CpG islands
4	Homo sapians calmodulin-like 5 (CALML5)
5	Homo sapiens Crm, cramped-like (Drosophila) (CRAMP1L)
6	Homo sapiens DEAD (Asp-Glu-Ala-Asp) box polypeptide 17 (DDX17)
7	Homo sapiens eukaryotic translation elongation factor 1 alpha 1 (EEF1A1)
8	Homo sapiens glycine amidinotransferase (L-arginine:glycine amidinotransferase) (GATM)
9	Homo sapiens isocitrate dehydrogenase 3 (NAD+) beta (IDH3B)
10	Homo sapiens LY6/PLAUR domain containing 3 (LYPD3), (C4.4A)
11	Homo sapiens peroxiredoxin 5 (PRDX5)
12	Homo sapiens TAP binding protein (tapasin) (TAPBP)
13	Homo sapiens TBC1 domain family, member 10A (TBC1D10A)
14	Homo sapiens transmembrane anterior posterior transformation 1 (TAPT1)
15	Homo sapiens unc-84 homolog B (C.elegans)
16	Homo sapiens WD repeat domain 71 (WDR71)
17	Homo sapiens WW domain binding protein 1 (WBP1)
18	Homo sapiens zinc finger, NFX1-type containing 1 (ZNFX1)
19	Hypothetical protein LOC201895
20	Hypothetical protein LOC283377

Table 4.6: List of positive interacting candidates with K5 (alphabetical order)

Positive interacting protein partners of K14

Number	Name identified by BLAST analysis
1	Calmodulin-like skin protein variant (CALML5)
2	Homo sapiens calponin 3, acidic (CNN3)
3	Homo sapiens calreticulin
4	Homo sapiens CD74 antigen
5	Homo sapiens chromodomain helicase DANN binding protein 3 (CHD3)
6	Homo sapiens coiled-coil domain containing 72 (CCDC72)
7	Homo sapiens cysteine-rich protein 2
8	Homo sapiens Fibulin 2
9	Homo sapiens immunoglobulin (CD79A) binding protein 1 (IGBP1)
10	Homo sapiens mitogen-activated protein kinase kinase kinase kinase 2
11	**Homo sapiens RAB34**
12	Homo sapiens signal transducer and activator of transcription 6, (STAT6)
13	**Homo sapiens transcription factor AP-2 beta (TFAP2B)**
14	**Homo sapiens tyrosine 3-monooxygenase/tryptophan 5-monooxygenase activation protein, Theta polypeptide (14-3-3)**
15	Homo sapiens unc-84 homolog B (C. elegans)
16	Homo sapiens zinc finger and BTB domain containing 4 (ZBTB4)
17	hypothetical protein LOC727957 isoform 1
18	**p86DM**
19	Rho guanine nucleotide exchange factor (GEF) 19
20	Uridine monophosphate kinase (UMPK protein)

Table 4.7: List of positive interacting candidates with K14 (alphabetical order)

4.2 Verification of the positive interacting candidates in mammalian cell culture system

Transcription factor AP2β, Rab34 a small GTPase of the ras superfamily, 14-3-3τ a member of 14-3-3 family proteins and the unannotated protein p86DM which were identified as K14 head domain interacting proteins by Sos recruitment technique were selected for further investigation to confirm their interaction with K14 in mammalian cell culture system.

Even though the above mentioned proteins were identified as interacting partners of K14 head domain, owing to the stability and expression pattern of K14 head domain in the cell culture system, full length K14 was used to verify the interaction with the identified candidate proteins.

To confirm the interaction, firstly expression of K14 head domain as GST fusion protein and subsequent efforts to perform pulldown assays of endogenously expressed candidates was not successful because of the aggregation of GST fusion protein. Similar kind of challenge was experienced when tried to express K14 head domain alone in mammalian cells.

To overcome these challenges, full length K14 was used to confirm the interaction by 'Bimolecular fluorescence complementation technique', which enables direct visualization of protein complexes in living cells and investigation of interactions in normal physiological cell environment.

Full length keratin protein was expressed along with 'N' terminal half of Venus-YFP and candidate proteins were expressed in fusion with 'C' terminal half Venus-YFP. Direct interaction of the expressed K14 and candidate protein, constituted full length active Venus-YFP.

4.2.1 Positive control for BiFC studies V1–Flag–p0071 WT and V2–HA–RhoA WT

The interaction of armadillo protein p0071 with RhoA a member of Rho-family of GTPases was reported by Wolf et al., 2006 using BiFC technique. So for the present study Venus tagged proteins of p0071 and RhoA were used as positive controls, which exhibited similar kind of fluorescence pattern as reported by authors (figure 4.10).

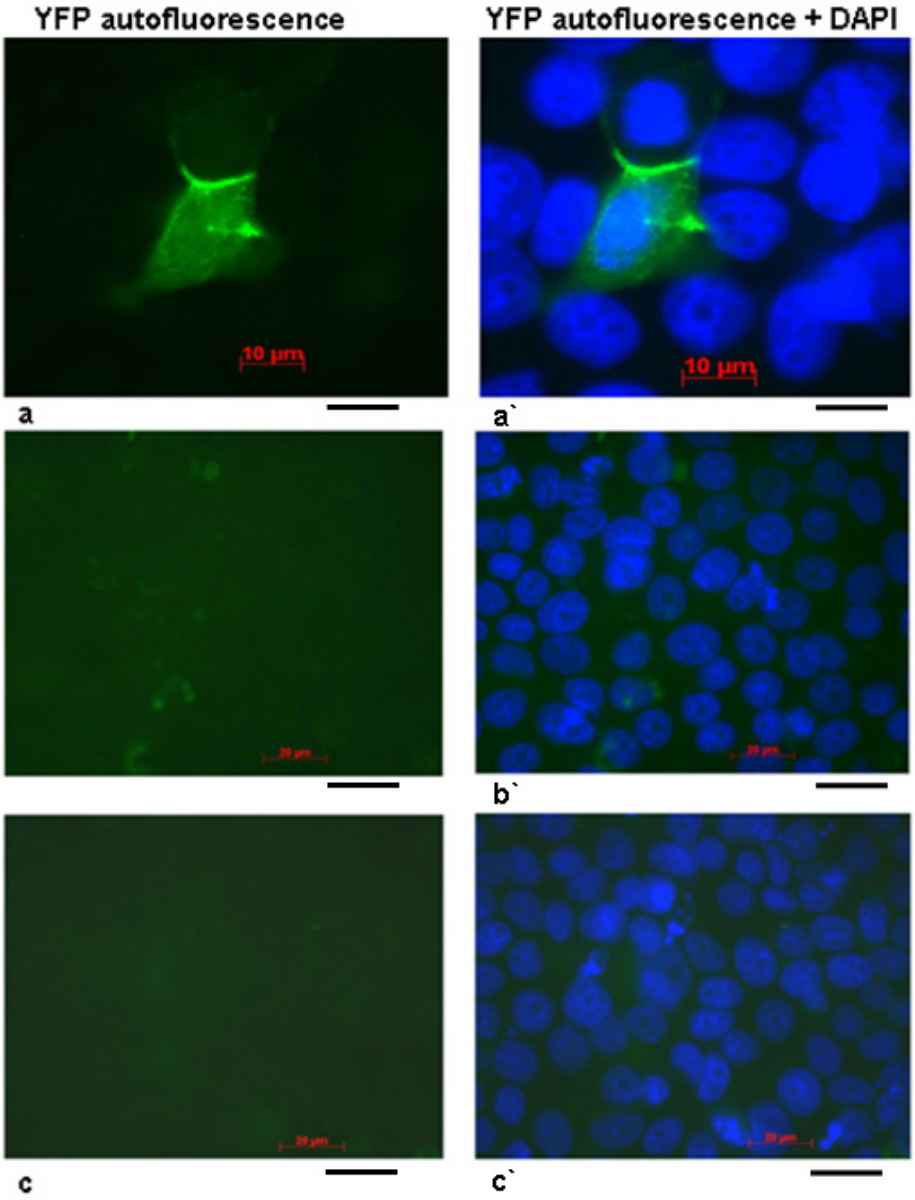

Figure 4.10: Transfection of Venus plasmids used as positive control for BiFC experiments

Association was determined by co-transfecting p0071-arm repeats fused to a Flag-tagged C-terminal YFP–Venus fragment (V1–Flag–p0071 WT) and the indicated Rho variants fused to the corresponding N-terminal part of YFP–Venus with a HA-tag (V2–HA–RhoA WT) (kind gift by Prof. Hatzfeld, Halle; Wolf et al., 2006). The green signal represents YFP autofluorescence.

a & a` : MCF7 cells were transiently cotransfected with V1–Flag–p0071 WT and V2–HA–RhoA WT, and were fixed using PFA after 48 hours of transfection. p0071 associates with wild-type RhoA at the midbody as shown by the authors and served as a positive control for BiFC experiments carried out in the present study.

b & b` : MCF7 cells were transiently transfected with V1–Flag–p0071 WT and were fixed using PFA after 48 hours of transfection. Absence of the green signal for YFP indicates there is no false or nonspecific signal from the YFP-Venus1 fragment.

c & c` : MCF7 cells were transiently transfected with V2–HA–RhoA WT and were fixed using PFA after 48 hours of transfection. Absence of the green signal for YFP indicates there is no false or nonspecific signal from the YFP-Venus2 fragment.

4.2.2 Confirmation of interaction between K14 and AP2β by BiFC

Interaction of K14 with AP2β a transcription activator was identified for the first time in yeast two hybrid screening studies. To check and confirm the relevance of this interaction in cultured mammalian cells, full length Venus tagged proteins of K14 and AP2β were expressed by cotransfecting in MCF-7 mammary epithelial cells.

Different combinations of the expression plasmids (Table No. 4.8) were transfected in the experiment in order to control and to avoid any false positive fluorescence.

Results of the positive control transfections are shown in next section of results.

Sl.No	Plasmid(s) transfected	Group	Fluorescence
1	K14-pVen1flag + AP2β-pVen2 HA	Test	+
2	K14-pVen1flag	Control	-
3	AP2β-pVen2 HA	Control	-
4	K14-pVen1flag + pVen2 HA	Control	-
5	pVen1flag + AP2β-pVen2 HA	Control	-

Table 4.8: Different transfection groups used in experiment to confirm direct interaction of K14 with AP2β

Full length K14 cDNA (1.73kb) was cloned in frame with amino terminal half of Venus-YFP (first 480bp from total 747bp of Venus-YFP). Flag tag was used to link carboxy end of Venus-YFP fragment with amino terminal end of keratin14 and also to facilitate folding of Venus-YFP fragment.

Full length AP2β cDNA (1.35kb) was cloned in frame with carboxy terminal half of Venus-YFP (last 267bp from total 747bp of Venus-YFP). HA tag was used to link carboxy end of Venus-YFP fragment with amino terminal end of AP2β which also helps in proper folding of Venus-YFP fragment to reconstitute full length active Venus-YFP.

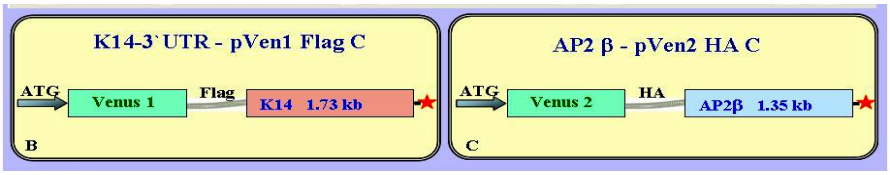

Figure 4.11: Schematic representation of the Venus-YFP constructs.

4.2.2.1 Cotransformation of full length cDNA inserted K14-pVen1flag and AP2β-pVen2 HA plasmids

In order to confirm the interaction of K14 and AP2β in mammalian cell culture system, Venus expression plasmids inserted with full length K14 and AP2β cDNA were cotransfected into MCF-7 cells. As a result of the direct interaction between the expressed proteins, Venus-YFP activity is reconstituted and led to accumulation of autofluorescence at the site of intracellular interaction (figure 4.12). A strong direct interaction was observed upon maturation of the YFP fluorescence along the expressed K14 filaments in the cytoplasm of transfected cells. Cotransformation efficiency of more than 40% was seen in all repetitive trials conducted to confirm the result.

The autofluorescence emitted by the reconstitution of active Venus-YFP when cotransfected in MCF-7 cells strongly suggests that K14 binds to AP2β and sequesters in cytoplasm of the cells.

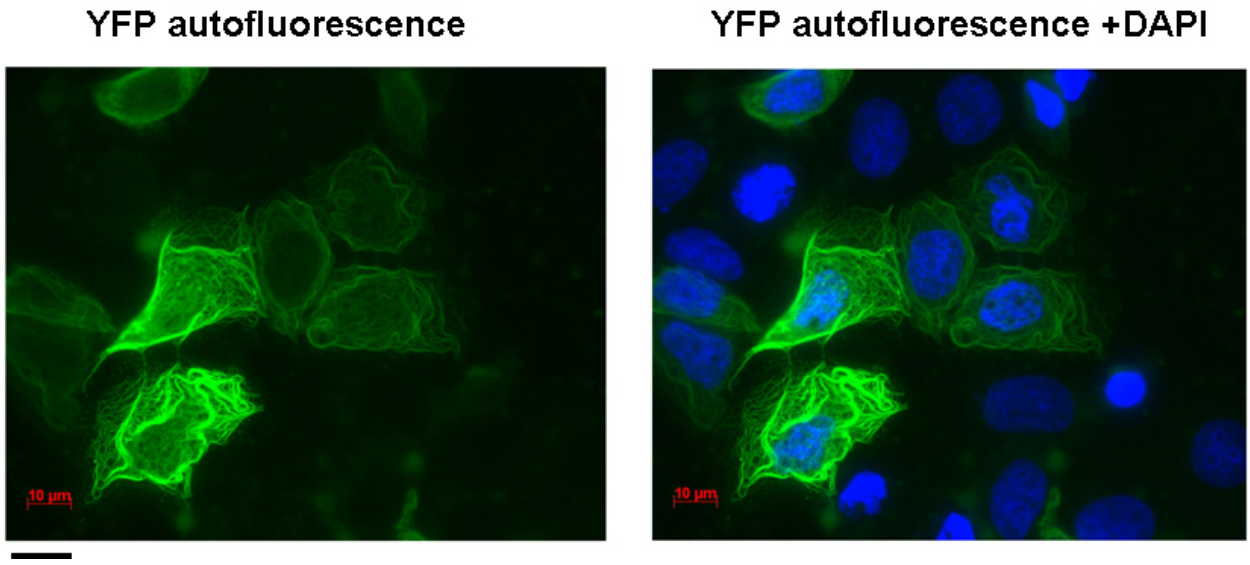

Figure 4.12: BiFC analysis of transiently transfected MCF7 cells with AP2β and K14 Venus constructs.
MCF7 cells were cotransfected with K14-Venus1Flag-N and AP2β-Venus2HA-C. Cells were fixed and analyzed after 48 hours of transfection. The green signal represents the YFP autofluorescence as a result of the formation of active YFP from the complementing halves due to the direct interaction between K14 and AP2β which are fused with the corresponding Venus halves. Distribution resembles to characteristic expression of endogenous keratin cytoskeleton. Scale bar 10 µm

4.2.2.2 Individual transformation of full length cDNA inserted K14-pVen1flag and AP2β-pVen2 HA plasmids

Venus expression plasmids inserted with full length K14 and AP2β were transfected individually into MCF-7 cells to check for emittance of false fluorescence signal from the individual Venus-YFP fragments. The results indicated that upon transfection of AP2β-pVen2 HA and K14-pVen1flag, there was no non specific fluorescence emitted from the individual Venus-YFP fragments (figure 4.13). Transfection efficiency with eYFP plasmid ranged between 55 to 65 %.

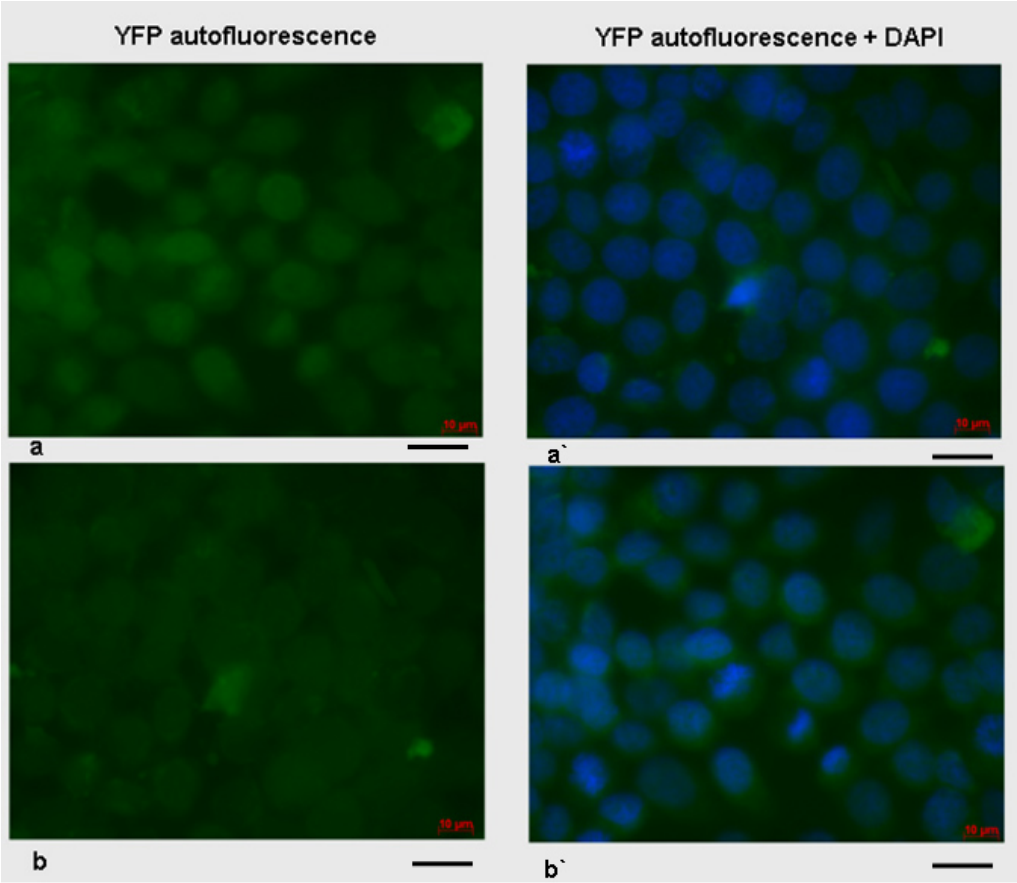

Figure 4.13: BiFC analysis of transiently transfected MCF7 cells with AP2β and K14 Venus constructs.

a & a` : MCF7 cells transiently transfected with AP2β-Venus2HA-C and analyzed after 48 hours of transfection. Absence of the green signal for YFP indicates there is no nonspecific signal from the YFP-Venus2 fragment.

b & b` : MCF7 cells transiently transfected with K14-Venus1Flag-N and analyzed after 48 hours of transfection. Absence of the green signal for YFP indicates there is no nonspecific signal from the YFP-Venus1 fragment. Scale bar 10 μm

4.2.2.3 Cotransformation of full length cDNA inserted and empty Venus plasmids

Venus plasmids inserted with full length cDNAs were cotransfected with their corresponding empty Venus vectors containing the Venus-YFP moiety required for the reconstitution of full length active YFP. In this set of experiment K14-pVen1flag was cotransfected with pVen2 HA and empty pVen1flag with out K14 was contransfected along with AP2β-pVen2 HA, to check for any nonspecific interactions between the Venus1-YFP and Venus2-YFP fragments or between expressed proteins (K14/AP2β) and Venus-YFP fragment. The results clearly indicated the absence of any non specific interactions in between either two Venus-YFP fragments or with the expressed protein (figure 4.14).

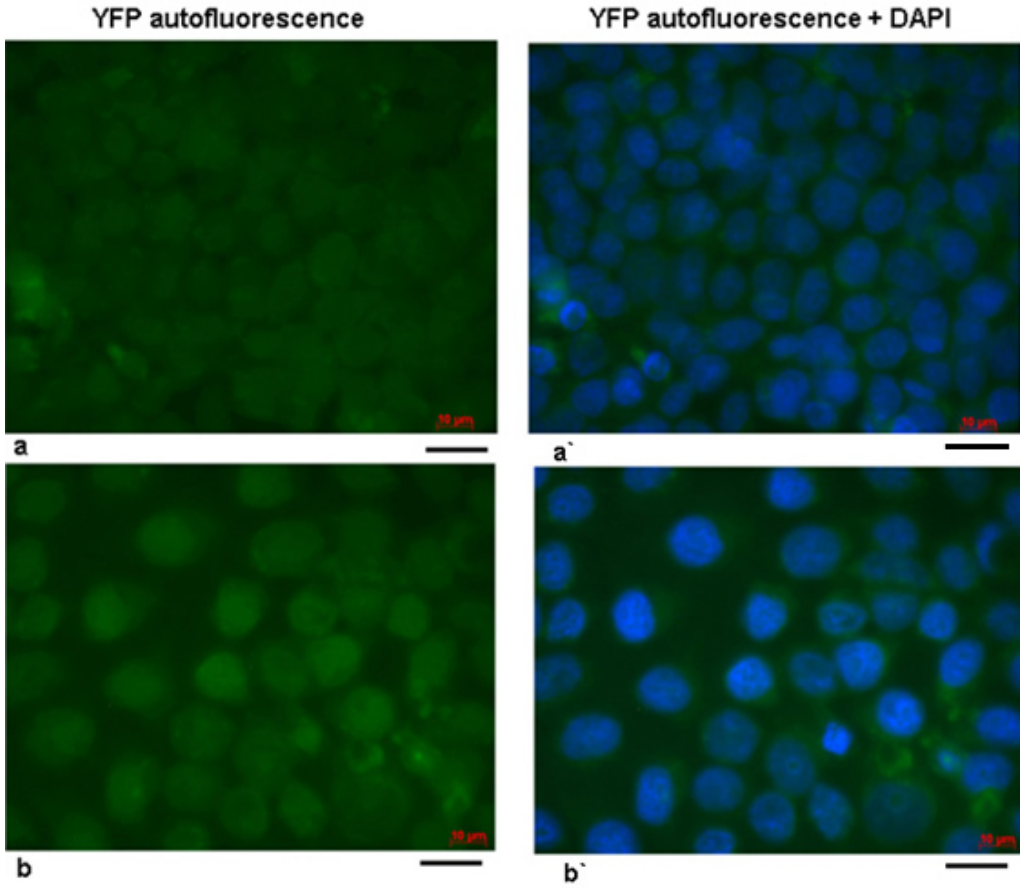

Figure 4.14: Negative control for BiFC analysis of transiently transfected MCF7 cells.

a & a` : MCF7 cells were cotransfected with AP2β-Venus2HA-C and empty Venus vector with the complementing half of the YFP pVenus1Flag-N, analyzed after 48 hours of transfection. Absence of the green signal for YFP indicates that the two complementing halves of the YFP do not form active YFP in presence of the fusion protein and it also doesn't interact with AP2β fused to Venus2 half of the full length YFP.

b & b` : MCF7 cells were cotransfected with K14-Venus1Flag-N and empty Venus vector with the complementing half of the YFP pVenus2HA-C, analyzed after 48 hours of transfection. Absence of the green signal for YFP indicates that the two complementing halves of the YFP do not form active YFP in presence of the fusion protein and it also does not interact with K14 fused to Venus1 half of the full length YFP. Scale bar 10 μm

Different sets of the above shown control experiments confirmed that, autofluorescence emitted by cotransfection of Venus constructs tagged to K14 and AP2β is only due to the direct interaction of K14 and AP2β thereby reconstituting the mature Venus-YFP.

These results confirm the interaction between two expressed proteins and strongly suggest that AP-2β is sequestered in the cytoplasm by interaction with K14 and also opens a new avenue for the first time to address a novel regulatory mechanism which controls the activity of AP-2β and possibly other AP-2 family members by interaction with keratins.

4.2.3 Confirmation of interaction between K14 and Rab34 by BiFC

A member of Rab GTPase family protein Rab34 was identified as an interacting partner and confirmed for its association with K14 in yeast by two hybrid method. To investigate for existence of similar kind of affinity between the two proteins in mammalian cell culture model, which can shed light on involvement of keratins in vesicle transport by binding or harboring proteins involved in transport, Venus-YFP fragments were expressed in fusion with proteins under investigation. Upon cotransfecting these two constructs in MCF-7 mammary epithelial cells, full length active Venus-YFP was reconstituted emitting autofluorescence along the keratin filaments.

In order to monitor the specificity of emitted fluorescence, different combinations of the expression plasmids (Table No. 4.9) were transfected in the experiment as controls.

Sl.No	Plasmid(s) transfected	Group	Fluorescence
1	K14-pVen1flag + Rab34-p ven2 HA	Test	+
2	K14-pVen1flag	Control	-
3	Rab34-p ven2 HA	Control	-
4	K14-pVen1flag + pVen2 HA	Control	-
5	pVen1flag + Rab34-p ven2 HA	Control	-

Table 4.9: Different transfection groups used in experiment to confirm direct interaction of K14 with Rab34

Full length K14 cDNA (1.73kb) was cloned in frame with amino terminal half of Venus1-YFP (first 480bp from total 747bp of Venus-YFP). Amino terminal of K14 was linked to carboxy end of Venus1-YFP fragment through 'Flag' tag which also to facilitates proper folding of Venus-YFP fragment while reconstitution.

Full length Rab34 cDNA (740bp) was cloned in frame with carboxy terminal half of Venus2-YFP (last 267bp from total 747bp of Venus-YFP). HA tag was used to link carboxy end of Venus2-YFP fragment with amino terminal end of Rab34 which also helps in proper folding of Venus2-YFP fragment to reconstitute full length active Venus-YFP.

4.2.3.1 Cotransformation of full length cDNA inserted K14-pVen1flag and Rab34-pVen2 HA plasmids

Venus plasmids tagged with full length K14 and Rab34 were transiently cotransfected in MCF-7 cells and observed for maturation of active Venus-YFP. Direct physical interaction of the two tagged proteins ensues the reconstitution of active Venus-YFP.

Cotransformation of MCF-7 cells with K14-pVen1flag and Rab34-pVen2 HA plasmids followed by incubation at lower temperature to facilitate the maturation of Venus-YFP, reconstituted active Venus-YFP from amino and carboxy Venus fragments emitting clear autofluorescence indicating a direct interaction between K14 and Rab34. Emitted fluorescence was distributed evenly throughout the cytoplasm of transfected cells similar to cytoskeletal network of keratin filaments.

Cotransformation efficiency of more than 40% was seen in all repetitive trials conducted to confirm the result.

The autofluorescence emitted by the reconstitution of active Venus-YFP when cotransfected in MCF-7 cells strongly suggests that K14 binds to Rab34 and sequesters in cytoplasm of the cells (figure 4.15).

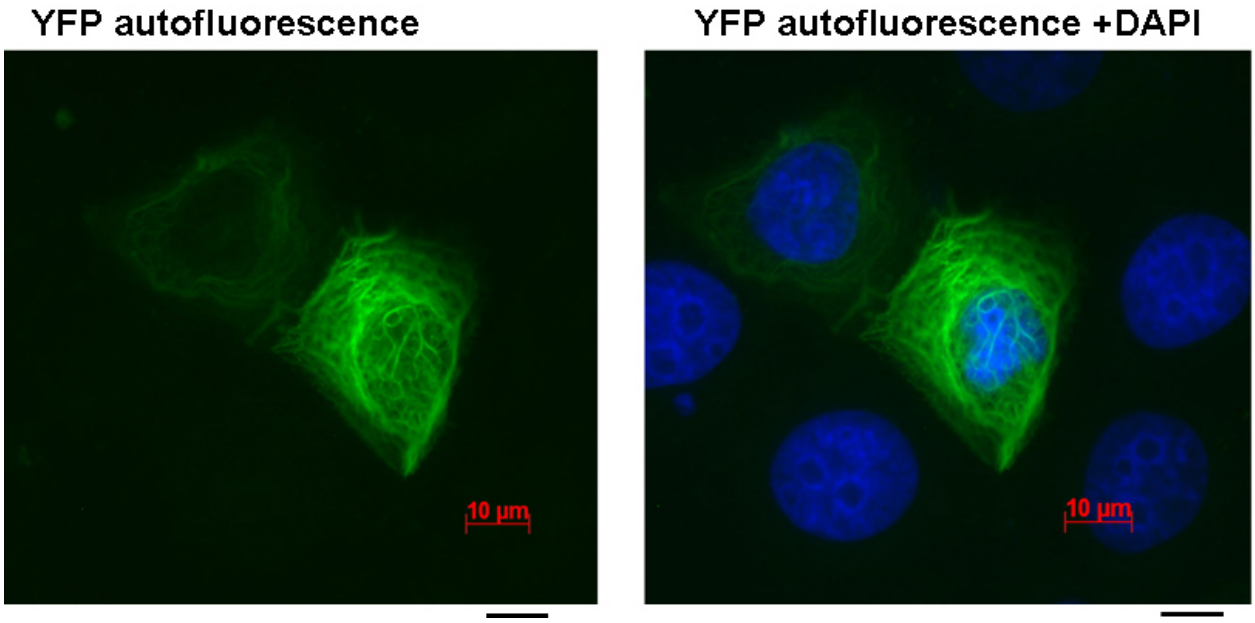

Figure 4.15: BiFC analysis of transiently transfected MCF7 cells with RAB34 and keratin 14 Venus constructs.

MCF7 cells were cotransfected with K14-Venus1Flag-N and RAB34-Venus2HA-C. Cells were fixed and analyzed after 48 hours of transfection. The green signal represents the YFP autofluorescence as a result of the formation of active YFP from the complementing halves due to the direct interaction between K14 and RAB34 which are fused

with the corresponding Venus halves. Distribution resembles to characteristic expression of endogenous keratin cytoskeleton. Scale bar 10 µm

4.2.3.2 Individual transformation of full length cDNA inserted K14-pVen1flag and Rab34-pVen2 HA plasmids

Transfection of MCF-7 cells with Venus expression plasmids inserted with full length K14 and Rab34 was done individually to verify emittance of fluorescence from the individual Venus fragment in the absence of its complementing fraction which is necessary to form full length active Venus-YFP.

The results indicated that upon transfection of Rab34-pVen2 HA and K14-pVen1flag, there was no non specific fluorescence emitted from the individual Venus-YFP fragments (figure 4.16). Transfection efficiency with eYFP plasmid ranged between 55 to 65 %.

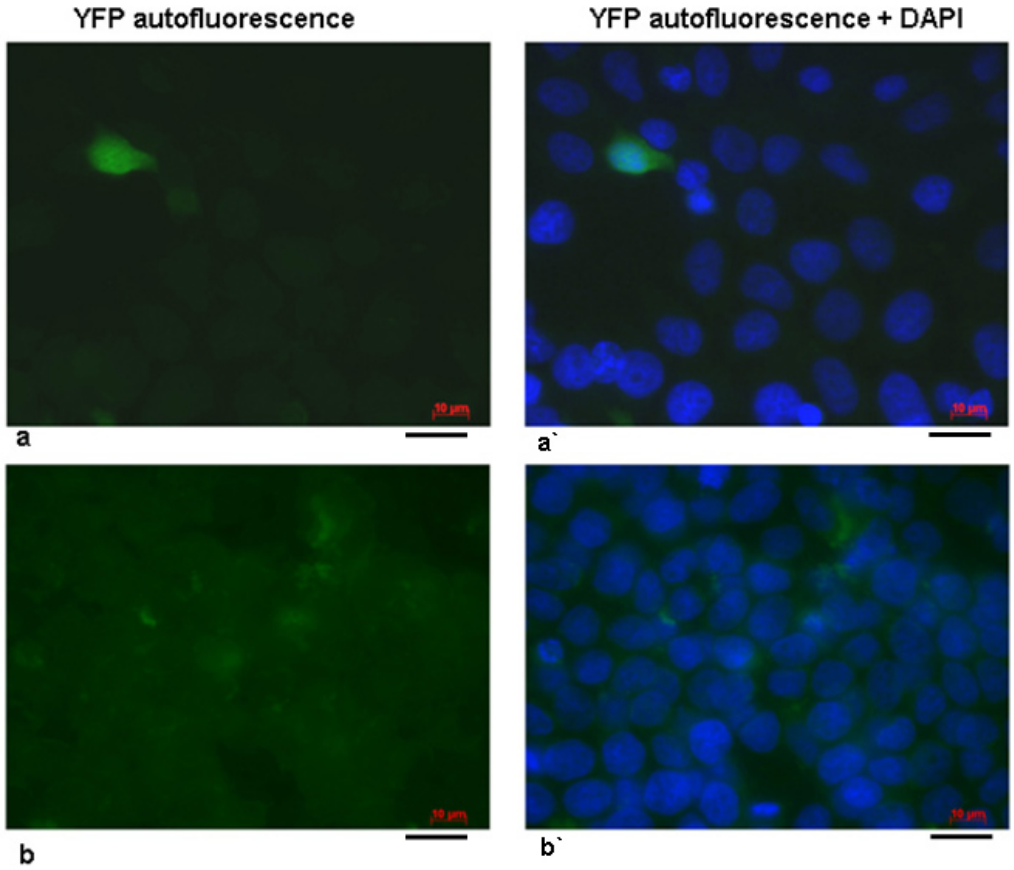

Figure 4.16: Negative control BiFC analysis of transiently transfected MCF7 cells with RAB 34 and keratin14 Venus constructs.

a & a` : MCF7 cells transiently transfected with RAB34-Venus2HA-C and analyzed after 48 hours of transfection. Absence of the green signal for YFP indicates there is no nonspecific signal from the YFP-Venus2 fragment.

b & b` : MCF7 cells transiently transfected with K14-Venus1Flag-N and analyzed after 48 hours of transfection. Absence of the green signal for YFP indicates there is no nonspecific signal from the YFP-Venus1 fragment. Scale bar 10 µm

4.2.3.3 Cotransformation of full length cDNA inserted and empty Venus plasmids

To confirm the result obtained in first part where it has shown the direct interaction between K14 and Rab34 is genuine and not due to nonspecific interaction of expressed proteins with Venus-YFP fragments, MCF-7 cells were cotransfected with K14-pVen1flag + pVen2 HA and Rab34-pVen2 HA + pVen1flag Venus plasmids.

The results clearly showed that, K14 tagged with Venus1 fragment does not interact with the Venus2 fragment in the absence of an interacting partner. The same was true for Rab34 tagged with Venus2 fragment (figure 4.17), which confirms the specificity of the detection system and thus the results obtained.

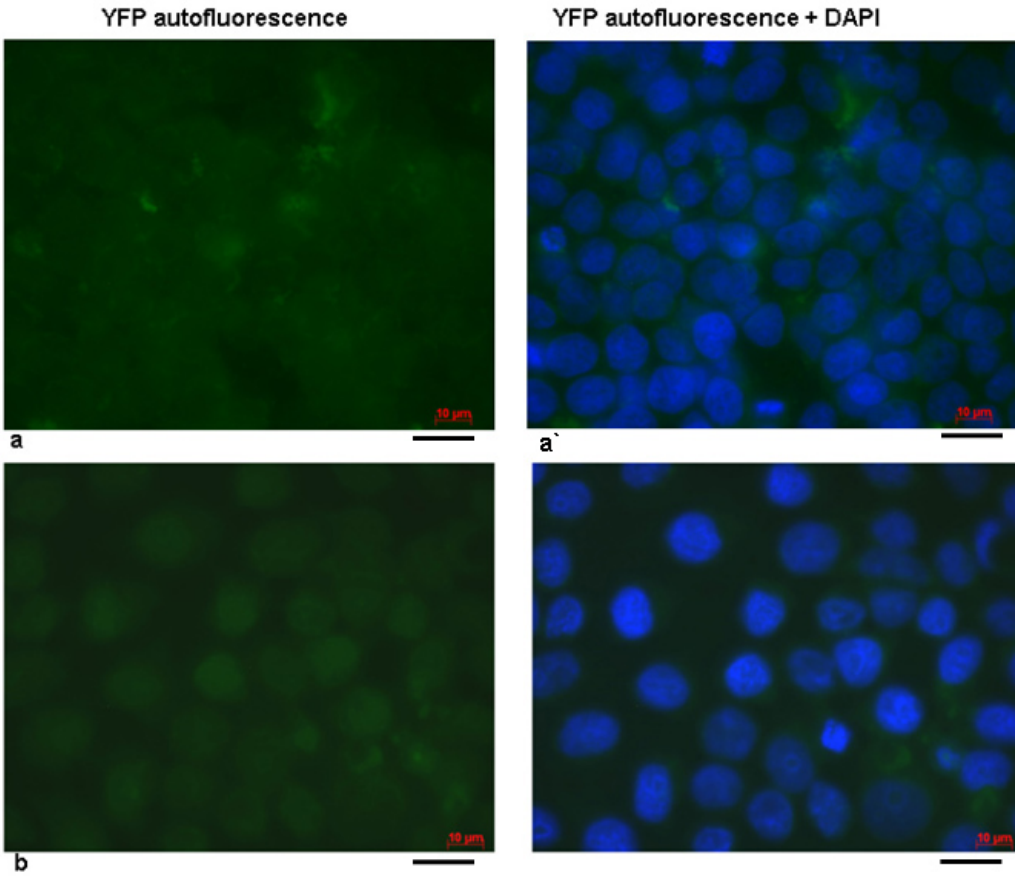

Figure 4.17: Negative control for BiFC analysis of transiently transfected MCF7 cells.

a & a` : MCF7 cells were cotransfected with RAB34-Venus2HA-C and empty Venus vector with the complementing half of the YFP pVenus1Flag-N, analyzed after 48 hours of transfection. Absence of the green signal for YFP indicates that the two complementing halves of the YFP do not form active YFP in presence of the fusion protein and it also doesn't interact with RAB34 fused to Venus2 half of the full length YFP.

b & b` : MCF7 cells were cotransfected with K14-Venus1Flag-N and empty Venus vector with the complementing half of the YFP pVenus2HA-C, analyzed after 48 hours of transfection. Absence of the green signal for YFP indicates that the two complementing halves of the YFP do not form active YFP in presence of the fusion protein and it also doesn't interact with keratin14 fused to Venus1 half of the full length YFP. Scale bar 10 µm

BiFC analysis confirmed the direct interaction between cytoskeletal protein keratin14 and Rab34 a transporter protein in the cytoplasm of MCF-7 cells. This result was supported by various control experiments conducted in parallel.

The finding of interaction between K14 with transporter protein Rab34 will further support the recent reports stating the role of keratin in vesicle transport. Rab proteins (Rab27) are involved in melanosome transport and distribution in melanocytes, Rab34 being the member of same family and its interaction with K14 hints that, this specific interaction might be having some role to play in uptake and redistribution of melanosomes in keratinocytes. Further investigations towards this aspect would be highly significant to elucidate the role of keratins in melanosome transport and redistribution in keratinocytes.

4.2.4 BiFC analysis for verifying interactions between K14 with 14-3-3τ and p86DM

Attempts to confirm the interaction of K14 with 14-3-3τ and p86DM in the similar lines to that of AP2β and Rab34 were not successful. Interaction of 14-3-3τ is dependent on phosphorylation of Ser33 like other members of 14-3-3 protein family. Since no artificial hyper-phosphorylation was induced in the experimental settings to look for the interaction, might be one of the reasons for not noticing the direct interaction with K14.

Several experiments performed by co-workers showed that p86DM do not interact with K14 directly. p86DM being identified for the first time, with its sequence analysis prediction pointing towards crucial role of this protein in many cellular process, led us to choose this protein for further investigation to characterize and to reveal its level of contribution in regulation/maintenance of cellular machinery.

4.2.5 Analysis of p86DM

Bioinformatic analysis of p86DM sequence identified in yeast two hybrid studies showed high level of sequence similarity with the sequence predicted in humans, mouse, fly and dog with the highest degree of identity being located at the C-terminus of coding sequence of orthologous proteins.

In humans 5 transcript variants of different sizes ranging from 898bp to 2.5kb (figure 4.18) comprising 4 exons in the smallest and 10 exons in the larger sequence was predicted.

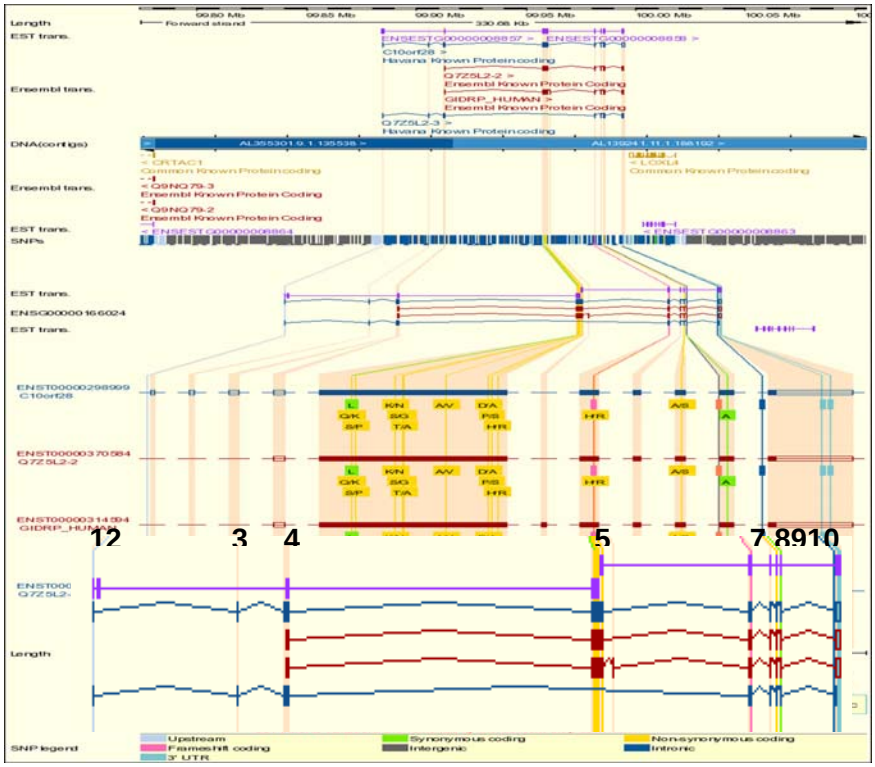

Figure 4.18: Sequence analysis of p86DM predicted 5 different transcript variants in humans with 4 to 10 number of exons.

4.2.5.1 Identification of p86DM coding sequence

To verify whether p86DM is encoded by a single functional gene or by multiple genes as predicted, total RNA was isolated from mammalian intestinal Caco2 cells, subjected to RT-PCR amplification in order to isolate full length cDNA. Specific primers were designed for each of the predicted sequence and PCR amplified product yielded product with two different sizes, the first one being about 900bp and the second with size of 2.5kb. This result was in par with that of the predicted ones (figure 4.19).

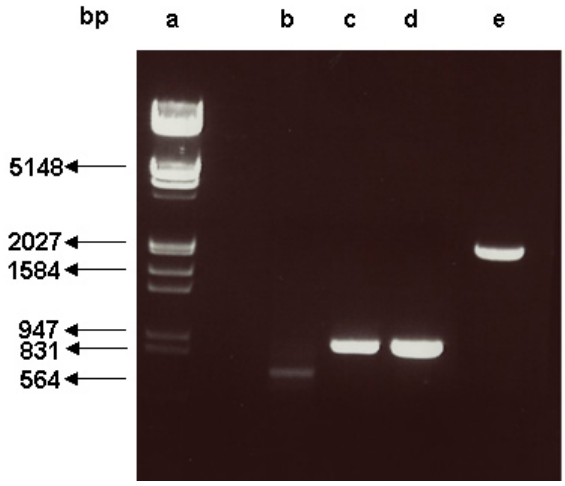

Figure 4.19: Size of PCR amplified cDNA products from Caco2 isloated RNA

Lane a : marker, Lane b - e : PCR amplified products using specific primer.

From the size profile obtained by PCR amplification using specific primers, it looked evident that the primers designed for different sized predicted genes, efficiently amplified the product. In order to confirm the amplified sequence, PCR amplified products were cloned into cloning vectors and transformed into E.coli. Column purified plasmid DNA was isolated from the transformed bacterial cultures.

Two of the predicted p86DM coding genes were of sizes 2449 and 2491bp respectively with a mere difference of 42bp but the latter one having an additional restriction site ‘Ava I’. The obtained largest PCR amplified fragment with an approximate size of 2.5kb was cloned in clonig vector and was subjected to restriction analysis with ‘Ava I’. Restriction results revealed that, the amplified product did not contain the specified restriction site ‘Ava I’ and hence confirms the expression of 2449bp fragment in Caco2 cells (Figure 4.20).

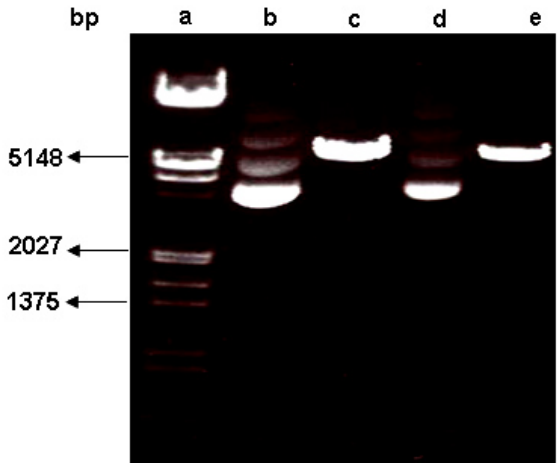

Figure 4.20: Restriction analysis with Ava I to differentiate between the two transcripts

Lane a : marker, Lane b &d : un cut plasmid inserted with PCR amplified product, Lane c & e: Plasmid restricted with Ava I enzyme

The vector backbone in which the PCR amplified product was inserted contained an Ava I restriction site. The single band with the size of 5.4kb reveals that, there is no second Ava I restriction present in the construct.

The PCR amplified fragments were sequenced and the results proved that p86DM is represented by only one functional gene, and the sequence of smaller fragments identified were found to be a part of 2.4kb gene identified.

4.2.5.2 Functional Studies

Bioinformatic analysis predicted a single transcript giving rise to an open reading frame of 776 amino acids in the mouse. The predicted protein carries an N-terminal 14-3-3 binding site, SH2 and SH3 motifs, a clathrin-heavy chain binding site, a coiled-coil domain and a C-terminal PDZ-binding site.

To elucidate the meaning of different predicted domains and in order to gain a first insight on the potential mechanism by which p86DM may act, a search for p86DM associated proteins was done. In this independent experiment, β-actin was identified as one of the p86DM interacting candidates.

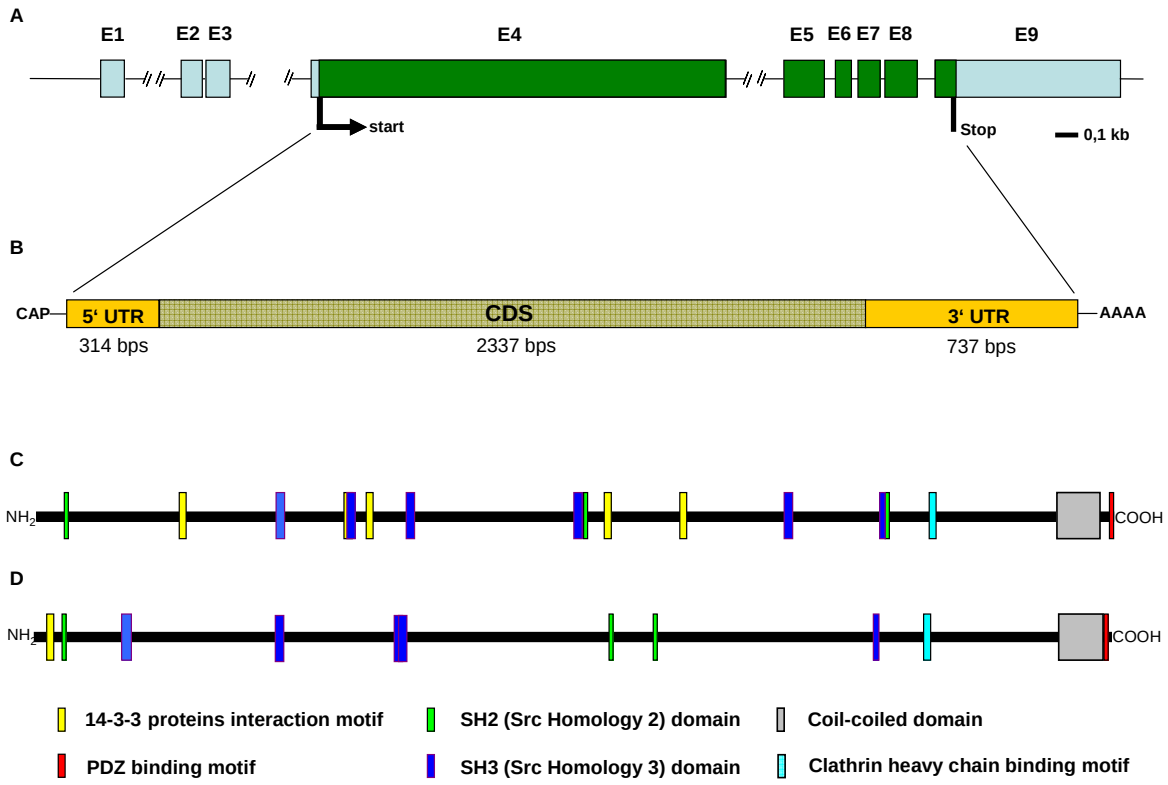

Figure 4.21: Schematic representation of p86DM gene, transcript and protein

A Human p86DM gene, on chromosome 10, encompasses ~110 kb with 9 exons. The coding sequence starts in exon 4 and ends in exon 9. **B** Processed mRNA with a coding sequence (CDS) of 2337 bps **C, D** predicted domain organization of human and mouse p86DM, respectively.

4.2.5.3 Interaction of p86DM with actin

As a further step to confirm the results from above mentioned independent experiment, an attempt to confirm interaction between actin and p86DM in MCF-7 mammary epithelial cells by BiFC was done.

In order to monitor the specificity of emitted fluorescence, different combinations of the expression plasmids (Table No. 4.10) were transfected in the experiment as controls.

Sl.No	Plasmid(s) transfected	Group	Fluorescence
1	p86DM-Ven1-N + Y-C-Actin	Test	+
2	p86DM-Ven1-N	Control	-
3	Y-C-Actin	Control	-
4	Y-C-Actin + p Ven1-N	Control	-

Table 4.10: Different transfection groups used in experiment to confirm direct interaction of p86DM with actin

Full length p86DM cDNA (2.4kb) was cloned in frame with amino terminal half of Venus1-YFP (first 480bp from total 747bp of Venus-YFP). Full length actin cDNA cloned in frame with carboxy terminal half of Venus2-YFP (last 267bp from total 747bp of Venus-YFP) was used.

4.2.5.3.1 Cotransformation of p86DM-pVen1 and Y-C-actin plasmids

In order to confirm the interaction of p86DM and actin in mammalian cell culture system, Venus expression plasmids inserted with full length p86DM and actin cDNA were cotransfected into MCF-7 cells. As a result of the direct interaction between the expressed proteins, Venus-YFP activity is reconstituted and led to accumulation of autofluorescence at the site of intracellular interaction (figure 4.22). A direct interaction was observed upon maturation of the YFP fluorescence spread all over cytoplasm of transfected cells. Cotransformation efficiency of more than 40% was seen in all repetitive trials conducted to confirm the result.
The autofluorescence emitted by the reconstitution of active Venus-YFP when cotransfected in MCF-7 cells strongly suggests that actin directly interacts with p86DM.

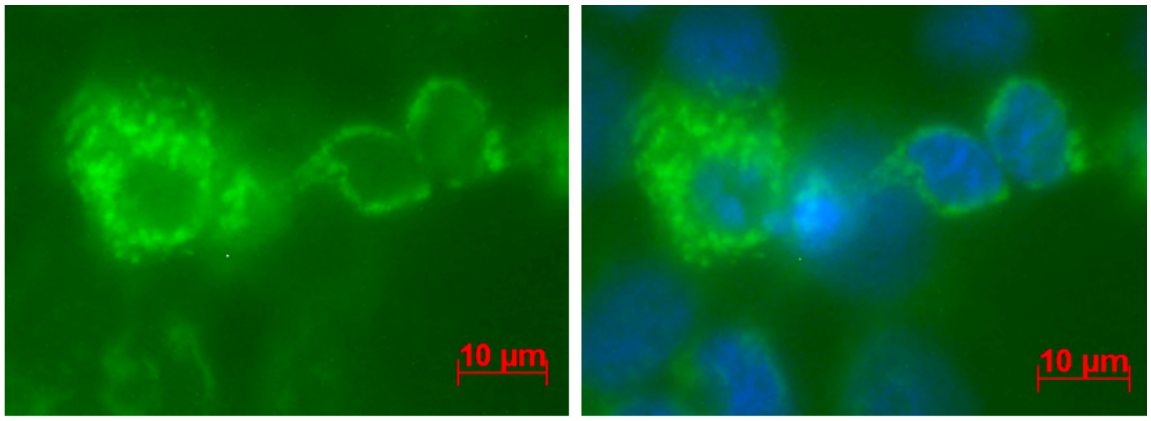

Figure 4.22: BiFC analysis of transiently transfected MCF7 cells with P86DM-Ven1-N and Y-C-actin Venus constructs.

MCF7 cells were cotransfected with P86DM-Ven1-N and Y-C-Actin. Cells were fixed and analyzed after 48 hours of transfection. The green signal represents the YFP autofluorescence as a result of the formation of active YFP from the complementing halves due to the direct interaction between P86DM and actin which are fused with the corresponding Venus halves.
a) Autofluorescence from the reconstituted Venus-YFP b) MCF-7 cells with DAPI staining

4.2.5.3.2 Individual transformation of full length cDNA inserted p86DM-Ven1-N and Y-C-actin plasmids

Venus expression plasmids inserted with full length p86DM and actin were transfected individually into MCF-7 cells to check for emittance of false fluorescence signal from the individual Venus-YFP fragments. The results indicated that upon transfection of p86DM-Ven1-N and Y-C-actin, there was no non specific fluorescence emitted from the individual Venus-YFP fragments (figure 4.23). Transfection efficiency with eYFP plasmid ranged between 55 to 65 %.

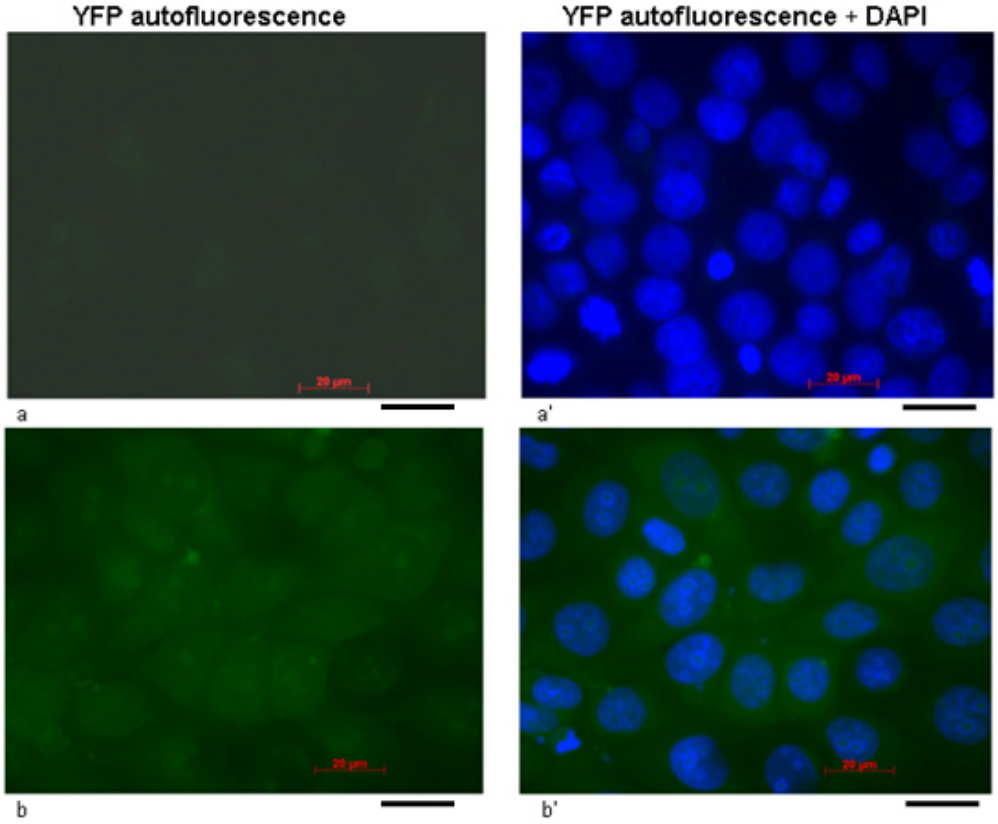

Figure 4.23: BiFC analysis of transiently transfected MCF7 cells.

a and a` : MCF7 cells transiently transfected with P86DM-Ven1-N and analyzed after 48 hours of transfection. Absence of the green signal for YFP indicates there is no nonspecific signal from the YFP-Venus1 fragment.

b and b` : MCF7 cells transiently transfected with Y-C-Actin and analyzed after 48 hours of transfection. Absence of the green signal for YFP indicates there is no nonspecific signal from the YFP-Venus1 fragment. Scale bar 20 µm

4.2.5.3.3 Cotransformation of full length cDNA inserted and empty Venus plasmids

To confirm the result obtained in first part where it has shown the direct interaction between K14 and Rab34 is genuine and not due to nonspecific interaction of expressed proteins with Venus-YFP fragments, MCF-7 cells were cotransfected with K14-pVen1flag + pVen2 HA and Rab34-pVen2 HA + pVen1flag Venus plasmids.

The results clearly showed that, K4 tagged with Venus1 fragment does not interact with the Venus2 fragment in the absence of an interacting partner. The same was true for Rab34 tagged with Venus2 fragment (figure 4.24), which confirms the specificity of the detection system and thus the results obtained.

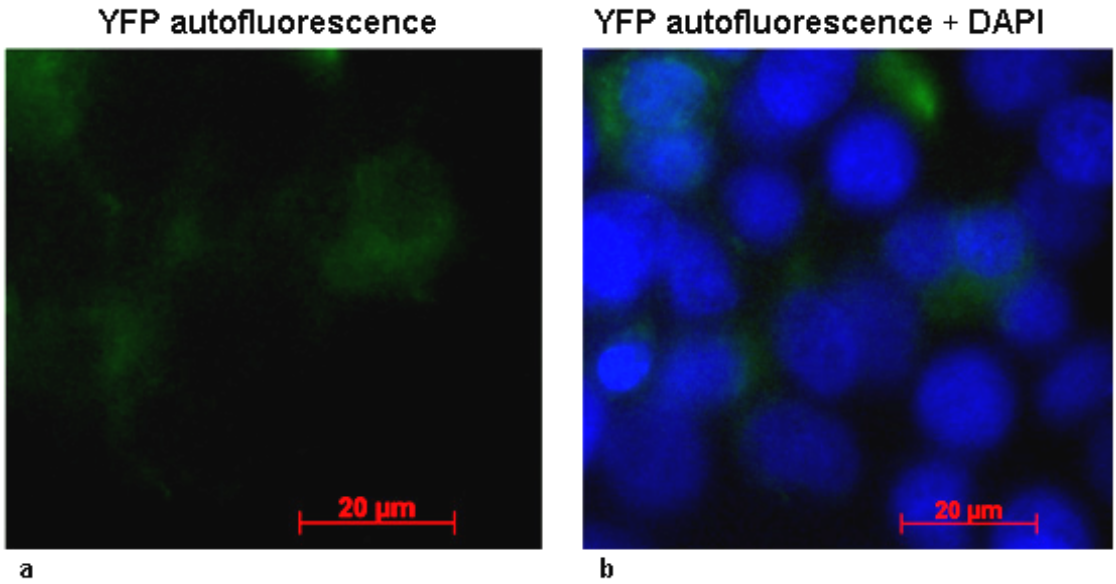

Figure 4.24: BiFC analysis of transiently transfected MCF7 cells.

MCF7 cells were cotransfected with Y-C-Actin and empty Venus vector with the complementing half of the YFP pVenus1-N, analyzed after 48 hours of transfection. Absence of the green signal for YFP indicates that the two complementing halves of the YFP do not form active YFP in presence of the fusion protein and it also doesn't interact with actin fused to second half of the full length YFP.

a) Autofluorescence from the reconstituted Venus-YFP b) MCF-7 cells with DAPI staining

An antiserum against a highly conserved C-terminal motif of p86DM was raised to examine the intracellular localization and tissue distribution of p86DM, By Western blotting and peptide competition experiments, the antiserum was found to be highly specific and detected a polypeptide of Mr 86 kDa in cultured cells (Wester. A., and Magin. TM).

To confirm the expression of p86DM and actin in cotransfected cells, cells were stained with the antiserum raised against p86DM and anti-YFP antibody which identifies the epitope on C-

terminal of YFP to look for the expression of actin. Staining images (Figure 4.25) supported the Venus-YFP fluorescence profile exhibited in BiFC experiments thereby confirming the interaction between p86DM and actin.

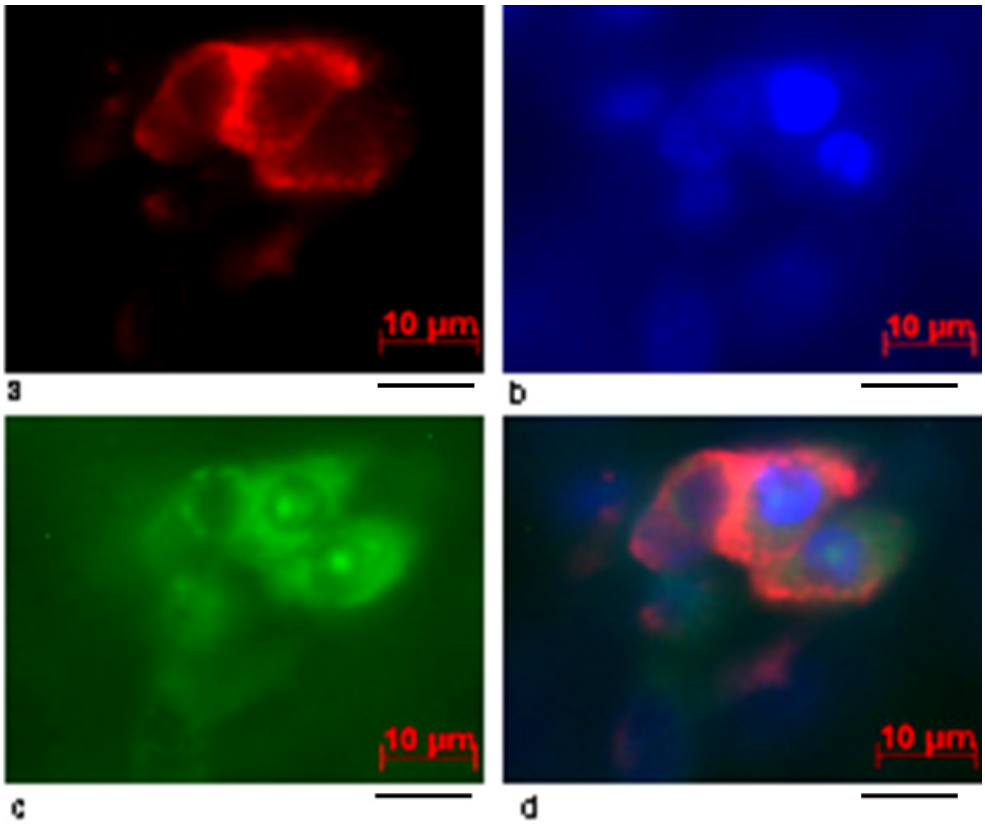

Figure 4.25: BiFC analysis along with staining of transiently transfected MCF7 cells.

MCF7 cells were cotransfected with p86DM-Ven1-N and Y-C-Actin. Cells were fixed and stained after 48 hours of transfection. Scale bar 10 µm.

a: Red signal represents expression of p86DM from the transfected p86DM-Ven1-N plasmid.

b: Transfected cells stained against C-terminal half of YFP using anti-YFP antibody. Blue signal represents expression of actin–YFP fragment fusion protein from Y-C-Actin plasmid

c: The green signal represents the YFP autofluorescence as a result of the formation of active YFP from the complementing halves due to the direct interaction between p86DM and actin which are fused with the corresponding Venus halves.

d: Mergerd signals from p86DM stained red, actin-YFP with blue and Venus- YFP autofluorescence from reconstituted Venus –YFP.

4.2.5.4 Expression of recombinant p86DM

For further investigation of functional significance and to elucidate the structural properties of p86DM, it was expressed as a recombinant protein in E.coli. Full length p86DM was cloned in frame with pET-SUMO expression vector in which p86DM was expressed as N-terminal SUMO fusion. Expression was optimized by testing different strains of E.coli at different induction

temperatures. It was observed that E.coli strain 'Rosetta' was most suitable when expression was induced at 27°C (figure 4.26). Purification of the expressed fusion protein was optimized by altering down stream processing conditions at various points.

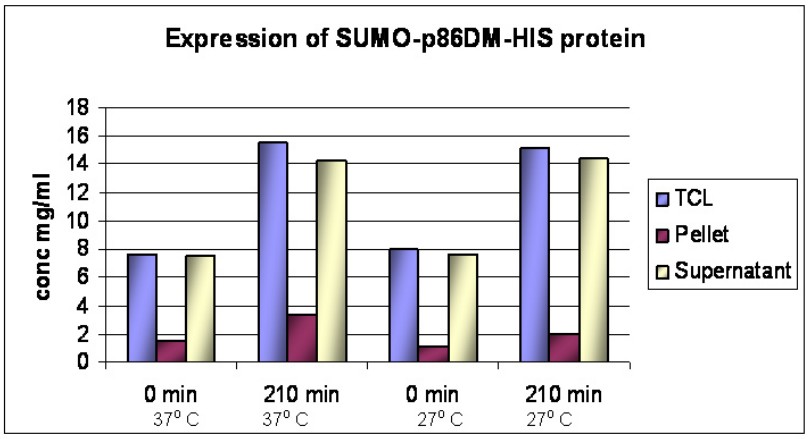

Figure 4.26: Expression profile of p86DM after 210 min of induction at 37°C and 27°C
p86DM was expressed as fusion protein with SUMO and His tags in *Rosetta* bacterial strain.

Purified protein with intact His tag can be used for further binding studies, His sumo tag was cleaved off by exposing to sumo protease, an enzyme which identifies the tertiary structure of the ubiquitin-like (UBL) protein and cleaves in a highly specific manner.

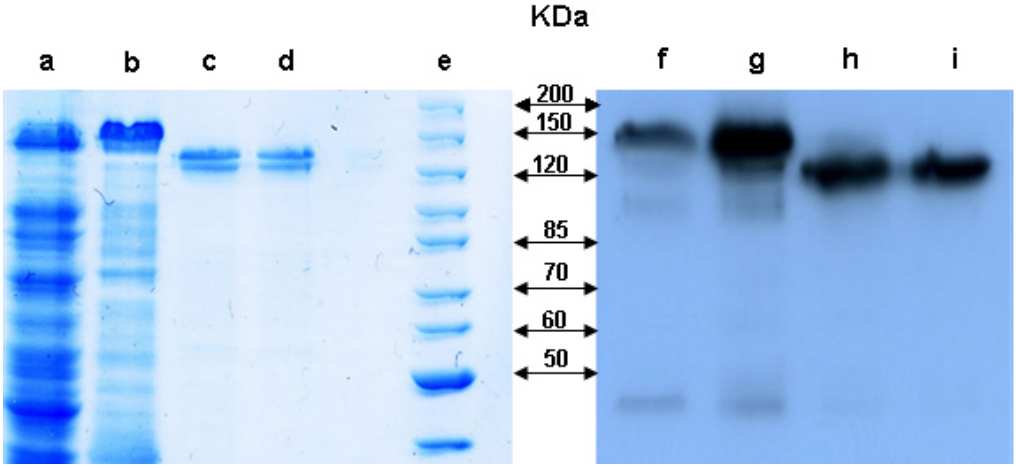

Figure 4.27: western blot analysis of recombinantly expressed p86DM followed by SUMO protease treatment to His-SUMO tag

Lane a & b: Coomassie staining of supernatant of cell lysates expressing recombinant p86DM in fusion with HOS-SUMO tag, Lane c & d: Coomassie staining of elutes treated with SUMO protease enzyme, Lane e : Marker, Lane f & g: Immuno blot of supernatant of cell lysates expressing recombinant p86DM in fusion with HOS-SUMO tag, Lane h & i: Immuno blot of elutes treated with SUMO protease enzyme.

5. Discussion

In order to understand how keratins act at the molecular level and how mutations in keratins cause pathological alterations, it is essential to have an in-depth understanding of keratin structure and its associated proteins. At the start of the work done in this thesis, very few keratin-associated proteins were known, including the structural proteins desmoplakin, filaggrin and plectin. The major work was to identify keratin-associated proteins which might act together with keratins to execute its actions beyond maintenance of cyctoarchitecture and might provide insight to molecular mechanisms responsible for functions of keratins in normal and diseased keratinocytes.

Keratins, being the major intermediate filament proteins of epithelia, display an outstanding degree of molecular diversity. The 54 human keratin genes which have been identified till date are expressed in highly specific patterns related to epithelial and stage of cellular differentiation, major of them being restricted to various compartments of hair follicles.

In the present study major focus was on epidermal keratins, K5 and K14.

K5 and K14 are expressed in the undifferentiated basal keratinocytes of stratified epithelium (Fuchs and Green, 1980), stratified follicular outer root sheath, basal and myoepithelial cells of complex glandular epithelial tissue (Purkis et al., 1990). During the process of terminal differentiation, expression of K5 and K14 is downregulated and a new set of keratins, K1 and K10 are expressed in the suprabasal spinous layer (Byrne et al., 1994). Most important function of K5 and K14 is to provide mechanical stability to epithelial cells and apart from this, these keratins have shown to be involved in other functions like vesicle transport. Mutations in genes encoding K5 and K14 lead to several skin disorders like Epidermolysis bullosa simplex (EBS), Naegeli-Franceschetti-Jadassohn syndrome (NFJS), Dermatopathia pigmentosa reticularis (DPR) and Dowling-Degos Disease (DDD). Thereby it raises the need for a detailed study in order to reveal the functions of keratins and keratin associated proteins, during physiological and pathological situations.

A closer look at the diseases caused due to mutations in K5 and K14 reveals that more disorders arise from mutation in K5 than from K14 and certain disorders like Dowling-Degos Disease (DDD) arise from K5 but not from K14, and disorder Recessive EBS-WC arises from due to mutated K14. This raises the question whether in a pair, both partners have the same function.

In order to verify keratin-associated proteins, we have performed screening studies cDNA library constructed with 500,000 cDNA fragments isolated rom human skin sample. These fragments were inserted randomly in yeast expression vector.

The screening was done using a novel genetic screening method 'Sos recruitment system'' in which the proteins like transcriptional activators/repressors, proteins that require post translational modification in the cytoplasm and the proteins /protein complex that are toxic to yeast can be identified which is not possible in the former Y2H screening techniques.

In this system, temperature sensitive yeast strain *S.cerevisiae* which carries mutated CDC45 gene, a homolog of human Sos protein. Bait is expressed as hSos fusion protein and prey is expressed as Myr fusion protein – myristylation signal containing gene. Upon physical interaction between the bait and the prey, anchors hSos to membrane there by activating the Ras signalling pathway which in turn enables the yeast to grow at restrictive temperature 37^{o}C.

All keratins have similar domain structure with a α-helical rod, flanked by non-helical head and tail domains. Type I and type II keratins form obligatory heterodimers via their highly conserved rod domains among different of keratins which are interrupted by non-α-helical linker sequences. The positively charged head domain permits the formation of filaments via antiparallel tetramers, while tail regulates the lateral association of individual filaments into bundles.

A significant similarity of 70% in the amino acid sequence was observed between the rod domains of stratified epithelial keratins K5/K14 with their embryonic and simple epithelial keratins K8/K18, where as sequences of head tail domains share only about 30%.

To get an insight into the differential properties of different keratin domains, head, rod and tail domains of K5 and K14 were individually expressed as fusion proteins with hSos and co-transformed along with cDNA library fragment containing pMyr.

The putative positive interacting candidates, which were isolated in the preliminary screening procedure, were confirmed for the interaction in yeast by replica plating on to the selective media followed by incubation at restrictive temperature.

More than 2400 interacting candidates were confirmed by yeast two hybrid screening were obtained from screening of 6 domains in-total of K5 and K14.

The purified plasmid DNA of these interacting yeast colonies was sequenced followed by bioinformatics analysis to identify the interacting candidates. Few of them are listed in the results section table 4.4 and table 4.5

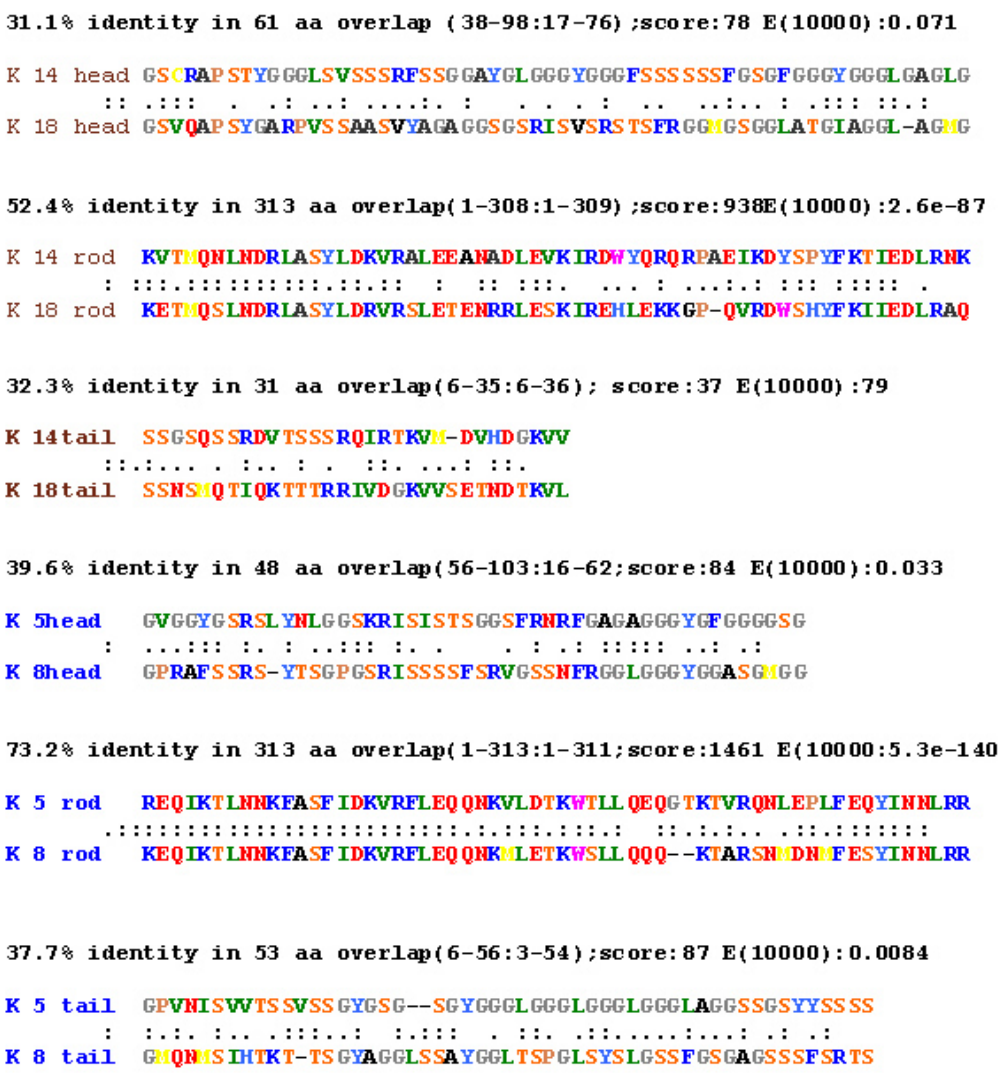

Figure 5.1: Domain sequence coparison of K5/ K14 with K8/K18. Rod domains showed greater similarities and are more consereved than head and tails domains.

We could identify wide array of proteins with diverse functions like calcium binding proteins: calponin, calmodulin, annexin, transporter proteins like GTPase family members proteins like Rab34, EP164 which play a direct role in vesicle transport. Membrane binding proteins like LYPD3, WW domain binding proteins like WBP1, TAPT1. Transcription factors like AP2ß, STAT6, translation elongation factor like EEF1A1, peroxyredoxin family of antioxidant enzymes like PRDX5 which reduce hydrogen peroxide to alkyl hydroperoxides and may play any antioxidant protective role in different tissues under normal conditions and during inflammatory process. Adapter protein 14-3-3 along with many hypothetical and un-annotated proteins were identified, out of which P86DM raises a special interest as bioinformatics domain analysis predicts to be involved in the cell polarity and migration of the cells. Disruption of the interaction between keratins and translation elongation factor (eEF1Bγ) depresses translation by

20% with the selective increase of 80S ribosomes in epithelial cells, which establish that the keratin cytoskeleton and protein synthesis machinery are functionally integrated (Kim et al., 2007).

Among the 40 listed candidates, RAB34, 14-3-3 theta, AP2β and P86DM were selected for further analysis and confirmation of their interaction with keratins in mammalian cell culture system.

To confirm the interaction in the mammalian cell system, bimolecular fluorescence complementation (BiFC) technique was used, which is based on the principle of formation of a mature fluorescent YFP from the two non-fluorescent fragments of YFP which are fused with the proteins whose interaction has to be studied. The physical interaction of the two proteins brings together the non-fluorescent fragments of YFP and forms a functionally active fluorescent complex. This method detects the direct physical interactions and has the advantage that autofluorescence reveals the confirmation of interaction thereby rendering the staining of cells non-essential.

Keratins and 14-3-3τ

Using 'Sos recruitment system' Theta isoform of 14-3-3 family of proteins has been identified as one of the interacting candidate with K14 head domain.

14-3-3 proteins were first described in the brain (Moore and Perez, 1967) and include seven members (β, γ, ε, η, σ, τ and ζ) that range in size between 28 and 33 kDa. 14-3-3 proteins are important regulators which are involved in many cellular processes like cell cycle regulation (Bridges and Moorhead, 2004; Hermeking, 2003; Hermeking and Benzinger, 2006) signal transduction and stress response (Fu et al., 1994; Yoshida et al., 2005), apoptosis (Datta et al., 2000), transcriptional regulation (Brunet et al., 2002), co-ordination of cell adhesion and motility (Santoro et al., 2003).

14-3-3 proteins regulate many cellular processes by binding to phosphorylated sites in diverse target proteins (Tzivion and Avruch, 2002). In general interaction of 14-3-3 proteins with target proteins is generally mediated through two canonical 14-3-3-binding motifs RSXpS/TXP or RXXXpS/TXP sequences, in which 'X' denotes 'any amino acid residue' and pS/T is phosphorylated (Yaffe, 2004).

To confirm the interaction between K14 and 14-3-3τ, bimolecular fluorescence complementation technique (BiFC) which allows visualizing the direct interactions was used. Upon co-transfection of Venus-tagged 14-3-3τ and K14 cDNAs into MCF-7 mammary epithelial cells, no fluorescence signal was observed which hinted towards absence of direct interaction between K14 and 14-3-3τ.

But it has been shown that 14-3-3 family proteins bind to keratin 18 in phosphorylation dependent manner with the mandatory phosphorylation of Ser33 for the association. Moreover the interaction of K18 with 14-3-3 proteins was observed only under induced hyperphosphorylated conditions by subjecting the transfected cells to heat or ocadiac acid treatment (Ku et al., 1998; Liao and Omary, 1996).

In the present study experimental settings with minimal deviation from normal physiological conditions were used to detect interaction between K14 and 14-3-3τ. It is possible that the stoichiometry of basal phosphorylation might be low in the cells studied here, which might be acting as a limiting factor for the interaction of the transfected Venus tagged K14 and 14-3-3τ proteins.

Keratins and Rab34

With the growing list of keratin-based genetic diseases hint at the role of keratins in skin pigmentation. EBS with mottled pigmentation (EBS-MP) is a rare EBS subtype, giving the skin a mottled appearance exhibiting hyper / hypo-pigmented skin. Until recently, all cases of EBS-MP had been linked to a single missense allele, P25L, in K5 (Uttam et al., 1996), which no longer might be true, since a missense mutation in the a-helical rod domain of K14, M119T (Harel et al., 2006), as well as the 1649delG mutation in K5 were reported with telltale signs of EBS-MP (Horiguchi et al., 2005). Patients suffering from EBS-MCE develop hyper- or hypo-pigmented patches as adults (Gu et al., 2003). Dowling-Degos disease (DDD) is typified by reticulate hyperpigmentation along with dark hyperkeratotic papules in skin known to be caused because of K5 haploinsufficiency (Betz et al., 2006). Naegeli–Franceschetti–Jadassohn syndrome caused by mutations located early in the head domain of K14 (Lugassy et al., 2006) causes mottled hyperpigmentation of the skin. Although the mechanism remains unclear, evidence supporting a novel role for keratin proteins in regulating skin pigmentation reveals that premature stop codons in the K5 gene affect melanosome distribution in keratinocytes (Betz et al., 2006; Liao et al., 2007). Also genetic mouse models with chemically induced mutations identify involvement of keratins in coat color determination (Fitch et al., 2003; McGowan et al., 2006; McGowan et al., 2007).

With all the above findings pointing towards the disturbed redistribution of melanosomes in skin, it becomes very important and interesting to understand the underlying mechanism in uptake of melanin granules packed in membrane-bound organelles termed ‘melanosomes’ from melanocytes - a neural-crest-derived, highly dendritic cell type to the neighboring keratinocytes and redistribution in keratinocytes. One hypothesis for melanosome uptake is endocytotic process and the redistribution through various transporter / motor proteins.

In the process of identifying keratin associated proteins, we have identified the protein Rab34 a member of small GTPases of ras superfamily as interacting partner of K14 head domain using Sos recruitment system.

Rab proteins are small GTPases of the ras superfamily that confer timing and target specificity to vesicle budding, tethering, docking, fusion, play essential roles in the endocytic and exocytic processes of transport vesicle formation within the eukaryotic secretory and endosomal pathways (Segev, 2001; Somsel Rodman and Wandinger-Ness, 2000; Zerial and McBride, 2001). They thus ensure accurate delivery of cargo macromolecules to the right target organelle. Most mammalian rabs are broadly expressed and regulate membrane transport between ubiquitous

compartments, such as endoplasmic reticulum and the golgi apparatus. However, certain cell types in higher eukaryotes harbor additional unique organelles that carry out tissue-specific functions. The best characterized are so-called lysosome-related organelles, which include melanosomes, the pigment organelle of melanocytes and of pigment epithelia in the eye. These proteins are also associated with particular vesicle membrane compartments and function in specific stages of the diverse vesicle trafficking events.

Rab34 is a 29-kDa protein present both in the cytosol and in the Golgi apparatus. Rab34 is present in the Golgi apparatus and cytosol (Wang and Hong, 2005) and it interacts with Rab7-interacting lysosomal protein (RILP) to regulate the morphology and spatial distribution of lysosomes(Wang and Hong, 2002). Rab34 is involved in the regulation of lysosome morphogenesis through cooperation with the dynein–dynactin complex (Jordens et al., 2001) Rab34 plays a crucial role in facilitating the formation of macropinosomes from the membrane ruffles (Wang and Hong, 2005). Rab34 is colocalized with actin to the membrane ruffles and macropinosome membrane (Sun et al., 2003). During macropinocytosis, Rab34 is associated with nascent macropinosomes and replaced by Rab5 at later stages. Overexpression of Rab34 elevates the number of macropinosomes, whereas the expression of a dominant-negative Rab34 prevents macropinosome formation induced by platelet-derived growth factor (PDGF) or PMA.

The direct interaction between Rab34 and K14 in the mammalian cell system was confirmed using bimolecular fluorescence complementation (BiFC) in cytoplasm of human MCF-7 cells.

Non fluorescent fragments of Venus were tagged to Rab34 and K14 cDNAs. Upon co-transfection into MCF-7 mammary epithelial cells, a direct physical interaction between the two proteins was observed in the form of autofluorescence emitted by the reconstituted mature YFP (Figure: 4.15). In endogenously keratin expressing MCF-7 cells K14 gets incorporated with the other type II keratins like K8/K9 to form the filamentous structure (Planko et al., 2007; Werner et al., 2004). Control transfections with empty vectors revealed no interaction, demonstrating the specificity of the interaction.

These data strongly suggest that Rab34 a member of transporter protein family directly interacts with K14. Understanding the significance of this interaction and further in-depth studies might definitely help in knowing process of import and regulation of melanosome by keratinocytes.

Keratins and AP-2β

The transcription factor family AP-2 consists of upto five members which are known to exhibit a highly homologous structure. AP-2 proteins form homo- or hetero-dimers with other AP-2 family members and bind specific DNA sequences. They are thought to stimulate cell proliferation and suppress terminal differentiation of specific cell types during embryonic development. Specific AP-2 family members differ in their expression patterns and binding affinity for different promoters. This protein functions as both a transcriptional activator and repressor, however their functions are considered to be different (Eckert et al., 2005). In skin AP-2β is expressed in the basal layer while AP-2β. is restricted to the sweat glands and AP-2γ is found in basal, spinous and granular layers (Byrne et al., 1994; Oyama et al., 2002; Panteleyev et al., 2003; Takahashi et al., 2000).

A role of AP-2 in epidermal differentiation is substantiated by studies of embryonic and adult skin in *Xenopus* demonstrate that the keratin gene-regulatory factor KTF-1 is identical with or closely related to AP-2 (Snape et al., 1991; Winning et al., 1991). This factor, also known as KER1 from human keratinocytes, is involved in regulation of keratin gene promoters during epidermal differentiation (Leask et al., 1991). The keratin proteins K1, K5, K10 and K14 as well as the EGFR which play a critical role in epidermal development and differentiation have been shown to harbor functional AP-2 binding sites in their promoters (Byrne et al., 1994; Koster et al., 2006; Leask et al., 1991; Maytin et al., 1999; Wang et al., 1997). Analysis of murine embryonic skin development revealed that AP-2 mRNA is expressed in a pattern similar to, but preceding that of basal keratin mRNAs (Byrne et al., 1994). Most recently, the conditional ablation of both AP-2α and γ has demonstrated their major role in terminal differentiation in skin epidermis (Wang et al., 2008).

The 5 members of the AP-2 family of helix-span-helix transcription factors determine the cell-type-restricted proliferation and the suppression of terminal differentiation of epithelia and additional tissues. Regulation of activity of AP-2 proteins still not well known.

All together more than 50 different type I and type II keratins form the major cytoskeleton of epithelial cells and are differentially expressed in all epithelia, creating protein scaffolds with unique properties. In addition to their well-established function as cytoskeletal scaffolds in epithelia, the disruption of which affects cytoarchitecture, recent papers have been reported establishing novel and unexpected keratin functions in cell proliferation, growth, survival and organelle transport.

In the yeast two hybrid screening for keratin associated proteins, we have isolated a clone encoding for the transcription factor AP-2β as a binding partner for the K14 head domain. Full length AP-2β cDNA was provided by Prof. Dr. Hubert Schorle, Bonn, was used for the further experiments.

The direct interaction between AP-2β and K14 was confirmed using bimolecular fluorescence complementation (BiFC), in the cytoplasm of human MCF-7 cells.

Upon co-transfection of Venus-tagged AP-2β and K14 cDNAs into MCF-7 mammary epithelial cells, a strong interaction between the two proteins was apparent that was highly reminiscent of staining these cells with a keratin antibody (Figure: 4.12). In fact, MCF-7 cells form an extensive cytoskeleton from endogenous keratins in which K14 becomes incorporated following transfection(Planko et al., 2007; Werner et al., 2004). Control transfections with empty vectors revealed no interaction, demonstrating the specificity of the interaction. These data strongly suggest that AP-2β is sequestered in the cytoplasm by interaction with K14.

In eukaryotes, transcription factors (like most proteins) are transcribed in the nucleus but are then translated in the cell's cytoplasm. Many proteins that are active in the nucleus contain nuclear localization signals that direct them to the nucleus. But for many transcription factors this is a key point in their regulation. Important classes of transcription factors such as some nuclear receptors must first bind to a ligand while in the cytoplasm before they can relocate to the nucleus.

We hypothesize that sequestration by distinct keratins represents a novel mechanism to regulate the activity of AP-2 transcription factors.

AP-2β can be a potential drug target as therapeutic agent in treatment of cancer (Deng et al., 2007). It has been validated as direct target gene mediating the anti-apoptotic function of PAX3/FKHR with a well known oncogenic role (Ebauer et al., 2007). AP-2 has been implicated to play a role in carcinogenesis, as well as in the development of the kidney. AP-2β expression was observed in the low-stage subtypes of renal cell carcinoma (Oya et al., 2004). AP-2β is reported to be a promising target for treatment of type 2 diabetes where it is known to regulate adipocytokine gene expression contribute to the pathogenesis of type 2 diabetes through regulation of adipocytokine gene expression, and that AP-2β may be a promising target for treatment or prevention of this disease (Maeda et al., 2005; Tsukada et al., 2006).

To understand and to elucidate the functional role of interaction between K14 and AP-2β , it becomes important to look for the molecular mechanism for the long-proposed scaffolding role of keratins and the signalling pathways regulate the AP-2β – K14 interaction.

Analysis of p86DM

We have isolated an unannotated protein as keratin associated protein using a genetic screening method 'Sos recruitment system' in yeast. We found this protein as interacting partner with K14 head and rod domain. Unfortunately the effort to prove its direct interaction with K14 in mammalian cell culture system using BiFC was not successful. At present, it appears that p86DM does not directly interact with K14, based on a number of experiments carried out by others in the lab.

p86DM still being unannotated in the database and sequence analysis of p86DM using bioinformatics tools predicted interesting functions like role in endocytosis, migration and regulation of tight junctions with relevant domains in its sequence. The predicted protein carries an N-terminal 14-3-3 binding site, SH2 and SH3 motifs, a clathrin-heavy chain binding site, a coiled-coil domain and a C-terminal PDZ-binding site, a domain organization similar to that of TJ-associated proteins.

These factors (see above) made us to select this protein for further investigation despite being not successful to identify the direct interaction in mammalian cells as the indirect interaction with functional significance cannot be ruled out.

Bioinformatics analysis predicted a single transcript giving rise to an open reading frame of 776 amino acids in the mouse and 5 isoforms for human p86DM gene. To verify whether p86DM is encoded by a single functional gene, total RNA was isolated from Caco-2 cells, full length cDNA was obtained by performing RT-PCR using the different set of primers according to the predicted isoforms with a coding sequence of 2337bp located in between exon 4 and exon 9. The multiple length cDNAs obtained by RT-PCR were sequenced and their analysis showed existence of a single functional gene for p86DM in cultured Caco-2 cells.

In order to gain a first insight on the potential mechanism by which p86DM may act, in an independent experiment (Wester.A and Magin.T.M) β-actin was identified as one of the p86DM associated proteins.

Immunofluorescence anylaysis in cultured epithelial cells demonstrated that at the apical plasmam membrane P86DM colocalized with actin at tight junctions (personal communication with Wester.A and Magin.T.M). The eukaryotic actin cytoskeleton has an important role in remarkable diverse processes, including cell migration, endocytosis, vesicle traffiking and cytokinesis, many of which are essential for survival of the cell (Goley and Welch, 2006). The dynamic assembly and disassembly of actin filaments and the formation of larger scale filament

structures are crucial aspects of actin's function, and are therefore under scrupulous control by over a hundred actin-binding proteins.

To investigate the interaction of p86DM with candidate proteins, its interaction with actin was investigated further. For this purpose we once again used BiFC technique which has successfully demonstrated the direct interactions between two proteins in previous experiments. Full length actin and p86DM were tagged with the non-fluorescent fragments of Venus-YFP, upon cotransfection in MCF-7 cells, autofluorescence as a result of formation of mature YFP revealed the interaction between actin and p86DM (Figure: 4.22). The cotransfected cells were stained for actin and p86DM, their staining profile and the images (Figure: 4.25) further supported the results obtained from BiFC experiment thereby confirming the interaction between actin and p86DM.

To carry out the further functional studies for p86DM, recombinant protein was expressed in E. coli with the SUMO-His tag (Figure: 4.27), which will be used in the further functional studies. The purified protein which has been cleaved off from SUMO-His tag, can be used for structural analysis and to raise p86DM specific monoclonal antibody.

Based on the preliminary set of results from the functional studies, p86DM enjoys the status of a promising candidate and requires thorough investigation to reveal the importance of its direct interaction with actin which might be involved in the local regulation of actin organization.

6. Summary

Keratins are an integral and important constituent of the epithelial cytoskeleton and protect epithelial cells against stress. In addition to their well-established function as cytoskeletal scaffolds in epithelia, recent findings have revealed that beyond maintenance of cytoarchitecture, keratins play important role in cell proliferation, growth, survival and organelle transport along with its associated proteins. To understand these novel keratin functions and to address the molecular mechanisms, the identification of keratin-associated proteins was a major prerequisite.

The aim of the present study was to find novel keratin associated proteins that might provide missing links. To this end, screening for the KAPs was carried out by a genetic approach 'Sos recruitment' technique based on temperature sensitive selection of positive interacting candidates in yeast to isolate K5 and K14 interacting proteins. As the first step, cDNA library was constructed with 500,000 cDNA fragments (size ranging from 500 bp to 4 kb) isolated from human skin sample. Yeast-two-hybrid screen was performed using head, rod and tail domains of epidermal keratins K5 and K14 as baits against cDNA library.

Screening in yeast yielded more than 2400 interacting candidates, out of which 200 selected cDNA fragments were sequenced.

It was observed that proteins affiliated with diverse functions seem to interact with K5 and K14. To name a few, small GTPase family members proteins (Rab34, EP164), membrane binding proteins (LYPD3), WW domain binding proteins (WBP1, TAPT1 etc), transcription factors (AP2β, STAT6), translation elongation factor (EEF1A1), 14-3-3theta a member of 14-3-3 family proteins along with many hypothetical and un-annotated proteins like p86DM were identified as interacting partners.

K14 head domain interacting candidates 'Rab34' a small GTPase of the ras superfamily reported to be involved in the regulation of lysosome morphogenesis (Jordens et al., 2001) and in formation of macropinosomes (Wang and Hong, 2005), regulator protein '14-3-3 theta', transcription factor 'AP2-β' a member AP-2 family of helix-span-helix transcription factors which determine the cell-type-restricted proliferation and the suppression of terminal differentiation of epithelia and additional tissues, and the anannotated protein 'p86DM' were selected for further analysis.

A direct interaction of full length K14 with AP-2β, and Rab34 was confirmed in cytoplasm of mammary epithelial MCF-7 cells by bimolecular fluorescence complementation (BiFC) technique.

These results strongly suggest:

1. Ras-related protein Rab-34 belonging to small GTPase Rab family directly interacts with K14. Understanding the significance of this interaction and further in-depth studies might definitely help in knowing process of import and regulation of melanosome by keratinocytes.
2. Direct interaction between K14 with AP-2β strongly suggests that AP-2β is sequestered in the cytoplasm by interaction with K14 and can be hypothesized that sequestration by distinct keratins represents a novel mechanism to regulate the activity of AP-2 transcription factors.
3. Preliminary set of results from the functional studies of p86DM displayed encouraging results and thus can be considered as a promising candidate and requires thorough investigation to reveal the importance of its direct interaction with actin.

It is worthwhile to note that, for the first time a detailed screen has been undertaken to identify keratin-associated proteins and less than 10% of the candidates obtained from Y2H screen have been sequenced so far. Further analysis of the already identified proteins and identifying the preserved un-sequenced samples will be beneficial towards understanding the molecular mechanism of keratin regulated functions.

References

1. Ameen, N. A., Figueroa, Y., and Salas, P. J. (2001). Anomalous apical plasma membrane phenotype in CK8-deficient mice indicates a novel role for intermediate filaments in the polarization of simple epithelia. J Cell Sci *114*, 563-575.
2. Apodaca, G., Katz, L. A., and Mostov, K. E. (1994). Receptor-mediated transcytosis of IgA in MDCK cells is via apical recycling endosomes. J Cell Biol *125*, 67-86.
3. Aronheim, A., Engelberg, D., Li, N., al-Alawi, N., Schlessinger, J., and Karin, M. (1994). Membrane targeting of the nucleotide exchange factor Sos is sufficient for activating the Ras signaling pathway. Cell *78*, 949-961.
4. Auerbach, D., Thaminy, S., Hottiger, M. O., and Stagljar, I. (2002). The post-genomic era of interactive proteomics: facts and perspectives. Proteomics *2*, 611-623.
5. Beil, M., Micoulet, A., von Wichert, G., Paschke, S., Walther, P., Omary, M. B., Van Veldhoven, P. P., Gern, U., Wolff-Hieber, E., Eggermann, J., *et al.* (2003). Sphingosylphosphorylcholine regulates keratin network architecture and visco-elastic properties of human cancer cells. Nat Cell Biol *5*, 803-811.
6. Betz, R. C., Planko, L., Eigelshoven, S., Hanneken, S., Pasternack, S. M., Bussow, H., Van Den Bogaert, K., Wenzel, J., Braun-Falco, M., Rutten, A., *et al.* (2006). Loss-of-function mutations in the keratin 5 gene lead to Dowling-Degos disease. Am J Hum Genet *78*, 510-519.
7. Bierkamp, C., McLaughlin, K. J., Schwarz, H., Huber, O., and Kemler, R. (1996). Embryonic heart and skin defects in mice lacking plakoglobin. Dev Biol *180*, 780-785.
8. Blouin, R., Kawahara, H., French, S. W., and Marceau, N. (1990). Selective accumulation of IF proteins at a focal juxtanuclear site in COS-1 cells transfected with mouse keratin 18 cDNA. Exp Cell Res *187*, 234-242.
9. Bretscher, A., Edwards, K., and Fehon, R. G. (2002). ERM proteins and merlin: integrators at the cell cortex. Nat Rev Mol Cell Biol *3*, 586-599.
10. Bridges, D., and Moorhead, G. B. (2004). 14-3-3 proteins: a number of functions for a numbered protein. Sci STKE *2004*, re10.
11. Brunet, A., Kanai, F., Stehn, J., Xu, J., Sarbassova, D., Frangioni, J. V., Dalal, S. N., DeCaprio, J. A., Greenberg, M. E., and Yaffe, M. B. (2002). 14-3-3 transits to the nucleus and participates in dynamic nucleocytoplasmic transport. J Cell Biol *156*, 817-828.
12. Byers, H. R., Maheshwary, S., Amodeo, D. M., and Dykstra, S. G. (2003). Role of cytoplasmic dynein in perinuclear aggregation of phagocytosed melanosomes and supranuclear melanin cap formation in human keratinocytes. J Invest Dermatol *121*, 813-820.
13. Byrne, C., Tainsky, M., and Fuchs, E. (1994). Programming gene expression in developing epidermis. Development *120*, 2369-2383.

14. Cadrin, M., Hovington, H., Marceau, N., and McFarlane-Anderson, N. (2000). Early perturbations in keratin and actin gene expression and fibrillar organisation in griseofulvin-fed mouse liver. J Hepatol *33*, 199-207.
15. Caldelari, R., de Bruin, A., Baumann, D., Suter, M. M., Bierkamp, C., Balmer, V., and Muller, E. (2001). A central role for the armadillo protein plakoglobin in the autoimmune disease pemphigus vulgaris. J Cell Biol *153*, 823-834.
16. Caulin, C., Ware, C. F., Magin, T. M., and Oshima, R. G. (2000). Keratin-dependent, epithelial resistance to tumor necrosis factor-induced apoptosis. J Cell Biol *149*, 17-22.
17. Chang, L., and Goldman, R. D. (2004). Intermediate filaments mediate cytoskeletal crosstalk. Nat Rev Mol Cell Biol *5*, 601-613.
18. Choi, H. J., Park-Snyder, S., Pascoe, L. T., Green, K. J., and Weis, W. I. (2002). Structures of two intermediate filament-binding fragments of desmoplakin reveal a unique repeat motif structure. Nat Struct Biol *9*, 612-620.
19. Choi, K. Y., Satterberg, B., Lyons, D. M., and Elion, E. A. (1994). Ste5 tethers multiple protein kinases in the MAP kinase cascade required for mating in S. cerevisiae. Cell *78*, 499-512.
20. Corden, L. D., and McLean, W. H. (1996). Human keratin diseases: hereditary fragility of specific epithelial tissues. Exp Dermatol *5*, 297-307.
21. Datta, S. R., Katsov, A., Hu, L., Petros, A., Fesik, S. W., Yaffe, M. B., and Greenberg, M. E. (2000). 14-3-3 proteins and survival kinases cooperate to inactivate BAD by BH3 domain phosphorylation. Mol Cell *6*, 41-51.
22. Deng, W. G., Jayachandran, G., Wu, G., Xu, K., Roth, J. A., and Ji, L. (2007). Tumor-specific activation of human telomerase reverses transcriptase promoter activity by activating enhancer-binding protein-2beta in human lung cancer cells. J Biol Chem *282*, 26460-26470.
23. Denk, H., Stumptner, C., and Zatloukal, K. (2000). Mallory bodies revisited. J Hepatol *32*, 689-702.
24. Drewes, G., and Bouwmeester, T. (2003). Global approaches to protein-protein interactions. Curr Opin Cell Biol *15*, 199-205.
25. Ebauer, M., Wachtel, M., Niggli, F. K., and Schafer, B. W. (2007). Comparative expression profiling identifies an in vivo target gene signature with TFAP2B as a mediator of the survival function of PAX3/FKHR. Oncogene *26*, 7267-7281.
26. Eckert, D., Buhl, S., Weber, S., Jager, R., and Schorle, H. (2005). The AP-2 family of transcription factors. Genome Biol *6*, 246.
27. Fields, S., and Song, O. (1989). A novel genetic system to detect protein-protein interactions. Nature *340*, 245-246.

28. Figueroa, Y., Wald, F. A., and Salas, P. J. (2002). p34cdc2-mediated phosphorylation mobilizes microtubule-organizing centers from the apical intermediate filament scaffold in CACO-2 epithelial cells. J Biol Chem *277*, 37848-37854.
29. Fitch, K. R., McGowan, K. A., van Raamsdonk, C. D., Fuchs, H., Lee, D., Puech, A., Herault, Y., Threadgill, D. W., Hrabe de Angelis, M., and Barsh, G. S. (2003). Genetics of dark skin in mice. Genes Dev *17*, 214-228.
30. Freedberg, I. M., Tomic-Canic, M., Komine, M., and Blumenberg, M. (2001). Keratins and the keratinocyte activation cycle. J Invest Dermatol *116*, 633-640.
31. Fu, H., Xia, K., Pallas, D. C., Cui, C., Conroy, K., Narsimhan, R. P., Mamon, H., Collier, R. J., and Roberts, T. M. (1994). Interaction of the protein kinase Raf-1 with 14-3-3 proteins. Science *266*, 126-129.
32. Fuchs, E. (1996). The cytoskeleton and disease: genetic disorders of intermediate filaments. Annu Rev Genet *30*, 197-231.
33. Fuchs, E., and Green, H. (1980). Changes in keratin gene expression during terminal differentiation of the keratinocyte. Cell *19*, 1033-1042.
34. Garrod, D., and Chidgey, M. (2008). Desmosome structure, composition and function. Biochim Biophys Acta *1778*, 572-587.
35. Geisler, N., Kaufmann, E., and Weber, K. (1985). Antiparallel orientation of the two double-stranded coiled-coils in the tetrameric protofilament unit of intermediate filaments. J Mol Biol *182*, 173-177.
36. Goley, E. D., and Welch, M. D. (2006). The ARP2/3 complex: an actin nucleator comes of age. Nat Rev Mol Cell Biol *7*, 713-726.
37. Gu, L. H., Kim, S. C., Ichiki, Y., Park, J., Nagai, M., and Kitajima, Y. (2003). A usual frameshift and delayed termination codon mutation in keratin 5 causes a novel type of epidermolysis bullosa simplex with migratory circinate erythema. J Invest Dermatol *121*, 482-485.
38. Guggino, W. B., and Stanton, B. A. (2006). New insights into cystic fibrosis: molecular switches that regulate CFTR. Nat Rev Mol Cell Biol *7*, 426-436.
39. Harel, A., Bergman, R., Indelman, M., and Sprecher, E. (2006). Epidermolysis bullosa simplex with mottled pigmentation resulting from a recurrent mutation in KRT14. J Invest Dermatol *126*, 1654-1657.
40. Helfand, B. T., Chang, L., and Goldman, R. D. (2004). Intermediate filaments are dynamic and motile elements of cellular architecture. J Cell Sci *117*, 133-141.
41. Hermeking, H. (2003). The 14-3-3 cancer connection. Nat Rev Cancer *3*, 931-943.
42. Hermeking, H., and Benzinger, A. (2006). 14-3-3 proteins in cell cycle regulation. Semin Cancer Biol *16*, 183-192.

43. Herrmann, H., Strelkov, S. V., Feja, B., Rogers, K. R., Brettel, M., Lustig, A., Haner, M., Parry, D. A., Steinert, P. M., Burkhard, P., and Aebi, U. (2000). The intermediate filament protein consensus motif of helix 2B: its atomic structure and contribution to assembly. J Mol Biol *298*, 817-832.
44. Hesse, M., Franz, T., Tamai, Y., Taketo, M. M., and Magin, T. M. (2000). Targeted deletion of keratins 18 and 19 leads to trophoblast fragility and early embryonic lethality. Embo J *19*, 5060-5070.
45. Hesse, M., Magin, T. M., and Weber, K. (2001). Genes for intermediate filament proteins and the draft sequence of the human genome: novel keratin genes and a surprisingly high number of pseudogenes related to keratin genes 8 and 18. J Cell Sci *114*, 2569-2575.
46. Horiguchi, Y., Sawamura, D., Mori, R., Nakamura, H., Takahashi, K., and Shimizu, H. (2005). Clinical heterogeneity of 1649delG mutation in the tail domain of keratin 5: a Japanese family with epidermolysis bullosa simplex with mottled pigmentation. J Invest Dermatol *125*, 83-85.
47. Huen, A. C., Park, J. K., Godsel, L. M., Chen, X., Bannon, L. J., Amargo, E. V., Hudson, T. Y., Mongiu, A. K., Leigh, I. M., Kelsell, D. P., *et al.* (2002). Intermediate filament-membrane attachments function synergistically with actin-dependent contacts to regulate intercellular adhesive strength. J Cell Biol *159*, 1005-1017.
48. Irvine, A. D., and McLean, W. H. (1999). Human keratin diseases: the increasing spectrum of disease and subtlety of the phenotype-genotype correlation. Br J Dermatol *140*, 815-828.
49. Ishida-Yamamoto, A., Tanaka, H., Nakane, H., Takahashi, H., and Iizuka, H. (1998). Inherited disorders of epidermal keratinization. J Dermatol Sci *18*, 139-154.
50. Jaquemar, D., Kupriyanov, S., Wankell, M., Avis, J., Benirschke, K., Baribault, H., and Oshima, R. G. (2003). Keratin 8 protection of placental barrier function. J Cell Biol *161*, 749-756.
51. Jordens, I., Fernandez-Borja, M., Marsman, M., Dusseljee, S., Janssen, L., Calafat, J., Janssen, H., Wubbolts, R., and Neefjes, J. (2001). The Rab7 effector protein RILP controls lysosomal transport by inducing the recruitment of dynein-dynactin motors. Curr Biol *11*, 1680-1685.
52. Kim, S., Kellner, J., Lee, C. H., and Coulombe, P. A. (2007). Interaction between the keratin cytoskeleton and eEF1Bgamma affects protein synthesis in epithelial cells. Nat Struct Mol Biol *14*, 982-983.
53. Kirfel, J., Magin, T. M., and Reichelt, J. (2003). Keratins: a structural scaffold with emerging functions. Cell Mol Life Sci *60*, 56-71.
54. Kischkel, F. C., Hellbardt, S., Behrmann, I., Germer, M., Pawlita, M., Krammer, P. H., and Peter, M. E. (1995). Cytotoxicity-dependent APO-1 (Fas/CD95)-associated proteins form a death-inducing signaling complex (DISC) with the receptor. Embo J *14*, 5579-5588.

55. Koster, M. I., Kim, S., Huang, J., Williams, T., and Roop, D. R. (2006). TAp63alpha induces AP-2gamma as an early event in epidermal morphogenesis. Dev Biol *289*, 253-261.
56. Kowalczyk, A. P., Bornslaeger, E. A., Borgwardt, J. E., Palka, H. L., Dhaliwal, A. S., Corcoran, C. M., Denning, M. F., and Green, K. J. (1997). The amino-terminal domain of desmoplakin binds to plakoglobin and clusters desmosomal cadherin-plakoglobin complexes. J Cell Biol *139*, 773-784.
57. Ku, N. O., Fu, H., and Omary, M. B. (2004). Raf-1 activation disrupts its binding to keratins during cell stress. J Cell Biol *166*, 479-485.
58. Ku, N. O., Gish, R., Wright, T. L., and Omary, M. B. (2001). Keratin 8 mutations in patients with cryptogenic liver disease. N Engl J Med *344*, 1580-1587.
59. Ku, N. O., Liao, J., and Omary, M. B. (1998). Phosphorylation of human keratin 18 serine 33 regulates binding to 14-3-3 proteins. Embo J *17*, 1892-1906.
60. Ku, N. O., and Omary, M. B. (2006). A disease- and phosphorylation-related nonmechanical function for keratin 8. J Cell Biol *174*, 115-125.
61. Ku, N. O., Soetikno, R. M., and Omary, M. B. (2003). Keratin mutation in transgenic mice predisposes to Fas but not TNF-induced apoptosis and massive liver injury. Hepatology *37*, 1006-1014.
62. Ku, N. O., Zhou, X., Toivola, D. M., and Omary, M. B. (1999). The cytoskeleton of digestive epithelia in health and disease. Am J Physiol *277*, G1108-1137.
63. Lane, E. B., and McLean, W. H. (2004). Keratins and skin disorders. J Pathol *204*, 355-366.
64. Langbein, L., and Schweizer, J. (2005). Keratins of the human hair follicle. Int Rev Cytol *243*, 1-78.
65. Leask, A., Byrne, C., and Fuchs, E. (1991). Transcription factor AP2 and its role in epidermal-specific gene expression. Proc Natl Acad Sci U S A *88*, 7948-7952.
66. Liao, H., Zhao, Y., Baty, D. U., McGrath, J. A., Mellerio, J. E., and McLean, W. H. (2007). A heterozygous frameshift mutation in the V1 domain of keratin 5 in a family with Dowling-Degos disease. J Invest Dermatol *127*, 298-300.
67. Liao, J., and Omary, M. B. (1996). 14-3-3 proteins associate with phosphorylated simple epithelial keratins during cell cycle progression and act as a solubility cofactor. J Cell Biol *133*, 345-357.
68. Lugassy, J., Itin, P., Ishida-Yamamoto, A., Holland, K., Huson, S., Geiger, D., Hennies, H. C., Indelman, M., Bercovich, D., Uitto, J., *et al.* (2006). Naegeli-Franceschetti-Jadassohn syndrome and dermatopathia pigmentosa reticularis: two allelic ectodermal dysplasias caused by dominant mutations in KRT14. Am J Hum Genet *79*, 724-730.
69. Maeda, S., Tsukada, S., Kanazawa, A., Sekine, A., Tsunoda, T., Koya, D., Maegawa, H., Kashiwagi, A., Babazono, T., Matsuda, M., *et al.* (2005). Genetic variations in the gene encoding TFAP2B are associated with type 2 diabetes mellitus. J Hum Genet *50*, 283-292.

70. Magin, T. M., Reichelt, J., and Hatzfeld, M. (2004). Emerging functions: diseases and animal models reshape our view of the cytoskeleton. Exp Cell Res *301*, 91-102.
71. Magin, T. M., Schroder, R., Leitgeb, S., Wanninger, F., Zatloukal, K., Grund, C., and Melton, D. W. (1998). Lessons from keratin 18 knockout mice: formation of novel keratin filaments, secondary loss of keratin 7 and accumulation of liver-specific keratin 8-positive aggregates. J Cell Biol *140*, 1441-1451.
72. Marks, M. S., and Seabra, M. C. (2001). The melanosome: membrane dynamics in black and white. Nat Rev Mol Cell Biol *2*, 738-748.
73. Mathur, M., Goodwin, L., and Cowin, P. (1994). Interactions of the cytoplasmic domain of the desmosomal cadherin Dsg1 with plakoglobin. J Biol Chem *269*, 14075-14080.
74. Maytin, E. V., Lin, J. C., Krishnamurthy, R., Batchvarova, N., Ron, D., Mitchell, P. J., and Habener, J. F. (1999). Keratin 10 gene expression during differentiation of mouse epidermis requires transcription factors C/EBP and AP-2. Dev Biol *216*, 164-181.
75. Mazzalupo, S., Wong, P., Martin, P., and Coulombe, P. A. (2003). Role for keratins 6 and 17 during wound closure in embryonic mouse skin. Dev Dyn *226*, 356-365.
76. McGowan, K. A., Aradhya, S., Fuchs, H., de Angelis, M. H., and Barsh, G. S. (2006). A mouse keratin 1 mutation causes dark skin and epidermolytic hyperkeratosis. J Invest Dermatol *126*, 1013-1016.
77. McGowan, K. A., Fuchs, H., Hrabe de Angelis, M., and Barsh, G. S. (2007). Identification of a Keratin 4 mutation in a chemically induced mouse mutant that models white sponge nevus. J Invest Dermatol *127*, 60-64.
78. Meads, T., and Schroer, T. A. (1995). Polarity and nucleation of microtubules in polarized epithelial cells. Cell Motil Cytoskeleton *32*, 273-288.
79. Moll, R., Franke, W. W., Schiller, D. L., Geiger, B., and Krepler, R. (1982). The catalog of human cytokeratins: patterns of expression in normal epithelia, tumors and cultured cells. Cell *31*, 11-24.
80. Mulari, M. T., Patrikainen, L., Kaisto, T., Metsikko, K., Salo, J. J., and Vaananen, H. K. (2003). The architecture of microtubular network and Golgi orientation in osteoclasts--major differences between avian and mammalian species. Exp Cell Res *285*, 221-235.
81. Oya, M., Mikami, S., Mizuno, R., Miyajima, A., Horiguchi, Y., Nakashima, J., Marumo, K., Mukai, M., and Murai, M. (2004). Differential expression of activator protein-2 isoforms in renal cell carcinoma. Urology *64*, 162-167.
82. Oyama, N., Takahashi, H., Tojo, M., Iwatsuki, K., Iizuka, H., Nakamura, K., Homma, Y., and Kaneko, F. (2002). Different properties of three isoforms (alpha, beta, and gamma) of transcription factor AP-2 in the expression of human keratinocyte genes. Arch Dermatol Res *294*, 273-280.

83. Paladini, R. D., Takahashi, K., Bravo, N. S., and Coulombe, P. A. (1996). Onset of re-epithelialization after skin injury correlates with a reorganization of keratin filaments in wound edge keratinocytes: defining a potential role for keratin 16. J Cell Biol *132*, 381-397.
84. Panteleyev, A. A., Mitchell, P. J., Paus, R., and Christiano, A. M. (2003). Expression patterns of the transcription factor AP-2alpha during hair follicle morphogenesis and cycling. J Invest Dermatol *121*, 13-19.
85. Parry, D. A., Steven, A. C., and Steinert, P. M. (1985). The coiled-coil molecules of intermediate filaments consist of two parallel chains in exact axial register. Biochem Biophys Res Commun *127*, 1012-1018.
86. Planko, L., Bohse, K., Hohfeld, J., Betz, R. C., Hanneken, S., Eigelshoven, S., Kruse, R., Nothen, M. M., and Magin, T. M. (2007). Identification of a keratin-associated protein with a putative role in vesicle transport. Eur J Cell Biol *86*, 827-839.
87. Porter, R. M., and Lane, E. B. (2003). Phenotypes, genotypes and their contribution to understanding keratin function. Trends Genet *19*, 278-285.
88. Purkis, P. E., Steel, J. B., Mackenzie, I. C., Nathrath, W. B., Leigh, I. M., and Lane, E. B. (1990). Antibody markers of basal cells in complex epithelia. J Cell Sci *97 (Pt 1)*, 39-50.
89. Rugg, E. L., and Leigh, I. M. (2004). The keratins and their disorders. Am J Med Genet C Semin Med Genet *131C*, 4-11.
90. Ryan, D. P., and Matthews, J. M. (2005). Protein-protein interactions in human disease. Curr Opin Struct Biol *15*, 441-446.
91. Salas, P. J. (1999). Insoluble gamma-tubulin-containing structures are anchored to the apical network of intermediate filaments in polarized CACO-2 epithelial cells. J Cell Biol *146*, 645-658.
92. Santoro, M. M., Gaudino, G., and Marchisio, P. C. (2003). The MSP receptor regulates alpha6beta4 and alpha3beta1 integrins via 14-3-3 proteins in keratinocyte migration. Dev Cell *5*, 257-271.
93. Schweizer, J., Bowden, P. E., Coulombe, P. A., Langbein, L., Lane, E. B., Magin, T. M., Maltais, L., Omary, M. B., Parry, D. A., Rogers, M. A., and Wright, M. W. (2006). New consensus nomenclature for mammalian keratins. J Cell Biol *174*, 169-174.
94. Segev, N. (2001). Ypt and Rab GTPases: insight into functions through novel interactions. Curr Opin Cell Biol *13*, 500-511.
95. Sinha, S., Degenstein, L., Copenhaver, C., and Fuchs, E. (2000). Defining the regulatory factors required for epidermal gene expression. Mol Cell Biol *20*, 2543-2555.
96. Sinha, S., and Fuchs, E. (2001). Identification and dissection of an enhancer controlling epithelial gene expression in skin. Proc Natl Acad Sci U S A *98*, 2455-2460.
97. Smith, E. A., and Fuchs, E. (1998). Defining the interactions between intermediate filaments and desmosomes. J Cell Biol *141*, 1229-1241.

98. Smith, F. (2003). The molecular genetics of keratin disorders. Am J Clin Dermatol *4*, 347-364.
99. Snape, A. M., Winning, R. S., and Sargent, T. D. (1991). Transcription factor AP-2 is tissue-specific in Xenopus and is closely related or identical to keratin transcription factor 1 (KTF-1). Development *113*, 283-293.
100. Somsel Rodman, J., and Wandinger-Ness, A. (2000). Rab GTPases coordinate endocytosis. J Cell Sci *113 Pt 2*, 183-192.
101. Stappenbeck, T. S., Lamb, J. A., Corcoran, C. M., and Green, K. J. (1994). Phosphorylation of the desmoplakin COOH terminus negatively regulates its interaction with keratin intermediate filament networks. J Biol Chem *269*, 29351-29354.
102. Steinert, P. M. (1990). The two-chain coiled-coil molecule of native epidermal keratin intermediate filaments is a type I-type II heterodimer. J Biol Chem *265*, 8766-8774.
103. Steinert, P. M., North, A. C., and Parry, D. A. (1994). Structural features of keratin intermediate filaments. J Invest Dermatol *103*, 19S-24S.
104. Strelkov, S. V., Herrmann, H., Geisler, N., Wedig, T., Zimbelmann, R., Aebi, U., and Burkhard, P. (2002). Conserved segments 1A and 2B of the intermediate filament dimer: their atomic structures and role in filament assembly. Embo J *21*, 1255-1266.
105. Sun, P., Yamamoto, H., Suetsugu, S., Miki, H., Takenawa, T., and Endo, T. (2003). Small GTPase Rah/Rab34 is associated with membrane ruffles and macropinosomes and promotes macropinosome formation. J Biol Chem *278*, 4063-4071.
106. Takahashi, H., Oyama, N., Itoh, Y., Ishida-Yamamoto, A., Kaneko, F., and Iizuka, H. (2000). Transcriptional factor AP-2gamma increases human cystatin A gene transcription of keratinocytes. Biochem Biophys Res Commun *278*, 719-723.
107. Takahashi, K., Coulombe, P. A., and Miyachi, Y. (1999). Using transgenic models to study the pathogenesis of keratin-based inherited skin diseases. J Dermatol Sci *21*, 73-95.
108. Tamai, Y., Ishikawa, T., Bosl, M. R., Mori, M., Nozaki, M., Baribault, H., Oshima, R. G., and Taketo, M. M. (2000). Cytokeratins 8 and 19 in the mouse placental development. J Cell Biol *151*, 563-572.
109. Tao, G. Z., Toivola, D. M., Zhou, Q., Strnad, P., Xu, B., Michie, S. A., and Omary, M. B. (2006). Protein phosphatase-2A associates with and dephosphorylates keratin 8 after hyposmotic stress in a site- and cell-specific manner. J Cell Sci *119*, 1425-1432.
110. Toivola, D. M., Baribault, H., Magin, T., Michie, S. A., and Omary, M. B. (2000). Simple epithelial keratins are dispensable for cytoprotection in two pancreatitis models. Am J Physiol Gastrointest Liver Physiol *279*, G1343-1354.
111. Tsukada, S., Tanaka, Y., Maegawa, H., Kashiwagi, A., Kawamori, R., and Maeda, S. (2006). Intronic polymorphisms within TFAP2B regulate transcriptional activity and affect adipocytokine gene expression in differentiated adipocytes. Mol Endocrinol *20*, 1104-1111.

112. Tzivion, G., and Avruch, J. (2002). 14-3-3 proteins: active cofactors in cellular regulation by serine/threonine phosphorylation. J Biol Chem *277*, 3061-3064.
113. Uttam, J., Hutton, E., Coulombe, P. A., Anton-Lamprecht, I., Yu, Q. C., Gedde-Dahl, T., Jr., Fine, J. D., and Fuchs, E. (1996). The genetic basis of epidermolysis bullosa simplex with mottled pigmentation. Proc Natl Acad Sci U S A *93*, 9079-9084.
114. Vasioukhin, V., Bowers, E., Bauer, C., Degenstein, L., and Fuchs, E. (2001). Desmoplakin is essential in epidermal sheet formation. Nat Cell Biol *3*, 1076-1085.
115. Wald, F. A., Oriolo, A. S., Casanova, M. L., and Salas, P. J. (2005). Intermediate filaments interact with dormant ezrin in intestinal epithelial cells. Mol Biol Cell *16*, 4096-4107.
116. Wang, D., Shin, T. H., and Kudlow, J. E. (1997). Transcription factor AP-2 controls transcription of the human transforming growth factor-alpha gene. J Biol Chem *272*, 14244-14250.
117. Wang, T., and Hong, W. (2002). Interorganellar regulation of lysosome positioning by the Golgi apparatus through Rab34 interaction with Rab-interacting lysosomal protein. Mol Biol Cell *13*, 4317-4332.
118. Wang, T., and Hong, W. (2005). Assay and functional properties of Rab34 interaction with RILP in lysosome morphogenesis. Methods Enzymol *403*, 675-687.
119. Wang, X., Pasolli, H. A., Williams, T., and Fuchs, E. (2008). AP-2 factors act in concert with Notch to orchestrate terminal differentiation in skin epidermis. J Cell Biol *183*, 37-48.
120. Wells, J. A., and McClendon, C. L. (2007). Reaching for high-hanging fruit in drug discovery at protein-protein interfaces. Nature *450*, 1001-1009.
121. Werner, N. S., Windoffer, R., Strnad, P., Grund, C., Leube, R. E., and Magin, T. M. (2004). Epidermolysis bullosa simplex-type mutations alter the dynamics of the keratin cytoskeleton and reveal a contribution of actin to the transport of keratin subunits. Mol Biol Cell *15*, 990-1002.
122. Wilson, A. K., Coulombe, P. A., and Fuchs, E. (1992). The roles of K5 and K14 head, tail, and R/K L L E G E domains in keratin filament assembly in vitro. J Cell Biol *119*, 401-414.
123. Winning, R. S., Shea, L. J., Marcus, S. J., and Sargent, T. D. (1991). Developmental regulation of transcription factor AP-2 during Xenopus laevis embryogenesis. Nucleic Acids Res *19*, 3709-3714.
124. Wojcik, S. M., Bundman, D. S., and Roop, D. R. (2000). Delayed wound healing in keratin 6a knockout mice. Mol Cell Biol *20*, 5248-5255.
125. Wong, P., Colucci-Guyon, E., Takahashi, K., Gu, C., Babinet, C., and Coulombe, P. A. (2000). Introducing a null mutation in the mouse K6alpha and K6beta genes reveals their essential structural role in the oral mucosa. J Cell Biol *150*, 921-928.
126. Wong, P., and Coulombe, P. A. (2003). Loss of keratin 6 (K6) proteins reveals a function for intermediate filaments during wound repair. J Cell Biol *163*, 327-337.

127. Yin, T., Getsios, S., Caldelari, R., Kowalczyk, A. P., Muller, E. J., Jones, J. C., and Green, K. J. (2005). Plakoglobin suppresses keratinocyte motility through both cell-cell adhesion-dependent and -independent mechanisms. Proc Natl Acad Sci U S A *102*, 5420-5425.

128. Yoshida, K., Yamaguchi, T., Natsume, T., Kufe, D., and Miki, Y. (2005). JNK phosphorylation of 14-3-3 proteins regulates nuclear targeting of c-Abl in the apoptotic response to DNA damage. Nat Cell Biol *7*, 278-285.

129. Zatloukal, K., Stumptner, C., Lehner, M., Denk, H., Baribault, H., Eshkind, L. G., and Franke, W. W. (2000). Cytokeratin 8 protects from hepatotoxicity, and its ratio to cytokeratin 18 determines the ability of hepatocytes to form Mallory bodies. Am J Pathol *156*, 1263-1274.

130. Zerial, M., and McBride, H. (2001). Rab proteins as membrane organizers. Nat Rev Mol Cell Biol *2*, 107-117.

131. Zhong, B., Zhou, Q., Toivola, D. M., Tao, G. Z., Resurreccion, E. Z., and Omary, M. B. (2004). Organ-specific stress induces mouse pancreatic keratin overexpression in association with NF-kappaB activation. J Cell Sci *117*, 1709-1719.

PROJECTS

1. **Identification and characterization of novel keratin associated proteins using a genetic interaction screening system**

Institue of Physiological chemistry

Guide : Prof. Thomas M. Magin

Brief project profile:

Cell architecture is mainly based on the interaction of cytoskeletal proteins, which include intermediate filaments, micro filaments, microtubules as well as type-specific membrane attachment structures and associated proteins.

Keratin 5 and keratin 14 form the major intermediate filaments of basal epidermis, their primary function is to impart mechanical strength to cells as highlighted by the dominant mutations causing inherited skin disorders. In order to understand the molecular mechanism of keratin dependent functions, we intend to identify novel keratin associated proteins.

Yeast two hybrid screen was performed using K5 and K14 as bait against a cDNA library prepared from human skin tissue. From the six baits used about 2000 positive interacting candidates were obtained, which included anticipated transporter proteins along with some unexpected and un-annotated proteins.

Among the different methods tested to confirm the interaction between positive candidates from the screen and keratins, bimolecular fluorescence complementation (Bifc) was found to be the most suitable method and thus was used to confirm the interaction for some of the short listed candidates. At present further functional studies are being carried out for characterization of some of the selected interacting candidates identified by screening experiments.

2. **Evaluation of estrogenic activity using MCF -7 human breast cancer cells**

Natural Remedies Ltd., Bangalore, INDIA. Team size: 1

Brief project profile:

This project is focused on discovering the potent phytoestrogens from the herbal extracts. Estrogenic activity is determined using an estrogen-dependent MCF-7 breast cancer cell proliferation assay.

3. **Nitric oxide scavenging activity in freshly isolated macrophages**

Natural Remedies Ltd., Bangalore, INDIA. Team size: 1

Brief project profile:

A mixture of water extracts of certain medicinal plants is being investigated for the nitric oxide scavenging activity in freshly isolated macrophages from the peritoneal cavity of mice. The nitric oxide release is stimulated using lipopolysaccharide (LPS) & the extract mixture is being tested for its scavenging activity by a microtitre plate assay method based on Griess reaction.

4. **Evaluation of anti-hyperglycemic effect of herbal extracts through the inhibition of intestinal enzymes in normal rats.**

Natural Remedies Ltd., Bangalore, INDIA. Team size: 1

Brief project profile:

We examined the inhibitory effects of different herbal extracts on starch and sucrose loading induced hyperglycemia in normal Wistar rats. Blood glucose level was estimated at different intervals after the carbohydrate loading to examine the inhibitory activity of the test extracts on disaccharidases in the small intestine of rats.

5. **Evaluation of anti stress property by swim endurance test**

Natural Remedies Ltd., Bangalore, INDIA. Team size: 1

Brief project profile:

The anti stress property of the herbal extracts was tested on Swiss albino mice, exposed to swim endurance test model of stress. Positive control compound and the test extracts were administered orally for 30 days. Reactivity of the mice, loss in body weight, length of endurance and incidence of mortality were graded and measured.

6. **Method Development For Isolation And Purification Of HBsAg Protein**

Yashraj Biotechnology Ltd., New Bombay, INDIA.

Brief project profile:

The project involves the method development for isolation & purification of the diagnostically important proteins (HBsAg, Cancer antigens) from the biological fluids of human origin, scale-up to production process & the study of stability properties of the purified proteins.

7. **Tool for finding ORF in a nucleotide sequence**.

Manvish InfoTech Ltd, Bangalore, INDIA,.

Guide: Dr. Raja Mugasimangalam. Team size: 3

Brief project profile:

A tool was developed using C programming language, to locate the Open Reading Frames (ORF) and its position in the original nucleotide sequence, along with six frame translations. The results obtained from this tool were similar to that of the currently available online tools. As a useful analytical tool, it also provided the percentage GC content. This utility is a useful and fast way to translate a sequence in combination with ORF analysis.

8. ***In-vitro* and *in-vivo* investigation on the hepatoprotective activity of certain medicinal plants.**

J.S.S College of Pharmacy, Ooty,

Guides :Dr.P.Vijayan. Team size: 1

Brief project profile:

The methanolic extracts of the root, root bark and stem of *Berberis tinctoria, ethanolic* extract of whole plant of *Phyllanthus amarus and* the total alkaloids isolated from the leaves of *Solanum pseudocapsicum* were investigated for its hepatoprotective activity against CCl_4 induced toxicity in freshly isolated rat hepatocytes, HepG2 cell line *in-vitro* and in animal models. The extracts were able to normalise the levels of ASAT, ALAT, ALP, TGL, total proteins, albumin, total bilirubin and direct bilirubin which were altered due to CCl_4 intoxication in freshly isolated rat hepatocytes and also in animal models.

9. **Comparative cytotoxic studies of synthetic drugs in established cell lines and primary culture.**

J.S.S College of Pharmacy, Ooty,

Guide : Dr. P. Vijayan & Ms. Sarita G.S Team size : 2

Brief project profile:

Eight drugs belonging to pyridine & mannich bases were selected for systematic screening for cytotoxicity as a means of identifying potential anti-tumor drug moieties. Long-term cytotoxicity studies were performed on HEp-2 and Vero cell lines and mouse lung & kidney primary cultures. The cytotoxic effect of all the eight drugs was estimated by dye exclusion, protein synthesis estimation and MTT assay methods. All studies confirmed that the drug activity was significant only at very high concentration.

COMPUTER KNOWLEDGE

- Windows, Linux, MS Office
- Working knowledge in C, HTML, ORACLE
- Working knowledge of Bioinformatics related software and tools like EMBOSS, GCG, Vector NTI, ClustalW, FASTA, BLAST, SCOP, FUGUE, J-Pred, 3DPSSM, PDB-BLAST, Swiss-Model, SwissPDB Viewer, PDB tool, RASMOL, Pfam.

PUBLICATIONS

- Comparative cytotoxic studies of synthetic drugs in established cell lines and primary culture, paper accepted for presentation at **52nd IPC** held at Hyderabad.
- Hepatoprotective effect of the alkaloid fraction of *Solanum pseudocapsicum* leaves, **Pharmaceutical Biology** –2003; *41: 443 - 448*
- The cytotoxic activity of the total alkaloids isolated from different parts of Solanum pseudocapsicum, Biol Pharm Bull. 2004 Apr;27(4):528-30.